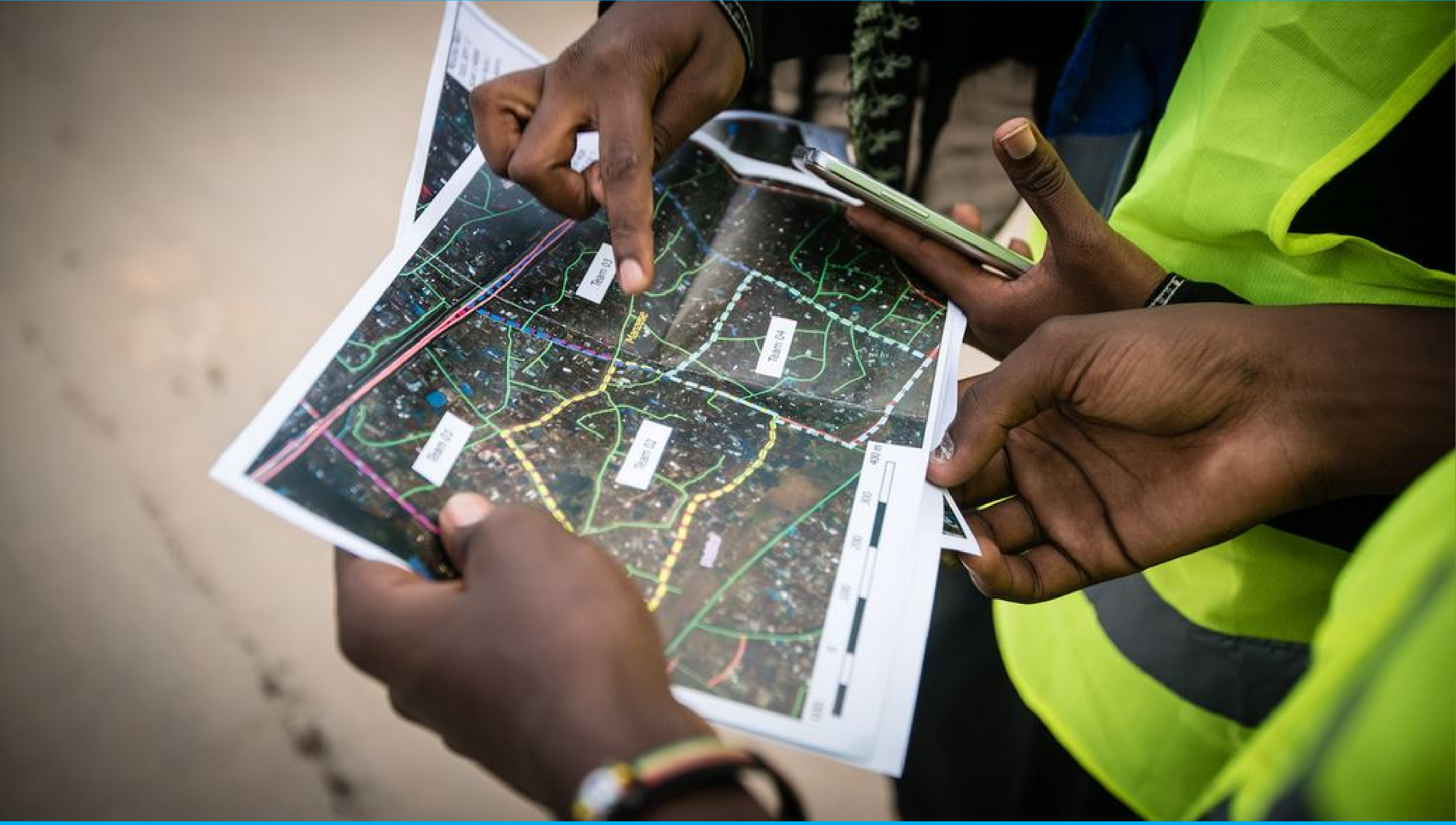

Technische Universiteit Delft

Community mapping for flood modelling

A case study of the *Ramani Huria* community mapping project in Dar es Salaam

Louise Petersson

TU Delft

Community mapping for flood modelling

A case study of the *Ramani Huria* community mapping project in Dar es Salaam

by

Louise Petersson

to obtain the degree of Master of Science in Civil Engineering
at the Delft University of Technology,
to be defended publicly on September 13th, 2019.

Student number:	4726634	
Thesis committee:	Dr. Ir. Hessel Winsemius,	TU Delft, chairman
	Dr. Ir. Marie-Claire ten Veldhuis,	TU Delft
	Prof. Dr. Zoran Kapelan,	TU Delft
	Ir. Govert Verhoeven,	Deltares

An electronic version of this thesis is available at http://repository.tudelft.nl/.
Cover image: *Ramani Huria* drainage mappers in Dar es Salaam.
http://ramanihuria.org/

Foreword

This thesis explores how community mapped data can be applied in a traditional hydrodynamic modelling software to improve flood predictions on neighbourhood scale. If you are only interested in how this can be done, proceed to appendix C. As you will notice, all steps in my methodology have not been done with open source software. I am sure that it is possible to overcome this with open source scripts, but unfortunately, the development of such scripts is outside the scope of my thesis. Here I propose *one* way to process community mapped data to become suitable for flood modelling, and I hope that this methodology will be improved and become accessible online. I believe that the open data community is only in the beginning of the journey to explore how design, development and governance can be supported by ICT and open source data. If you have any ideas or questions about my work, or if you want to get access to my raw data or results, feel free to drop an email to lepetersson8890@gmail.com.

Now that I have got your attention - let's avoid to make the open data community to yet another platform created by men, for men. Please stay inclusive, and credit other people's work properly. I will see you around!

Louise

Abstract

The current intensification of the hydrologic cycle, in combination with expanding settlements in flood prone areas, makes an increasing share of the global population exposed to flood risks. Many parts of the world are, however, still lacking the data needed for flood risk management and risk reduction. The recent development of information and communication technologies has remarkably lowered the costs to collect data for flood resilience, which has accommodated the rise of community mapping projects to fill data gaps in resource-strained environments. This thesis utilises drainage data collected by the *Ramani Huria* community mapping project in Dar es Salaam, Tanzania, to investigate if community mapped drainage data can improve flood predictions on neighbourhood scale. A coupled 1D-2D hydrodynamic model is developed of Kijitonyama ward, and is run with and without *Ramani Huria*'s drainage data implemented in the 1D schematisation. The simulated flood depth for the scenarios is validated with citizen's observations on flood depth during a rain event on 3 March, 2019. The developed model is then applied to investigate the impact of solid waste accumulation in the drainage system on floods, by closing the drainage segments that were recorded as blocked in Kijitonyama ward by *Ramani Huria* staff the morning after the simulated event. An experimental scenario is also run, to examine the impact of blocked culverts. The results show that community mapped drainage data indeed can enhance the performance of hydrodynamic models, as the model output corresponds better with the validation data when implementing *Ramani Huria*'s drainage data in the 1D schematisation, compared with a scenario run with only a 2D schematisation. The scenarios run with solid waste blockages do not influence the model output when comparing with citizen's observations, but increase the water level in the drainage segments located upstream of the blockages.

Acknowledgements

First of all, I would like to thank **Dr. Hessel Winsemius**, associate professor and hydrologist at TU Delft, for connecting me with most of the people mentioned below. Your position at TU Delft has only started and your creativity is already making a difference for sustainable development in Dar es Salaam. Thank you for investing your talent in the common good. I also want to thank the other members of my assessment committee, **Govert Verhoeven**, **Marie-Claire ten Veldhuis** and **Zoran Kapelan** for your support and pep talk during this sometimes very difficult process. I could not have been more lucky to get your supervision. Furthermore, I give special thanks to **Elia Dominic**, mapping supervisor at Humanitarian OpenStreetMap Team Tanzania (HOT), whose support of my data collection is invaluable for the outcome of this thesis. Also special thanks to **Immaculate Mwanja** at HOT for supporting me during my stay in Dar es Salaam, especially with carrying out my surveys. Stay strong and focused - the future belongs to women like you.

Furthermore, I would like to thank:

Humanitarian OpenStreetMap Team Tanzania

William Evans	Johanes Petro
Ivan Gayton	Glory Pastory
Innocent Maholi	Lovenes Charles
Wombura Kimacha	Emanuel Kombe

Mappers performing the flood extent and blockage survey (HOT)

Wilfred Raban Chomba	Hamisi Salehe
Deogratias Gabriel	Frank Majaliwa
Baraka Barton	Benedicto Adamu
Ramadhani Omari	

Deltares, Delft
Rinske Hutten

My partner in crime
Markus Pleij

You are all contributors to this thesis. It has been an honour to work with you all, and I hope to meet you again in one way or another. I am convinced that openness, curiosity and hard work is the key to combat the challenges of climate change, and you have all inspired me to continue down this road. Thank you.

Love and thanks to:

My mental support team
Agnes, William, Maike, Fransje, Irene, Carina, Jacintha

Min familj
Victoria, Caroline, Stefan

Louise Petersson
Göteborg, augusti 2019

Contents

Abbreviations

CMDD	Community Mapped Drainage Data
DS	Downstream
DTM	Digital Terrain Model
GPS	Global Positioning System
ICT	Information and Communication Technologies
ISO	International Organisation for Standardisation
JOSM	Java OpenStreetMap
HOT	Humanitarian OpenStreetMap Team (www.hotosm.org)
NGO	Non-Governmental Organisation
ODK	Open Data Kit Collect application
OSM	Open StreetMap (www.openstreetmap.org)
TAHMO	TransAfrican HydroMeteorological Observatory (www.tahmo.org)
TARURA	Tanzania Rural and Urban Road Agency
TURP	Tanzania Urban Resilience Program
UDSM	University of Dar es Salaam
US	Upstream
VGI	Volunteered Geographic Information

Dictionary

Swahili	English
ramani huria	open map
kata	ward/wards
mtaa	sub-ward
mitaa	sub-wards

Chapter 1

Introduction

Climate change and rapid urbanisation pose severe challenges to cities worldwide. Intensified precipitation and rising sea levels, in combination with expanding settlements in flood prone areas, cause an increased global flood risk. As of 2018, 55% of the world's population is living in urban areas, projected to rise to 68% in 2050 [65]. At the same time, at least 10% of the world's population is living coastal areas, less than 10 metres above sea level [1]. Many areas are still lacking the spatial data that is needed for disaster preparedness, disaster response and basic governance functions. This can be explained by the fact that geographic information, traditionally, has been expensive and technologically complicated to produce. Since the new millennium, however, it is increasingly available for anyone with Internet access to create geographic information. *Volunteered Geographic Information* (VGI) arose in the early 2000's, through projects like Open StreetMap (OSM), an online world map which can be edited by anyone [2].

The severe earthquake in Haiti in 2010 made the global development community realise the potential of VGI in resource-strained environments. Remotely located OSM volunteers could rapidly produce online maps of the affected areas in Haiti by adding features to aerial imagery, which guided the local disaster response [3]. Since, there is a growing scientific awareness that the added value of VGI in a certain context depends on its resources and the completeness of available data sets [4]. This thesis explores this further, by developing a flood model with drainage data collected by the community mapping project *Ramani Huria* in Dar es Salaam, Tanzania.

1.1 Problem statement

The current intensification of the hydrologic cycle, in combination with expanding settlements in flood prone areas, make an increasing share of the global population exposed to flood risks [1][5][6]. This calls for risk management and risk reduction. Many parts of the world are, however, still lacking basic geographical and hydrological data, given the traditionally high barriers to produce it. Furthermore, the urbanisation is so rapid in many areas that it is non-beneficial to carry out expensive surveys that soon get outdated [7].

1.2 General research motivation

The development of the user-generated *Web 2.0* and VGI has remarkably lowered the costs to collect the data needed to build flood resilience. The Internet has allowed for data abundant, rather than data scarce, platforms where geographical information can be produced and stored. In the last decade, the potential of VGI to fill crucial data gaps in resource-strained environments has been realised, which has accommodated the rise of *community mapping* projects to collect geographical and and hydrological data. The community mapping project *Ramani Huria* is, to the best of the author's knowledge, the only large-scale community mapping project in the world that has recorded the urban drainage system of a whole city. This drainage data can be used in hydrodynamic modelling to predict the flood impact of rain events, which, in turn, can support decision making, flood resilience plans, risk reduction and urban development. Now that this data is in place, it is of interest to investigate if community mapped data can contribute to flood risk management in resource-strained environments. Furthermore, it is of interest to examine if models built with community mapped drainage data can be used to detect causes of flooding.

1.3 Specific research motivation

Previous research has utilised drainage data that was collected by *Ramani Huria* in 2015 to build a flood model of Manzese ward in Dar es Salaam [8]. This study revealed that the drainage data was insufficient for reliable hydrodynamic modelling, as it only included the width and depth of cross sections, missed data on elevation of the drains related to ground level, and segments were missing or disconnected in the data set. Since 2017, *Ramani Huria* is applying a new mapping methodology, recording more detailed attributes of each drainage segment, and performs analyses of the consistency and connectivity of the drainage network. Therefore, it is of interest to examine if this improved data collection method can contribute to better flood predictions. Research has identified solid waste blockages in the drainage system as a potential amplifier of flooding in urban areas [9]. As Dar es Salaam is facing problems with solid waste management, it is also relevant to examine how this impacts the flood situation in the city.

1.4 Research objective

The main objective of this thesis is to investigate if community mapped drainage data (CMDD) can contribute to the understanding of floods in resource-strained environments. This will be examined by *model development* of a coupled 1D-2D hydrodynamic model of Kijitonyama ward in Dar es Salaam, utilising CMDD from *Ramani Huria* in the 1D schematisation. The model output will be validated with the local community's reports on flood depth from the modelled rain event. This information will be collected in a *flood extent survey*, using a methodology developed by *Ramani Huria*. Furthermore, the impact of solid waste in the drainage system on flooding will be investigated, by adding data on solid waste blockages to the model. Information on solid waste blockages in the study area will also be collected in a survey. This is referred to as the *model application* phase. It should be noted that the main focus of this thesis is to *develop* a model built with CMDD.

Being one of the first model schematisations built with CMDD, it is important to support local capacity building in Tanzania and knowledge transfer by producing a transparent workflow of the model setup. Hence, the first sub-objective of this thesis is to explore *how* hydrodynamic models can be built with CMDD. This result will be shared with the open data community for further exploration and development, and is summarised in appendix C. The second sub-objective is to examine if CMDD can contribute to better flood predictions on neighbourhood scale, and the third and final sub-objective is to investigate the impact of solid waste on flooding.

Table 1.1 summarises the research questions to be answered in this thesis.

Table 1.1: Research questions.

Main objective	Investigate if community mapped drainage data (CMDD) can contribute to the understanding of floods in resource-strained environments
Research questions	
1	Can community mapped drainage data improve flood predictions on neighbourhood scale? (Model development)
2	What is the impact of solid waste in the drainage system on flooding on neighbourhood scale? (Model application)

The research questions will be answered by running 6 scenarios in SOBEK 2.16, see table 1.2. The scenarios are explained further in section 5.3.

Table 1.2: Scenarios.

Phase	Scenario	Description
Development	**1**	Only 2D schematisation
	2a	Coupled 1D-2D model without adjusted bed levels (see section 5.1.6) and constant friction values
	2b	Coupled 1D-2D model with adjusted bed levels and constant friction values
	2c	Coupled 1D-2D model with adjusted bed levels and distributed friction values
Application	**3a**	Coupled 1D-2D model with segments blocked according to the results of the solid waste blockages survey
	3b	Experimental coupled 1D-2D model with a third of the culverts in a part of the study area being blocked

1.5 Thesis outline

Chapter 2 introduces a theoretical framework for the study by reviewing literature and concepts that are relevant for hydrodynamic modelling with CMDD. Chapter 3 aims to provide a thorough understanding of the case study, *Ramani Huria* community mapping project in Dar es Salaam. Chapter 4 presents all data sets that constitute the flood model, which is presented in chapter 5. Chapter 6 presents the results of the performed surveys and the model simulations. Chapter 7, 8 and 9 finish the thesis with discussion, conclusion and an outlook for future research.

Chapter 2

Theoretical framework

This chapter introduces a theoretical framework for the study by reviewing the strands of literature that are relevant for flood modelling with community mapped data. The chapter starts with exploring climate change and rapid urbanisation and how this leads to increasing flood risks globally. Then, the field of community mapping is described, and the chapter ends with the hydrologic principles and hydraulic theories that are applied in flood modelling.

2.1 Climate change and flood risks

Research has observed a global increase in temperature during the 20^{th} century, especially since the 1970's [10][11][12]. Even if the future trend of temperature changes is uncertain, there is a consensus prevailing that continued future warming is 'very likely' [13][14]. The theoretical implication of increased temperature on the hydrologic cycle[1] is described by the *Clausius-Clapyeron* relation, stating that maximum atmospheric moisture content increases with temperature [13][15][16]. This, in turn, is anticipated to cause an intensification of the hydrologic cycle, increasing the rate of precipitation, evaporation and runoff [17]. Huntington [13] gathers scientific evidence of hydrologic variables that confirms this anticipation; precipitation over land increased about 2% on a globally averaged basis from 1900-1998 [18][19]. The world continental runoff from major rivers increased about 3% from 1910-1975 [20][21]. Researchers do, however, note that the effect of increased global precipitation on runoff varies greatly over different climate zones; runoff is likely to increase in high altitudes and equatorial regions, but decrease in mid-latitude and some subtropical regions due to increased evaporation [22][23][24]. Extreme hydrological conditions are expected to be intensified, leading to extreme droughts followed by severe flooding in many areas [17].

This intensification of the hydrologic cycle poses challenges to an urbanising world. As of 2018, 55% of the world's population is living in urban areas, projected to rise to 68% in 2050 [25]. The fastest urban population growth until 2050 is expected to arise in Sub-Saharan Africa [26][27]. Hanson et al. [5] note that 13 out of the 20 most populated cities in the world as of 2005 were port cities. These cities form a crucial component in the global economy but are at the same time vulnerable to extreme coastal water level events and subsidising soils, especially in delta regions. McGranahan et al. [1] show that 10% of the world's population is living in the Low Elevation Coastal Zone, that is the area along the coast that is less than 10 metres above sea level. They note that coastal populations are at risk of flooding, particularly when high tides combine with storm surges and/or high river flows. This risk is exacerbated by certain features of urban development; built-over land increases runoff peaks due to decreased infiltration capacity of the soil, and drained wetlands remove buffers against tidal floods [1].

[1] The hydrologic cycle is explained in section 2.3.1.

The European Union Floods Directive [28] defines a *flood* as ”*the temporary covering of land not normally covered by water*”. Three flood types can be distinguished in literature; *coastal-*, *river-* and *flash floods* [29][30]. Jonkman [6] also adds *drainage problems* to the classification, which can also be labelled *pluvial flooding* or *sewer flooding* [31]. The different flood types are described in table 2.1.

Table 2.1: Flood types and their causes. After Jonkman [6].

Flood type	**Flood cause**
Coastal floods/storm surges	Wind storms and low atmospheric pressure cause set-up of water levels on the coast.
Flash floods	Occur after local rainfall with high intensity (convective storms), leading to a quick level rise of water bodies. The time available to predict flash floods in advance is limited.
River floods/fluvial floods	Flooding of rivers outside their regular boundaries. Caused by high precipitation levels (not necessarily in the flooded area), melting snow or blockage of the flow. Extreme river discharges can generally be predicted in some period in advance.
Drainage problems/pluvial floods	Floods independent of overflowing water bodies. Caused when the runoff caused by rainfall exceeds the conveyance capacity of the drainage system at the location [31].

Floods caused by insufficient drainage capacity, pluvial floods, are of certain interest in this thesis. The study area chosen for the study is mainly exposed to pluvial floods, see section 3.3. Jonkman [6] states that pluvial flooding mainly causes economic damage and normally does not pose threat to human life due to limited water levels. The topic has nonetheless gained more attention in recent years, as the globally increasing urbanisation results both in more runoff and more properties at risk, which would be aggravated by intensified precipitation [31][32]. Further consequences of pluvial flooding are exposure to contaminants in stagnant water and severe disruption of transportation networks, causing potentially life-threatening indirect effects [33][34][35]. Pluvial floods can further be intensified by elevated sea levels in coastal areas due to backwater effects in the drainage infrastructure, or due to substantial groundwater infiltration [36][37].

Several definitions of flood risks can be found in literature. The European Union Floods Directive [28] states that *flood risk* means “*the combination of the probability of a flood event and of the potential adverse consequences for human health, the environment, cultural heritage and economic activity associated with a flood event*”. Alternatively, it can be determined by three parameters: the probability of occurrence of an event, the amount of people and assets that would be directly impacted by the event, and the vulnerability of the exposed population and assets [32]. Butler [31] argues that pluvial flood risk management has moved from a probability-based approach, considering only the *likelihood* of a flood event in the design of urban drainage systems, towards a risk-based approach, where both the probability *and* the consequence of a flood is concerned. This tendency is reflected in the European Union Floods Directive [28].

It is evident that flood risks are of a very multi-faceted character. Ostrom [38] argues that problems caused by climate change traditionally are conceptualised as ”global” problems, but are, in fact, ”*the cumulative result of actions taken by individuals, families, small groups, private firms, and local, regional, and national governments*” [38]. Hence, the solving of flood problems requires collective action. Conventional collective-action theory predicts that no institutions or individuals will voluntarily change their behaviour to overcome the challenges of climate change, even if individual actions would contribute to the common good. Instead, external authorities like global-level institutions must impose sanctions and incentives for change. Contrarily, Ostrom argues that it is better to encourage *polycentric* efforts to reduce risks imposed by climate change. Socio-ecological systems are often relying on a distribution of responsibilities across different scales, which requires multilevel decision making and information exchange. This seminal work has triggered an increasing scientific awareness that polycentric governance is beneficial in natural resources management [39].

Within water resources, the traditional sectoral and fragmented approach to water resources management has often led to governing bodies with conflicting interests [40]. Catchments are formed according to geophysical characteristics and do not respect administrative boundaries. Hence, the field of *integrated water resources management* has emerged since the 1990's, incorporating polycentric decision making and practices. *The Dublin principles* were formulated at the International Conference on Water and the Environment in Dublin in 1992, where principle number 2 states that "*Water development and management should be based on a participatory approach, involving users, planners and policymakers at all levels*"[40]. This approach is reflected in the case study of this thesis, see chapter 3.

The principle of polycentric governance is also reflected in the *Sendai Framework for Disaster Risk Reduction* [41], adopted in 2015. It dictates that there has to be a more *"people-centered"* approach to disaster risk reduction, where governments should engage with relevant stakeholders, including groups like women, youth and poor. This is especially relevant in developing countries, where the mortality and economic losses from disasters are *"disproportionately higher"* [41]. It states that this requires open exchange of data, which should be easily accessible, up-to-date and science-based, complemented by traditional knowledge.

In the last decade, the development of Internet and smartphones have made public participation in monitoring, data collection, planning and decision making possible in a way that has never been accessible previously. Paul et al. [39] show how a polycentric approach is beneficial over a monocentric, both in pre-disaster, in-disaster and post-disaster management. They argue that a participatory approach to data collection can support multidirectional information provision and enhance hydrological risk reduction. Mc Granahan et al. [1] state that most of the data needed for flood risk management is found at the local scale, and that the lead time of top-down implemented environmental policies are usually too long to decrease the vulnerability of people living in flood prone areas. One way of involving citizen in data collection for building disaster resilience is the emerging field of *community mapping.* This will be described in the next section.

2.2 Volunteered Geographic Information

Community mapping is the action of producing a map together *with or by* the residents of a certain location, often featuring local knowledge and resources [42]. It can be understood as a form of *Volunteered Geographic Information* (VGI), a term coined by Goodchild in 2007 [43]. Being the very first notion of this emerging field, it is worth quoting here;

> They [the mapping volunteers] are largely untrained and their actions are almost always voluntary, and the results may or may not be accurate. But collectively, they represent a dramatic innovation that will certainly have profound impacts on geographic information systems (GIS) and more generally on the discipline of geography and its relationship to the general public. I term this *volunteered geographic information* (VGI), a special case of the more general Web phenomenon of user-generated content...[43].

VGI, in turn, can be seen as *crowdsourcing* of geospatial information. Felstiner [44] defines crowdsourcing as "*the act of taking a job traditionally performed by a designated agent (usually an employee) and outsourcing it to an undefined, generally large group of people in the form of an open call.*" Examples of crowdsourced data are Wikipedia[2], the free online encyclopaedia, and Open StreetMap[3] (OSM, see section 2.2.2), an online world map which can be edited by anyone [2]. The field of VGI, as defined by Goodchild, has emerged as a consequence of *Web 2.0*, that is the development of the user-generated World Wide Web [43][45]. Since the early 2000's, it is increasingly available for anyone with Internet access to create geographic information, which was accommodated by several coincides around the new millennium. The Global Positioning System (GPS) was fully operational in 1995, implemented by the US Department of Defence, and the selective availability of the GPS signal was removed in the year 2000. This gave way to affordable GPS receivers, and home computers and user-generated websites

[2]www.wikipedia.org

[3]www.openstreetmap.org

were on the rise [7]. VGI has put mapping, a task that for centuries has been reserved to official agencies, in the hands of anyone that want to contribute to online maps [46]. This section will introduce different forms of VGI, namely geographical citizen science, crisis mapping and community mapping. This will support the framing of the case study in this thesis, the *Ramani Huria* community mapping project, see section 3. Figure 2.1 depicts the relation between the concepts described in this section.

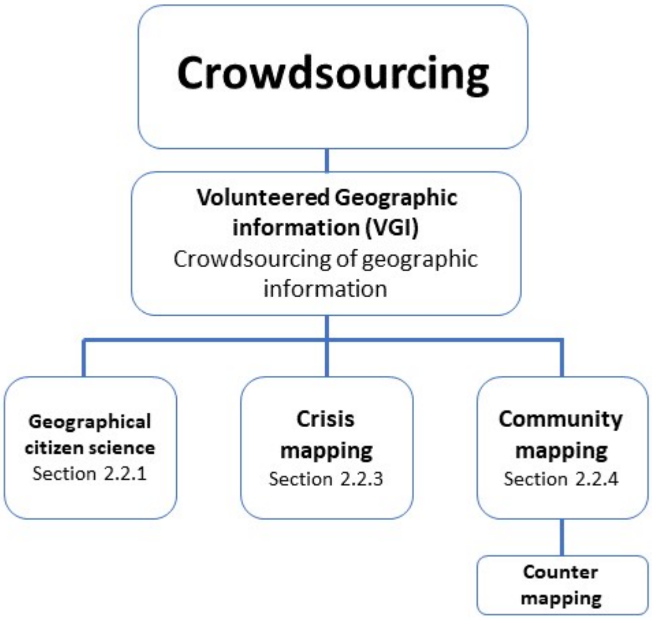

Figure 2.1: Forms of VGI.

The review of VGI is outlined as follows. Section 2.2.1 introduce the broader field of *citizen science*, where VGI is frequently applied. Then, OSM will be introduced in detail in section 2.2.2. Section 2.2.3 describes the Haiti earthquake in 2010, as it profoundly affected the further development of OSM, and realised the potential of web-based community mapping in data scarce, resource-strained environments. This affects the power of maps, as will be illustrated in section 2.2.4. Section 2.2.5 and 2.2.6 discuss the quality and authority of VGI data, which leads to a framework for community mapping in developing countries, described in section 2.2.7.

2.2.1 Citizen science

Depending on the level of participation of the mapping volunteers, VGI can be described as a form of *citizen science* [47]. This is science where non-professionals are involved in data collection, but also in other parts of the research process. Specifically, VGI can be seen as a form of *geographical* citizen science, as the location of data points is an integral part. Haklay [48] define a framework that classifies the level of participation in citizen science activities, see Figure 2.2.

At the first level, the participants merely serve as sensors and provide data to scientists by collecting information. Haklay labels this as 'classic' citizen science, as it has been around long before the rise of VGI, for example as crowd-sourced bird counts or rain gauge monitoring. The second level, *distributed intelligence*, makes use of the participant's cognitive ability. It can include both data collection and basic data processing and analysis by the participants, and usually includes basic training and tests to check the quality of the participant's work. At the third level, the problem definition is set by the participants, and a data collection method is formulated with scientists and experts. The participants are then included in the data collection, but require expert assistance to analyse the results. Examples of this can be found within environmental justice campaigns, where communities gather scientific evidence to set action plans for an environmental conflict. The fourth level is labelled *extreme citizen science*, where participants potentially can be involved in analysis, publication and utilisation of the results. Paul et al. [39] argue that this method is not widely accepted in the academic world, as it requires involvement of scientists on a profound level regarding the social and ethical aspects of their work.

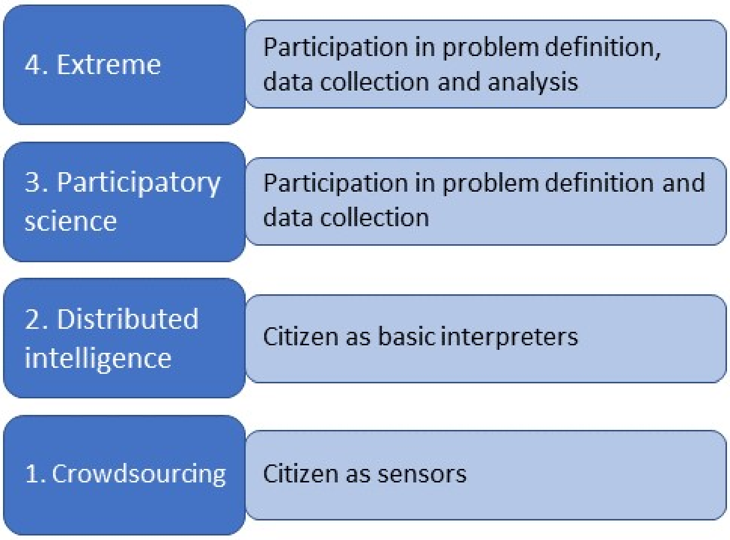

Figure 2.2: Levels of participation in citizen science. After Haklay [48].

Haklay [48] notice that participants can move up and down the participation ladder within a research project, especially if it spans over a long period of time. Furthermore, he notes that it is not clear which projects that should be labelled citizen *science*. Even if data collection in OSM is not carried out for a scientific purpose, he notes that it is a process producing verifiable results, using scientific instruments like aerial imagery and GPS receivers, and that it in its essence do not differ from what professional cartographers have done for centuries. He concludes that a geographical citizen science project focus on *recording* observations, rather than locating community views or reporting events, which leaves OSM being a crowd-sourcing citizen science project.

VGI has been accommodated by the development of information and communication technologies (ICT) in the last decade. The earliest examples of large-scale, digital VGI projects, dating around 2010 (see section 2.2.3 and 2.2.4), made use of stand-alone GPS devices and home computers. Only ten years later, smartphones are now equipped with sensors like mobile network, FM and GPS receivers, camera, accelerometer, compass and microphones, making them suitable for scientific data collection [48]. Davids et al. [49] suggest that smartphone-based data collection activities should be a part of science and engineering curricula, aiming for standardised data collection methods and open access. In their research, they engage second- and third-year engineering bachelor's degree *student citizen scientists*.

Having outlined the general concept of citizen science, the review continues with describing OpenStreetMap (OSM) in more detail, as it is a main online platform in the case study of this thesis.

2.2.2 OpenStreetMap

OSM was founded by Steve Coast at University College London in 2004, intended to be a free world map. Haklay and Weber [7] argue that the motive of OSM is to provide accurate, digital geographical information, which, in Europe, is "*considered to be expensive and out of the reach of individuals, small businesses, and community organizations*". This initial motive has later been accompanied by the potential of OSM to cover spatial data gaps in resource-strained environments, as will be illustrated below. Haklay and Weber [7] also highlight that OSM have an advantage over national mapping agencies in that it allows for rapid geospatial changes, where commercial geographical information products are too expensive to apply in regular update surveys.

The OSM website, *www.openstreetmap.org*, contains four parts, see Table 2.2. Only registered users can edit the online map, which makes it possible to trace the information source in case of copyright disputes [7]. The basic object types in OSM are *nodes* and *ways* [2]. This thesis will use the terms *nodes* and *segments*, as this is the terminology used in the *Ramani Huria* community mapping project, see chapter 3. Nodes are described by a single coordinate (*geopoint*), and segments by a list of nodes on a line (*geotrace*). The objects are assigned with *tags*, describing attributes of the objects [43]. The tags consist of a *key* and a *value*. The objects can either be mapped remotely by digitising features from aerial imagery, or be collected in the field with mobile GPS devices.

Table 2.2: OpenStreetMap features. Based on Haklay & Weber [7].

Feature	Description
Map interface	Allows users to inspect the OSM world map in its current state, see Figure 2.3
OSM *wiki*	Contains guidance on appropriate mapping practices and documentation of the technical infrastructure of OSM, *https://wiki.openstreetmap.org*
Edit function	Allows users to upload map features or correct errors on the map
Export function	Allows users to download all current raw OSM data within a specified area in an XML format for further application or processing

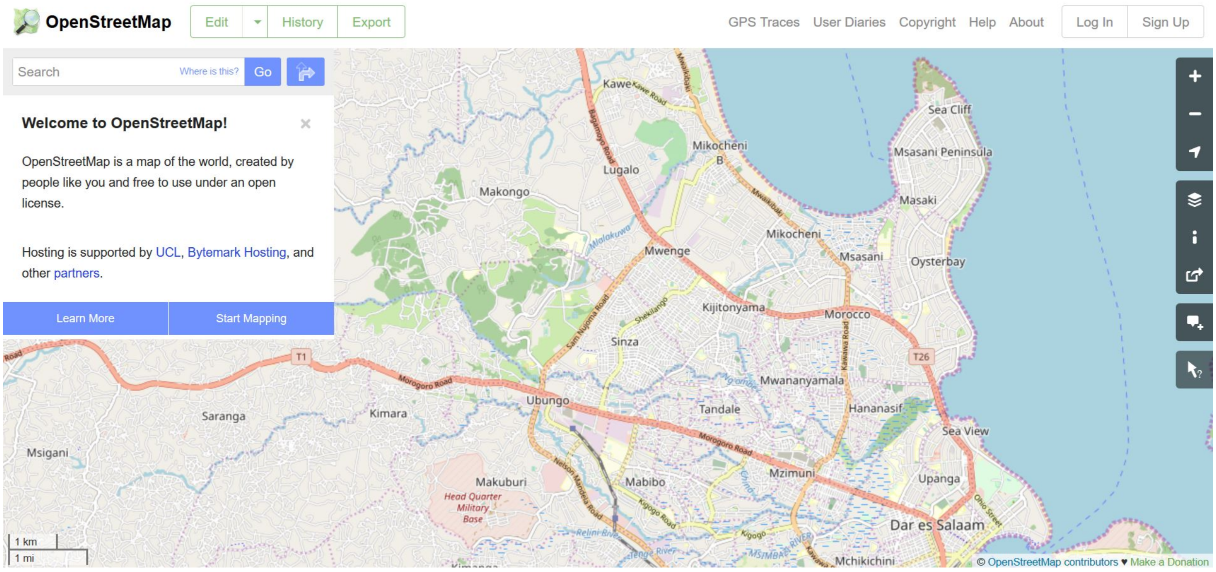

Figure 2.3: OpenStreetMap, www.openstreetmap.org, as of April 2019. The map is showing the northeastern parts of Dar es Salaam.

The OSM web site offers a basic export function, where all objects within a specified area can be downloaded as *.osm*-files. More refined export tools with additional functions are also available, for example the HOT Export Tool[4], where the data can be downloaded as *.shp*- or *.gpkg*-files. The OSM web site contains a simple online editor where users can add, update, or delete objects on the map [7]. More extensive editing and analysing can be performed in the desktop editor Java OpenStreetMap (JOSM). It offers functionalities such as linking OSM features to photos and audio notes and is supported by several plug-ins. JOSM requires internet connection to download and upload OSM data, but the editing can be done offline [50]. Figure 2.4 depicts the JOSM interface.

2.2.3 The rise of crisis mapping

The Haiti earthquake of 12 January 2010, causing the death of least 230'000 people [51], marks a turning point in the history of VGI. The available spatial data of Haiti at the time was not detailed enough to guide the disaster response; road maps and information on critical assets, infrastructure and buildings were absent, which disabled the logistics of humanitarian aid work [45]. As a response, satellite imagery companies produced high-quality aerial images of post-earthquake Haiti and made them available online within 24 hours after the event [45][3]. Still, these images were lacking the geographic information (tags) needed to create useful disaster management maps, a process that would

[4]export.hotosm.org

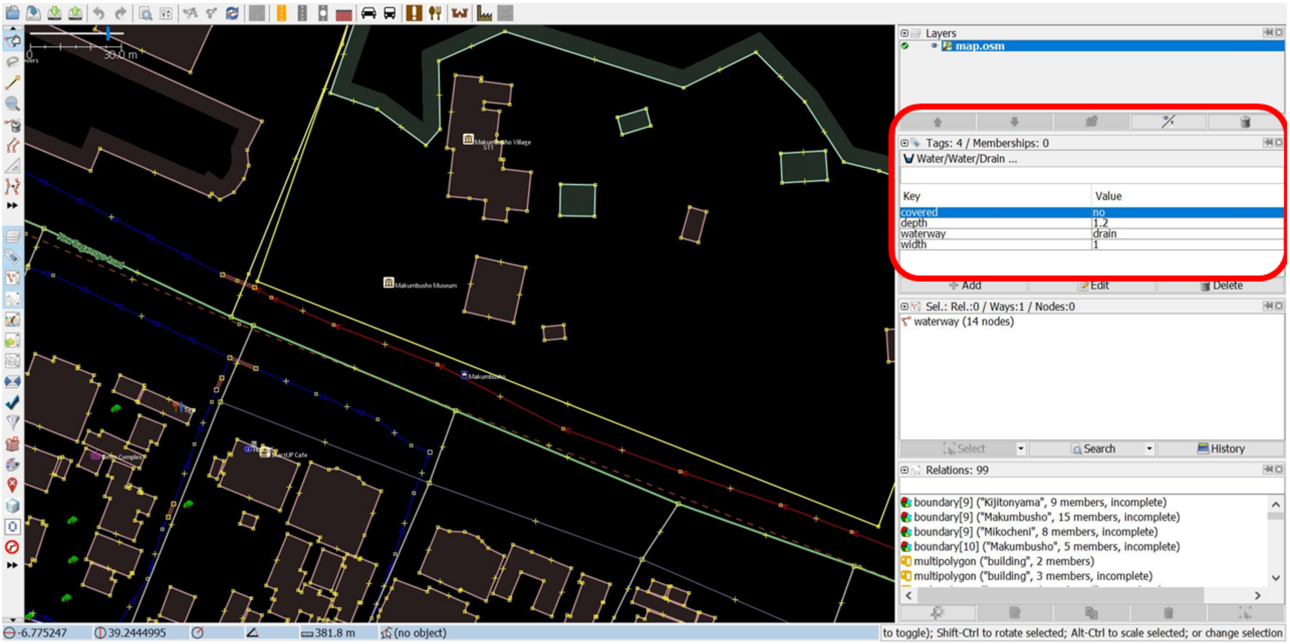

Figure 2.4: Data dowloaded from OSM, opened in JOSM. To the right the tags of the selected feature (highlighted in red) are displayed; it is a covered drain that is 1.2 m deep and 1 m wide.

take years to accomplish for professionals to cover an area of Haiti's size [45]. At this point, people and organisations around the world realised that geo-tracing could be done remotely, using online tools. OSM was already well-established as a community, but held only a fraction of the road network on Haiti, and had never been applied in a large-scale organised humanitarian aid effort. The year before the earthquake, at the annual OSM conference *State of the Map* in July 2009, the potential of open data in humanitarian and development work had been addressed [3]. Now, OSM volunteers downloaded the released aerial images, traced the outlines of streets, buildings and assets, and uploaded the traced objects to the OSM server. This was complemented by volunteers present in Haiti, who could add tags with additional information to the features, using mobile GPS devices [45]. The OSM data was used by, among others, United Nations agencies to operate the logistics of the disaster response [3].

This process was the result of a strategy developed by a few members of the OSM community, that later was institutionalised as the Non-Governmental Organisation (NGO) Humanitarian OpenStreetMap Team (HOT)[5]. A full description of the foundation of HOT in the aftermath of the Haiti earthquake is given by Soden & Palen [3]. Since this, HOT is developing methods to produce open data in data scarce environments. This includes mapping technologies, as will be described in the case study of this thesis (see section 3.2.2), but also social events that enhance data collection. *Mapathons*, for example, gather volunteers that bring their own laptops and contribute to a designated mapping task in the *HOT tasking manager*[6]. The tasks can be proactive, or serve as a direct disaster response, as was the case during the Haiti earthquake, and several disasters since [52]. In 2012, Ziemke [53] notes the rise of *crisis mapping*, that has been sparked by handheld GPS units, OSM and increasing Internet accessibility.

2.2.4 The power of maps

The Haiti earthquake shows how many resource-strained environments still are lacking vital spatial information. This has consequences not only for disaster management, but for the capacity of all types of governance. Harley [54] argues that mapping is not a neutral process, but rather a reflection of the perceptions of the individuals that perform it. Throughout history, the access to maps and mapping technologies has only been available to a usually privileged and powerful elite. Maps are, hence, a product of power and produce power [55]. This argument was, however, formulated in 1989, when mapping still was a privilege reserved for national mapping agencies. Now that the hegemony of these

[5] www.hotosm.org
[6] https://tasks.hotosm.org

agencies is challenged through the rise of VGI, the power of maps is changing. This can be illustrated by the community mapping project *Map Kibera* in the informal settlement Kibera in Nairobi, Kenya. The project was launched in October 2009 by local OSM contributors that realised that Kibera, being home to more than one million people [56], was not included on OSM or any other online map. Kibera was, however, frequently surveyed by foreigners for academic purposes, but the results of these mapping efforts were not available to the residents of Kibera [57].

Governance requires maps. Kibera is facing problems like poor sanitation, lack of facilities of water, electricity and sewage, which require spatial information to be understood, analysed and solved. The required data includes, for example, locations of water points, electric lights, toilets and clinics [57]. The *Map Kibera* project realised that this information could be collected by the local community and uploaded to OSM. The project started by recruiting 13 young people, one from each village in Kibera, training them for two days in using GPS devices and OSM, and then let them spend three weeks mapping their home villages - Kibera was now put on the map for the first time. Today, *Map Kibera* is a community information project that includes ongoing digital mapping and citizen journalism [57] and is supporting the initiation of community mapping projects in other locations. One of the projects that *Map Kibera* have supported is *Ramani Huria* in Dar es Salaam which is studied in this thesis, see chapter 3. As of April 2019, the *Map Kibera* blog was last updated on November 9$^{\text{th}}$, 2018, reporting on how the government demolishes schools in Kibera, illustrating the spatial impact of the demolitions on a map[7]. This type of reporting can be seen as *counter mapping*, a 'political act' [58] aiming to counter elitist cartography, carried out by communities to represent themselves and stake claims to resources [42]. There are, however, examples of community mapping projects that involve local authorities, see section 2.2.7.

Kibera is one of the earliest examples of community mapping in the digital era, as it produces maps *with and by* the residents of Kibera. The project shows that maps no longer are tools to purely manifest power, as argued by Harley [54], but that they have the capacity to *empower* local communities, thanks to the rise of Web 2.0 and VGI. Community mapped data can support residents to address local problems in areas where data acquired by qualified agencies for any reason is missing. This raises questions about the quality and authority of VGI data, which will be addressed in the following sections.

2.2.5 Quality of VGI

The quality of geographic information is traditionally assessed according to quantitative quality measures from the International Organisation for Standardisation (ISO), see Table 2.3. VGI is, however, produced by heterogeneous contributors, using different tools and platforms, with different levels of detail and precision [59]. This lack of standardisation introduce errors and variable quality of VGI data sets. Many researchers have analysed the quality of OSM data, comparing it with spatial data from national mapping agencies [60][61][62][63]. Haklay [60] labels the OSM road data in London as "fairly accurate", as it has a 80% overlap with road data from the official Ordnance Survey. Studies in Sweden [64] and Germany [65] show a "good" coherence of OSM and authoritative road network data.

Table 2.3: Quality metrics of geographic information quality according to ISO/TC 211. After Senaratne et al. [59]. *http://www.isotc211.org/*

Quality metric	**Definition**
Completeness	Describes the relationship between represented objects and their conceptualisations, either as absence of data (errors of omission) or presence of excess data (errors of commission)
Consistency	Coherence of the data structure
Accuracy	Refers to the degree of closeness between a measurement of a quantity and the accepted true value of that quantity. This can be positional accuracy, or thematic accuracy, referring to consistent attributes and classifications.

[7] http://www.mapkibera.org/blog/2018/11/09/the-plight-of-schools-demolished-in-kibera/

The quality assurance provided by traditional mapping agencies consists of procedures to control quality during the data acquisition, and by comparing samples of the compiled data with reference sources. While the studies outlined above focus on the latter procedure, Goodchild & Li [66] suggests that quality of VGI data can be improved by focusing on measures during the acquisition phase. They highlight the ability of groups to perform extensive validation and cross-checking of data collected by individuals. The validity of an observation can be strengthened by additional observations from the same or nearby points. Several researchers refer to *Linus' law* [66] [67] [59], predicting that the efforts of a crowd will converge to the truth. *Linus' law* comes from the context of software engineering and the experience that the bugs in a piece of software are most likely to be found and corrected if a large number of engineers has access to it and can review it. Goodchild & Li [66] note that the success of this law in the OSM context depends on the number of contributors and their interest in the mapped area, especially when it comes to tagging the mapped features. Other possibilities to assure VGI data quality is to introduce moderators and gatekeepers, that is individuals promoted with special privileges to delete and protect content based on their previous contributions, or data mining such as outlier detection and cluster analysis [59].

It is noteworthy that the majority of all studies on quality of OSM data has been carried out in Europe [68]. One of few exceptions is Iliffe [50] that analyses OSM road data in Tandale ward in Dar es Salaam, in terms of positional accuracy and completeness. The results show that all roads in the OSM data set lie within a 10 m buffer zone of the road data provided by the Dar es Salaam City Council (DCC). Furthermore, the OSM data holds a much more extensive road network than the DCC data set. This can not be seen as errors of commission (see Table 2.3), but is a consequence of the fact that the official map held by the ward officer was outdated and did not contain all roads in Tandale ward [50].

2.2.6 A new understanding of authority

It is evident that the traditional understanding of authority of geographic information is challenged by the rise of VGI, and that the understanding of authority depends on available resources in different contexts. If OSM data is perceived as non-authoritative in contexts where detailed geographic data from national mapping agencies is present, but is proved to be more extensive and as accurate as official data in Tanzania, the mechanisms that make a data set authoritative must be outlined. This will contribute to the understanding of the value of VGI in resource-strained environments.

Literature makes a distinction between *authority* and *credibility*. *Authority* is defined as the "*power or right to give orders, make decisions, and enforce obedience*" [69], whereas *credibility* is defined as "*the quality or state of being credible; capacity to be believed or believed in*" [70]. Put differently; authority can be *given* or assigned to an institution, but credibility is *earned*. Flanagin & Metzger [46] summarise attributes that traditionally have given credibility to national mapping agencies, see table 2.4. They note that the credibility of these agencies arose in an era of data scarcity; when the costs and barriers to collect geographic information were high, allowing mapping agencies to serve as *gatekeepers* and filter the available information. These official mapping agencies have an incentive to maintain their credibility by assuring high data quality.

Table 2.4: Traditional indicators of credible data. After Flanagin & Metzger [46].

Indicator	Attributes enhancing credibility of geographic data
Quality	Completeness, consistency and accuracy, see table 2.3
Meta data	Transparent documentation of information sources and acquisition methods
Accountability	Clear responsibility for the data quality assurance
Gatekeepers	People with incentives to uphold high quality standards, either to maintain good reputation or out of economic interest

Contrarily, the user-generated Web 2.0 consists of data *abundance*, making the indicators in table 2.4 difficult to fulfil. As shown, researchers suggest how the practices around VGI can be improved to assure VGI data quality [66][59], which presumably can be extended to practices on meta data documentation and accountability transparency. On the other hand, it can be argued that the premise of data scarcity underlying the indicators in table 2.4 is no longer true, thanks to the rise of Web 2.0 and VGI. It can, hence, not be concluded that data sets are not credible if they do not fulfil these indicators. Instead, the framework for credible data sets must be reformulated and adjusted to an era of data abundance and low barriers to produce geographic information. Flanagin & Metzger [46] argue that this era has uncoupled credibility from authority, which may lead to a *"shift from a model of single authority based on information scarcity and hierarchy, to a model of multiple distributed authorities based on information abundance and networks of individuals"* [46].

The data abundant Web 2.0 seems to add different assets depending on the available geographic information in a certain context. The added value of VGI in planned, mapped and industrially advanced areas lies in endemic knowledge about the physical environment, and current information about local conditions [46]. But in contexts where authoritative data sets are incomplete or absent, VGI has the potential to, additionally, fill gaps of data needed for basic governance. This makes Iliffe [50] draw the conclusion that a different framework must be applied for community mapping in developing countries, which is presented in the next section.

2.2.7 A framework for community mapping in developing countries

Iliffe [50] developed his framework by studying *Ramani Tandale*, a community mapping project carried out in 2011 in Tandale ward in Dar es Salaam. *Ramani Tandale* will be described in more detail in section 3.2.1. The results show that community mapping enables the collection of VGI to a quality and extent previously unseen in industrially developing countries. The framework is depicted in Figure 2.5 and its components are explained below.

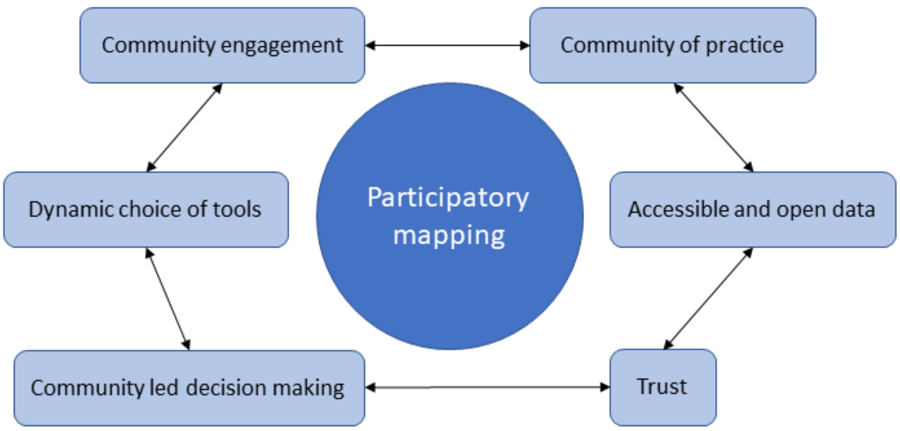

Figure 2.5: A conceptual framework of community mapping. After Iliffe [50].

Community engagement

Community forums are essential to community mapping. In *Ramani Tandale*, open community forums were held at the Tandale ward office, attended by representatives from the local government and community members[8]. The forums can support awareness of the mapping activity, discussions on mapping priorities and methods, and also present results and maps to the community.

Community of practice

Community mapping is composed of many different communities, which all have different objectives. This includes the community being mapped, but also civil society, local or national government, and national or international non-governmental organisations. Together they form a *community of practice*, coalescing around the community being mapped.

[8]https://matharevalley.wordpress.com/2011/08/09/community-mapping-starts-in-tandale-dar/

Community led decision making

The priorities of what is being mapped, and how, is led by the community itself. Methods can initially be demonstrated by *catalysts*, with some community members becoming catalysts during the mapping process, supporting the next iteration and sustainability of community mapping.

Trust

As the data is collected by the community for the community, Iliffe [50] argues that this generates authority of community mapped data. The following quote from an interview with the town planner for Kinondoni Municipality and the ward executive officer of Tandale illustrates this argument[9]:

> **Mark:** "In your professional opinions, is this data [community mapped data from *Ramani Tandale*] authoritative?"
> **Juliana:** In my professional opinion, yes, because this is really data [...] this is the best map, this is the recent best map ever for this area, so I think this is really official and because it belongs to the community, and whenever you want to succeed in the community, like us, we are local authority, we are working with the community. You have to work with the community at the best, and they have to understand you, they have to appreciate you, and they have to be really onboard with you while planning for them. This is what will take them there.
> **Osiligi:** I can say that this is the real picture of Tandale, so it should get all the blessing from the government, or any other authority, because very precisely it shows everything and it reflects the real picture of the area. There is not any lying here. I do think that the authorities which bless this to be used by anyone should do it immediately without questioning, because it is the real fact about the places where you took the pictures, and it's going to help us ([50], p. 214).

Accessible and open data

The data from community mapping and the materials produced from it need to be accessible as open data.

Dynamic choice of tools

The data collection methods must be comprehensible for the members of the mapping community, especially with regards to their experience with ICT.

2.3 Flood modelling of urban areas

In this thesis, community mapped data is applied to develop a flood model. The model setup is described in chapter 5. This section introduces the hydrological processes and hydraulic theories that are applied in flood modelling.

2.3.1 The urban hydrologic cycle

A hydrologic model is an attempt to represent the *hydrologic cycle*, which describes how water circulates through the hydrosphere, see figure 2.6. The cycle has no beginning or end; water *evaporates* into the atmosphere, where it is transported as water vapour until it condenses and *precipitates* on the land and the oceans [71]. Precipitation on land is followed by several hydrologic processes; the water may be *intercepted* by vegetation, *infiltrate* deep into the ground and recharge the ground water storage, flow through the unsaturated zone in the soil as *subsurface flow* or discharge as *surface runoff*. This thesis is focused on *urban hydrology*, that is, the water cycle in urban environments. Here, the surface runoff is of certain interest, as this hydrologic process causes inundation of infrastructure and properties. As will be illustrated in the next chapter, it can also have life-threatening consequences.

Urbanisation is followed by *land use change*, and the ground is often covered with artificial surfaces like asphalt or bricks. This increases the amount of surface runoff in relation to infiltration. As water travels faster over hard surfaces than natural surfaces, the precipitation reaches downstream water courses faster in urban areas than in natural systems. This increases the *peak flow* of the water, and therefore also the inundation [31]. This effect can be reduced by the construction of *drainage systems*

[9] The interview is recorded and available here: https://www.youtube.com/watch?v=TdPdO7EWCxot=3s

that lead the surface water in drains to the closest water course, rather than over land. This thesis is developing a model of an urban drainage system utilising drainage data that has been collected with a community mapping approach, see chapter 3.

2.3.2 Model concepts

Hydrologic models can be used to predict the behaviour of the processes described above. This can be done through extrapolation of knowledge of a certain water system, either in space to other catchments with similar properties, or in time. Hydrologic models can also be used to design artificial experiments to predict system response to changes in system characteristics, such as land use change or intensified precipitation. Gharari [72] argues that it should be "from the highest interest for decision makers to understand the effect of their decision on hydrological behaviour and therefore the future status of a system". A *flood model* can be seen as a hydrologic model specifically aimed at predicting the spatial distribution of the water depth that appears for a certain rainfall event.

The performance of hydrologic models is dependent on data availability. Long-term measurements of precipitation and discharge, *time series*, are important data sets that serve as forcing and validation data in hydrology. The models contain *parameters* that describe the relations between the fluxes in the hydrologic cycle, such as the infiltration capacity of the soil and the evaporation rate. The parameter values can either be assigned via measurements, or be calibrated if no data is available. In that case, an appropriate *parameter range* must be set for the calibration process. The models also contain *boundary conditions*, that is known values at the border of the model space. This can, for example, be measured discharge in a stream that flows into the area of interest, or a known water level in a river. This value limits the possible solutions to the differential equations that are solved in the model computation, see section 2.3.3 below.

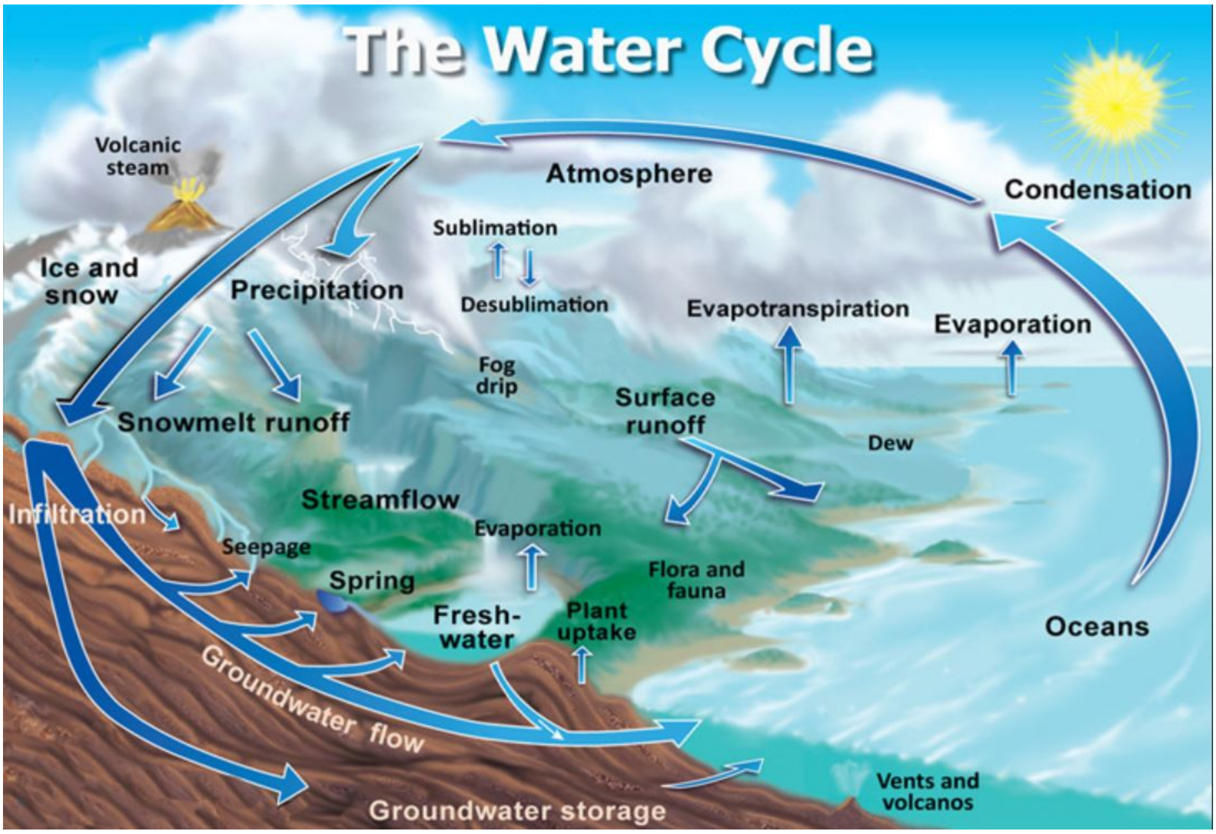

Figure 2.6: The water cycle. By John Evans and Howard Periman, USGS - http://ga.water.usgs.gov/edu/watercycle.html, Public Domain, https://commons.wikimedia.org/w/index.php?curid=26818355.

This thesis develops a *physically-based* model, which consists of finite elements that represent physical entities of the modelled area. A *1D schematisation* consists of nodes and links that represent, for example, drain segments or small natural water courses. A water course can be represented in a 1D schematisation if it is realistic to assume that the velocity distribution over each channel cross-section is uniform, which is usually the case in urban drainage systems [31]. Here, attributes such as cross section dimensions and construction material are assumed to be constant for each model element. A *2D schematisation*, on the contrary, can capture lateral variations in the velocity field, which is suitable when predicting how surface runoff distributes on a flood plain. Here, each model element is a *grid cell* with constant parameter values for e.g. soil infiltration and land roughness. A *coupled 1D-2D model* simulates the interaction between 1D and 2D model components, like a urban drainage system and its surrounding topography. The intersection of the grid cells are *computational nodes* where the differential equations presented in section 2.3.3 are solved [31].

Physically-based models can be *lumped*, where all model elements are assumed to have the same parameter values, or *distributed*, where the parameter values are different in each grid cell [71]. Lumped models can be applied if no distributed data is available, or if it seems reasonable that a distributed representation of the parameters will not give more accurate model output. This depends, for example, of the grid cell size i relation to the size of the model space. Distributed models require more computational power and introduce the risk of *equifiniality*, when the same model output can be obtained with different parameter sets, which challenges the causal mechanisms of the model [73]. On the other hand, they offer spatially distributed results, which is of interest when modelling flood depth in urban areas.

2.3.3 Hydraulics

The modelling software used in this thesis, SOBEK (see chapter 5), allows for coupled 1D-2D modelling of unsteady flow, that is, flow that varies over time. The distribution of surface runoff is calculated in each computational node for each time step by solving the so-called *Saint-Venant equations*, stating the conservation of mass and momentum in space and time [31]. The continuity equation in 1D reads

$$\frac{\delta A}{\delta t} + \frac{\delta Q}{\delta x} = 0 \qquad (2.1)$$

where [74]

$A(x,t)$	total cross-sectional area of water course [m^2]
$Q(x,t)$	discharge [m^3/s]

and the momentum equation in 1D, x-direction

$$\frac{\delta Q}{\delta t} + \frac{\delta}{\delta x}\left(\frac{Q^2}{A_F}\right) + gA_F\frac{\delta \zeta}{\delta x} + \frac{gQ|Q|}{C^2RA_F} - w_f\frac{\tau_{wind}}{\rho_w} + gA_F\frac{\xi Q|Q|}{L_x} = 0 \qquad (2.2)$$

where[10]

[10] SOBEK user manual, version 1.00

A_F flow area [m^2]
C Chézy coefficient [m$^{1/2}$/s]
g gravitational acceleration [m/s^2]
ζ water level [m]
L_x length of branch segment [m]
Q discharge [m^3/s]
R hydraulic radius [m]
t time [s]
w_f water surface width [m]
x distance along the channel axis [m]
ρ_w density of fresh water [kg/m^3]
τ_{wind} wind shear stress [N/m^2]
ξ extra resistance coefficient [s^2/m^5].

For 2D schematisations, such as overland flow, the equations above are solved in two dimensions (x and y). The first term in equation 2.2 describes the Eulerian acceleration [75], the second the convergence of the cross-sectional area of the flow (excluding storage area), the third the water level gradient, the fourth the bed level friction, the fifth the influence of the wind force and the sixth the influence of extra resistance[11]. The *bed level* is understood as the lowest point in the cross section, that is, the ground level in the 2D schematisation, and the bottom of a drain segment in the 1D schematisation[12]. The *surface level* is the highest point of the cross section, and if the water level rises over the surface level, there is a flood at the location, compare with figure 4.3.

The *friction factor* or *roughness factor*, included in term four in equation 2.2, is an important factor in hydraulics. It describes the resistance to flow when a fluid flows over land in 2D schematisations, and the resistance created by the walls of the drainage segment or waterway in 1D schematisations. Hence, it is of importance to know the hydraulic roughness of the land and the drainage when building flood models, which depends on the material of the feature. There are many formulas to describe this, of which SOBEK makes use of the *Chézy* bed friction value in solving the equations above. For this thesis, *Manning* roughness values are assigned, as this is widely applied with empirically derived values for many different materials. The Chézy coefficient is then calculated in the computation by SOBEK[13] using

$$C = \frac{R^{1/6}}{n_m} \tag{2.3}$$

where

C Chézy coefficient [m$^{1/2}$/s]
R hydralic radius [m]
n_m Manning coefficient [s/m$^{1/3}$].

A constant Manning value will be assumed for the land roughness in the study area, and the impact of distributed friction values in the 1D schematisation will be investigated, see section 5.3.

[11] Ibid.
[12] Ibid.
[13] SOBEK user manual, version 1.00

Chapter 3

Case study

The flood model developed in this thesis (see chapter 5) utilises drainage data collected by the *Ramani Huria* community mapping project in Dar es Salaam, Tanzania. This chapter aims to provide a thorough understanding of this project and its context. The chapter begins with introducing the flood situation in Dar es Salaam. Subsequently, *Ramani Huria*'s background, organisation and data collection methods are outlined. The chapter ends with a presentation of the study area, *kata ya* Kijitonyama, that will be modelled in terms of flood extent using *Ramani Huria* data.

3.1 Urbanisation and flood problems in Dar es Salaam

Dar es Salaam, the largest city in Tanzania, is undergoing a rapid and unplanned growth. Its population was estimated to be around 2.5 million in 2002 [76], and around 6 million as of 2019[1,2,3], making it to one of the fastest growing cities in the world [77]. It is divided into five municipalities, which are divided into wards (*kata*) which consist of sub-wards (*mitaa*). The location of Dar es Salaam is shown in figure 3.1. Situated where the Msimbazi river basin meets the Indian Ocean, the city is vulnerable to fluvial, pluvial and flash floods, sea-level rise and coastal erosion [78]. The rapid population growth rate leaves the city highly unplanned, with around 70% of the inhabitants living in informal settlements [76]. The city centre is characterised by a very high building density on lands susceptible to flood risks, mainly in the Msimbazi river basin. The region is experiencing biannual wet seasons, one occurring in October-December, and one more intense in March, April and May. The city suffers from flash floods during the wet seasons, leading to loss of life, housing and major disruptions on transportation infrastructure. On 15 April 2018 a state of flood emergency was declared that called for evacuation of all people living in flood prone areas. 15 people lost their lives during this storm event [79].

This situation calls for institutional coordination and integrated planning, to allow for rapid response in emergency situations and proactive disaster mitigation. The World Bank [79] finds that data and information are lacking to make accurate assessments of the exposure and adaptive capacity of the population and assets in Dar es Salaam. The Tanzanian Urban Resilience Programme[4] (TURP) was established in 2017 by the government of Tanzania, the World Bank Group and the UK Department for International Development to support the Tanzanian government in the management of urban climate risks. The community mapping project *Ramani Huria 2.0*, that has collected the drainage data utilised in this thesis, is supervised by TURP. The project can be seen as an initiative to collect the data needed to enhance disaster resilience in Dar es Salaam. *Resilience* is defined by the United Nations Office for Disaster Risk Reduction as *"The ability of a system, community or society exposed to hazards to resist, absorb, accommodate to and recover from the effects of a hazard in a timely and efficient manner, including through the preservation and restoration of its essential basic structures and functions"*[5].

Dar es Salaam is facing challenges with solid waste management. The absence of solid waste services imposes sanitation problems and induces floods when rivers and drains are blocked by plastics and debris [9]. Figure 3.2 shows the solid waste accumulation in Ng'ombe river on 23 February 2019.

[1] http://worldpopulationreview.com/world-cities/dar-es-salaam-population/
[2] https://www.cia.gov/library/publications/the-world-factbook/fields/350.htmlTZ
[3] https://populationstat.com/tanzania/dar-es-salaam
[4] https://www.worldbank.org/en/programs/tanzania-urban-resilience-program
[5] https://www.unisdr.org/we/inform/terminology

Figure 3.1: Location of Dar es Salaam in Tanzania. By © Sémhur / Wikimedia Commons, CC BY-SA 4.0, https://commons.wikimedia.org/w/index.php?curid=6681218.

3.2 *Ramani Huria* community mapping project

This section seeks to provide a description of the background, organisation and data collection methods of the *Ramani Huria* community mapping project. It will support the understanding of how *Ramani Huria*'s data collection methods has evolved over time. It will also relate the project to the literature on community mapping presented in chapter 2. The information provided here is based on *Ramani Huria* blog posts, the case study carried out by Iliffe [50] in *kata ya* Tandale, and interviews with employees at Humanitarian OpenStreetMap Team Tanzania and the World Bank in Dar es Salaam.

3.2.1 Background

After the successful crowd-sourced mapping of Haiti in response to the earthquake in 2010, the potential of VGI data in resource-strained environments was realised by the global development community. In Dar es Salaam, a pilot community mapping project was initiated in 2011 by the World Bank[6], in collaboration with Ardhi University[7], representatives from *Map Kibera* (section 2.2.4) and local NGOs. The ward executive officer in *kata ya* Tandale, the study area of the project, was also involved. Tandale is unplanned to a large extent, situated along the Ng'ombe tributary of the Msimbazi river. Figure

[6] https://www.knowledgesharingfordev.org/story/urban-community-mapping. The World Bank called the project *Urban Community Mapping*; the name *Ramani Tandale* was given by the mappers [50]. *Ramani* means *map* in Swahili.

[7] Ardhi University in Dar es Salaam is devoted to research and education in land based disciplines such as urban and regional planning, land administration, real estate etc. http://www.aru.ac.tz/

Figure 3.2: Solid waste in Ng'ombe river upstream of the bridge between Kijitonyama and Tandale, 23 February 2019. Photo by the author; thanks to Ahmed Mwanyenza.

3.3 shows the representation of Tandale on OSM in May 2019. The study area of this thesis, *kata ya* Kijitonyama (see section 3.3), is situated on the northern side of Ng'ombe river. Note how the two *kata* differ in their spatial structure; Kijitonayma is a planned *kata*, which is anticipated from the more regular road pattern compared to Tandale.

Students in urban and regional planning from Ardhi university were trained by *Map Kibera* catalysers to use GPS devices and to collect and upload data to OSM. The intention was to let the students bridge an assumed capacity gap among residents in Tandale in terms of experience with ICT. The mapping was initiated with a community forum at the Tandale ward office, attended by representatives from local *kata* and *mitaa*, community members and the students from Ardhi university[8]. The forum identified what the community thought should be put on the map; roads, pharmacies, schools, drainage and features relating to water access, sanitation, flood impact and solid waste disposals. The mapping was then carried out during four weeks in August 2011, resulting in a detailed map of Tandale, that later was used by the local authorities to aid a cholera outbreak [50].

The positive outcome of *Ramani Tandale* made the World Bank in Tanzania decide to aim for an up-scaling of the project and put all flood prone *kata* in Dar es Salaam on the map. The application for grants for *Ramani Huria*[9] *1.0* was sent in early 2012 and was accepted in September 2014. The NGO Humanitarian OpenStreetMap Team (HOT), that were founded in the aftermath of the Haiti earthquake (section 2.2.3), were contracted to launch the project. HOT had not been operating in Tanzania previously. Now, they trained a small group of students from Ardhi university and mapped several *kata* in the first half of 2015, using the methodology that had been developed in *Ramani Tandale*; start up with a community forum to define the community's priorities, let *mappers* collect data in the field and pass the collected data to *data cleaners* that edit it in JOSM (see section 2.2.2) and upload it to OSM, and close the mapping campaign with another community forum. At this time, the equipment used in the field was field papers to take notes and GPS devices. The field work was guided by aerial imagery taken

[8] https://matharevalley.wordpress.com/2011/08/09/community-mapping-starts-in-tandale-dar/
[9] *Ramani huria* means *open map* in Swahili.

Figure 3.3: *Kata ya* Tandale as represented on OSM in May 2019. Before *Ramani Tandale* in 2011, this area was a blank spot on OSM and other platforms [50].

by drones of the flood prone areas[10] that was digitised with the HOT tasking manager[11] in "mapping parties"[12].

HOT, together with the student group, facilitated an up-scaling of *Ramani Huria 1.0* during the summer months. The first *summer school* of *Ramani Huria*, launched in July 2015, was called 'Community Mapping for Flood Resilience' and aimed to map 14 *kata* prone to fluvial flooding and flash floods[13]. The resulting maps were used to run flood impact scenarios in QGIS[14]. It attracted 150 students from the University of Dar es Salaam (UDSM) and Ardhi University, as well as community members from 10 of the 14 *kata* that were mapped. After this big mapping effort, *Ramani Huria* and HOT Tanzania continued as a group of development workers and graduates from Ardhi university supporting several smaller projects in 2016, like mapping of sanitation facilities[15] and possible bicycle routes[16]. Workshops were held in late 2016 and early 2017 with *kata* officers, revealing that the drainage and inundation maps created by *Ramani Huria 1.0* had instigated measures for flood resilience on local level, including regular community clean ups of clogged drains, discouragement of dumping waste in drainage systems and construction improvements of the drainage system[17].

The mapping project was extended further in the *Ramani Huria 2.0* summer school in 2017, engaging 300 students in urban planning and geomatics from Ardhi university as a part of their industrial training[18]. The purpose this year was to map 35 *kata* to collect data for flood resilience. The students

[10] http://ramanihuria.org/drone-aerial-imagery-used-for-commuity-mapping-for-flood-resilience-in-ndugumbi-ward/
[11] https://tasks.hotosm.org/
[12] http://ramanihuria.org/3rd-mapping-party-20th-june-2015/
[13] http://ramanihuria.org/scale-up-workshop-6th-july-2015/
[14] QGIS is a free and open source geographic information system application. www.qgis.org
[15] http://ramanihuria.org/mapping-dar-es-salaams-water-sanitation-hygiene-facilities/
[16] http://ramanihuria.org/participating-dar-es-salaams-cycle-caravan-mapping-bicycle-routes/
[17] http://ramanihuria.org/weos-discuss-map-use-beyond-flood-resilience/
[18] http://ramanihuria.org/three-hundred-students-map-flood-resilience-dar-es-salaam/

were divided in specialised teams, focusing on drainage mapping, data processing in GIS, digitise aerial imagery (*remote mapping*) and community outreach[19]. The drainage data utilised in this thesis was collected during this mapping campaign. The data collection methods of *Ramani Huria* implemented in 2017, which still are in use and developed as of 2019, are described in section 3.2.2. After the summer school in 2017, HOT Tanzania continued with a smaller number of employees and students, now also performing other mapping projects in Tanzania. The local organisation Open Map Development Tanzania[20] (OMDTZ) was founded in December 2017 to deal with local contractors.

In the launch of *Ramani Huria 2.0* in 2017, the drainage mapping methodology was improved. The drainage data from *Ramani Huria 1.0* only included the width and depth of cross sections, missed data on elevation of the drains related to ground level, and segments were missing or disconnected in the data set [8]. The survey was now developed to map all drainage attributes necessary for hydrodynamic modelling[21]. These attributes are described in section 4.1.1 and implemented in a model setup in chapter 5.

This thesis makes use of a flood extent survey to validate the developed flood model, see chapter 6. *Ramani Huria* started to develop the flood extent methodology in late 2017, using a community mapping approach;

> After consulting with the appropriate subward leaders, students go door-to-door and explain the project to community members. If the citizens are interested, the students will then show them how to operate the Opendatakit Collect (ODK) app and ask them to fill out the survey form accordingly. New community members are brought down to the river by the students and directed through the app. From their point on the river, the community members are instructed to walk directly away from the river to survey houses along the way – identifying whether or not they are hit by flooding. The student accompanies the community member for 1 or 2 houses and then leaves the trainee to continue on solo to complete the survey[22].

The flood extent survey carried out in this thesis, and how it builds upon *Ramani Huria*'s methodology, is explained in section 4.2.1. The summer school of 2018 attracted more than 600 students to participate in *Ramani Huria* for their industrial training[23]. The outcome was 44 *kata* being fully mapped, and the production of "threats and assets" reports where each *kata* was analysed in terms of flood risks in collaboration with community members[24]. The continued work of *Ramani Huria* in 2018 and 2019 includes finalisation of drainage mapping in all *kata*, determine grain size distribution of soils across Dar es Salaam to support erosion analyses[25] and trace the outlines of *shinas*, the most granular administrative divisions that exist in Tanzania[26]. This is work carried out by around 40 contracted people, based at HOT Tanzania's/OMDTZ's office in Dar es Salaam, with several mapping teams out in the field on a daily basis. *Ramani Huria* is projected to end in July 2019; Figure 3.4 provides a time line of the project.

[19] http://ramanihuria.org/art-drainage-mapping-dar-es-salaam/
[20] http://omdtz.or.tz/
[21] https://medium.com/@h.c.winsemius/using-community-mapping-for-flood-modelling-c04976d3e982
[22] http://ramanihuria.org/community-outreach-for-flood-extent-mapping-hananasif-ward/
[23] http://ramanihuria.org/two-hundred-subwards-of-dar-es-salaam-to-be-mapped-by-university-students-in-the-next-six-weeks/
[24] ttp://ramanihuria.org/community-meetings-for- flood-resilience-plan/
[25] http://ramanihuria.org/assessing-the-geomorphological-characteristics-of-soil-in-dar-es-salaam/
[26] http://ramanihuria.org/hyperlocal-boundary-mapping/

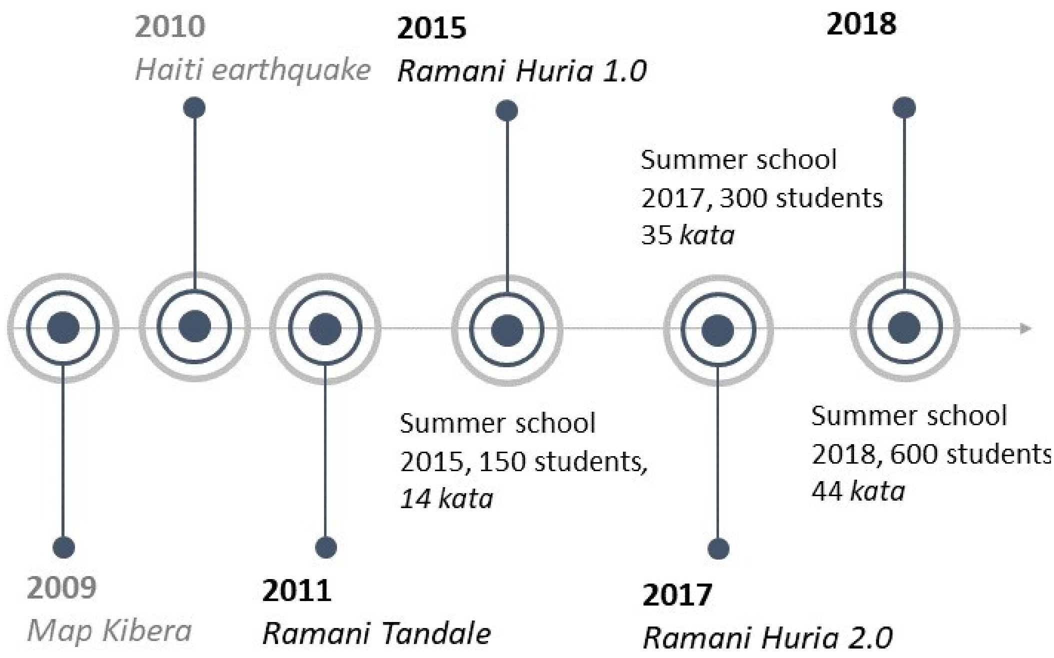

Figure 3.4: Time line of *Ramani Huria*.

3.2.2 *Ramani Huria*'s data collection and organisation

This section describes the data collection methods and organisational structure of *Ramani Huria*. An overview is depicted in Figure 3.5.

The Open Data Kit Collect application (ODK) is at the core of *Ramani Huria*'s data collection since 2017. It is a survey application allowing for advanced questionnaires, with the additional function that it can add geopoints and geotraces to each data entry, making use of the GPS in the smartphone that records the survey. *Ramani Huria* took part in the development of the ODK application to its current function; at the start of *Ramani Huria 2.0* in 2017, the application could not record geotraces with sufficient accuracy. *Ramani Huria* tested and developed the geotracing function in collaboration with the ODK developers[27], making it fit-for-purpose to record the stretch of drainage segments. The surveyor starts the geotrace at the beginning of the drainage segment, walks along it, and ends the geotrace at the end of the segment. A new geotrace is started if the elevation from the starting point of the trace is exceeding approximately 10 centimetres[28]. The drainage mapping team starts with identifying the most downstream point of an area, where the drainage system reaches a water body, records a geopoint and labels it as *outflow* in the ODK application. Then, they map the drainage system starting from the most downstream point and walk upstream. In this way, the beginning of a geotrace is always the downstream point of a segment, and the end of the geotrace is the upstream point. The cross sections of drainage segments are measured with measuring sticks and tape measures, see Figure 3.6.

The questionnaires in the ODK application are created as *XLSForms*[29]. XLSForm is a form standard to author advanced forms in Excel. The functions include, for example, meta data, GPS accuracy thresholds, conditional questions, constraints, calculations and multiple language support. The questions are programmed in Excel using a certain syntax, and then the XLSForm is uploaded to a server. The surveyors then connect to this server in the ODK application, download the form, perform the survey and upload the results again. *Ramani Huria* makes use of the *KoBo Toolbox*[30] server.

[27] https://www.hotosm.org/updates/2017-11-05_ramani_huria_building_open_tools_to_map_drains
[28] This practice is not documented on the *Ramani Huria* OSM Wiki, but was applied when the author joined the drainage mappers in *mtaa wa* Gongo la Mboto, 28 February 2019
[29] http://xlsform.org/en/
[30] https://www.kobotoolbox.org/

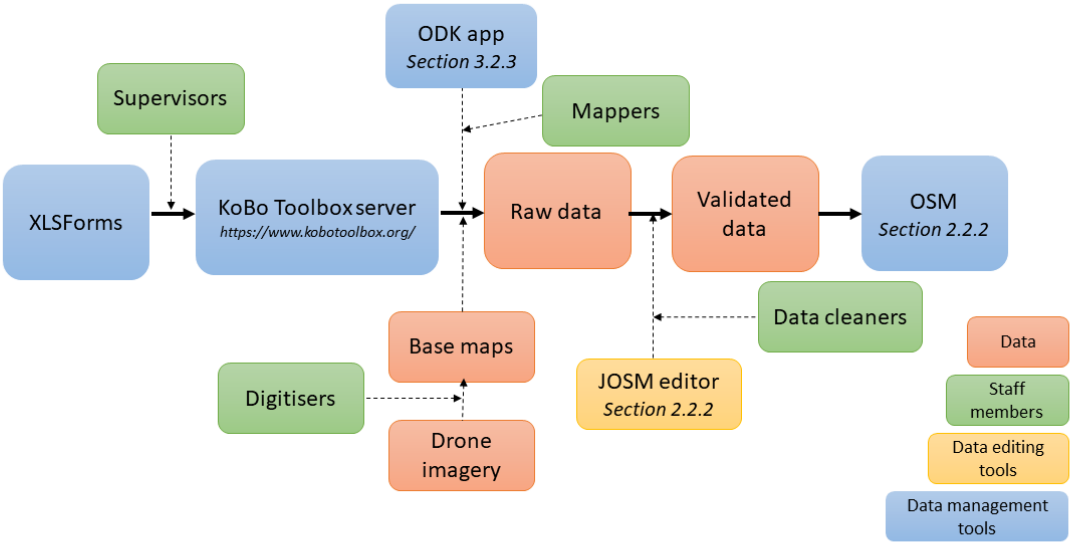

Figure 3.5: Components of *Ramani Huria*'s data collection methods. Thanks to Lovenes Charles.

Figure 3.6: Mapping of a culvert on 12 September 2017, using measuring stick, tape measure and smartphone. http://ramanihuria.org/art-drainage-mapping-dar-es-salaam/.

The organisational structure of *Ramani Huria* build upon the methodology that developed organically in *Ramani Tandale* [50]. *Supervisors* manage the XLSForms and keep track of the work process. *Mappers* are out in the field collecting data and upload the survey results to the *KoBo Toolbox*. *Data cleaners* download the results and validate it JOSM (see section 2.2.2) before uploading the data to OSM. There are also *digitisers* at HOT Tanzania/OMDTZ, that make maps from aerial imagery, supporting both local and international projects. They contribute to *Ramani Huria* through making base maps that guide the mappers when they are in the field. HOT Tanzania/OMDTZ is making their own aerial imagery of Dar es Salaam with drones that are built at their office, see Figure 3.7. The drone body is built from bamboo and the plastic parts are printed by their own 3D-printer.

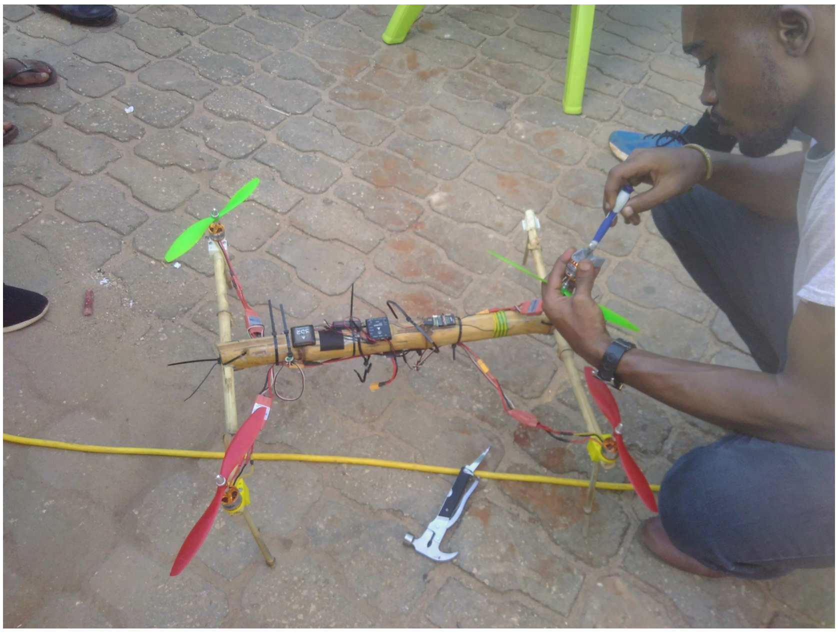

Figure 3.7: Wombura Kimacha is preparing OMDTZ's drone for take-off on 15 February 2019. This drone type, *MwanzaMwanzi*, is developed by Bornlove Ntikha. Photo by the author.

3.2.3 *Ramani Huria* related to literature

As *Ramani Huria* is building upon the foundation set during *Ramani Tandale* in 2011, it clearly relates to the framework for community mapping in developing countries [50] presented in section 2.2.7. The project has, however, expanded over time, adding new dimensions to the understanding of community mapping. Community mapping is defined, recalling section 2.2, as "the action of producing a map together *with or by* the residents of a certain location" [42]. This certainly applies to *Ramani Tandale*, and, for example, *Ramani Huria*'s flood extent survey described above, but not all data sets fulfil this. Since the launch of *Ramani Huria 2.0* in 2017, the project is increasingly collecting data that requires training, like the drainage mapping, soil sample survey and the development of drones and elevation measurements. This development is accommodated by the rise of *Web 2.0*, that has lowered the barriers to produce geographic information, but the data produced from these technologies cannot be categorised as community mapped according to the presented framework. Neither can it be labelled as *Volunteered* Geographic Information, as it is produced by professional supervisors, mappers and data cleaners.

Ramani Huria was initiated by the World Bank, not by scientist. The collected data is, however, of scientific interest, as it adds information to a very data scarce environment that face challenges linked to climate change and rapid urbanisation. Furthermore, Haklay [48] argues that OSM in itself is a crowd-sourcing citizen science project as it records geographic observations with scientific instruments (compare with Haklay's ladder on levels of participation in citizen science in Figure 2.2). As shown above, hundreds of students have participated in *Ramani Huria*'s summer schools as a part of their industrial training at university. There is a clear link to the academia in *Ramani Huria.* However, it can be discussed who the citizen scientists are if we perceive *Ramani Huria* as a citizen science project- the students and employees, or the communities they reach out for in their data collection. If we call

Ramani Huria's summer school students *student citizen scientists*, as suggested by Davids et al. [49], we can define *Ramani Huria*'s drainage data collection as a 'distributed intelligence' citizen science project according to Haklay's ladder on levels of participation, as it involves data collection and basic interpretation. Ultimately, one could argue that *Ramani Huria* is an 'extreme citizen science' project, as the problem definition and data collection methods were formulated by the community of Tandale in 2011.

Given the absence of an existing framework that comprehensively can capture *Ramani Huria* in its current state, it is clear that this project has added a new dimension to the value of VGI and how open data can support governance and resilience building in resource-strained environments.

3.3 Study area: *kata ya* Kijitonyama

The study area selected for this thesis is *kata ya* Kijitonyama in Kinondoni municipality. The aim of the selection process was to identify an area prone to pluvial flooding, to be able to investigate the added value of *Ramani Huria*'s drainage data on flood predictions. The process started with studying the topography of Dar es Salaam, locating *kata* situated outside or at the border of the Msimbazi river basin. This was complemented with discussions with experienced drainage mappers. Then, the available drainage data of the identified *kata* was studied, revealing that the data in Kijitonyama was most complete, as some of the other considered *kata* missed data on elevation in relation to reference roads. It was also of importance that Kijitonyama is located close to two weather stations, see section 4.1.4. Figure 3.8 shows the outline of *kata ya* Kijitonyama and the Msimbazi river basin.

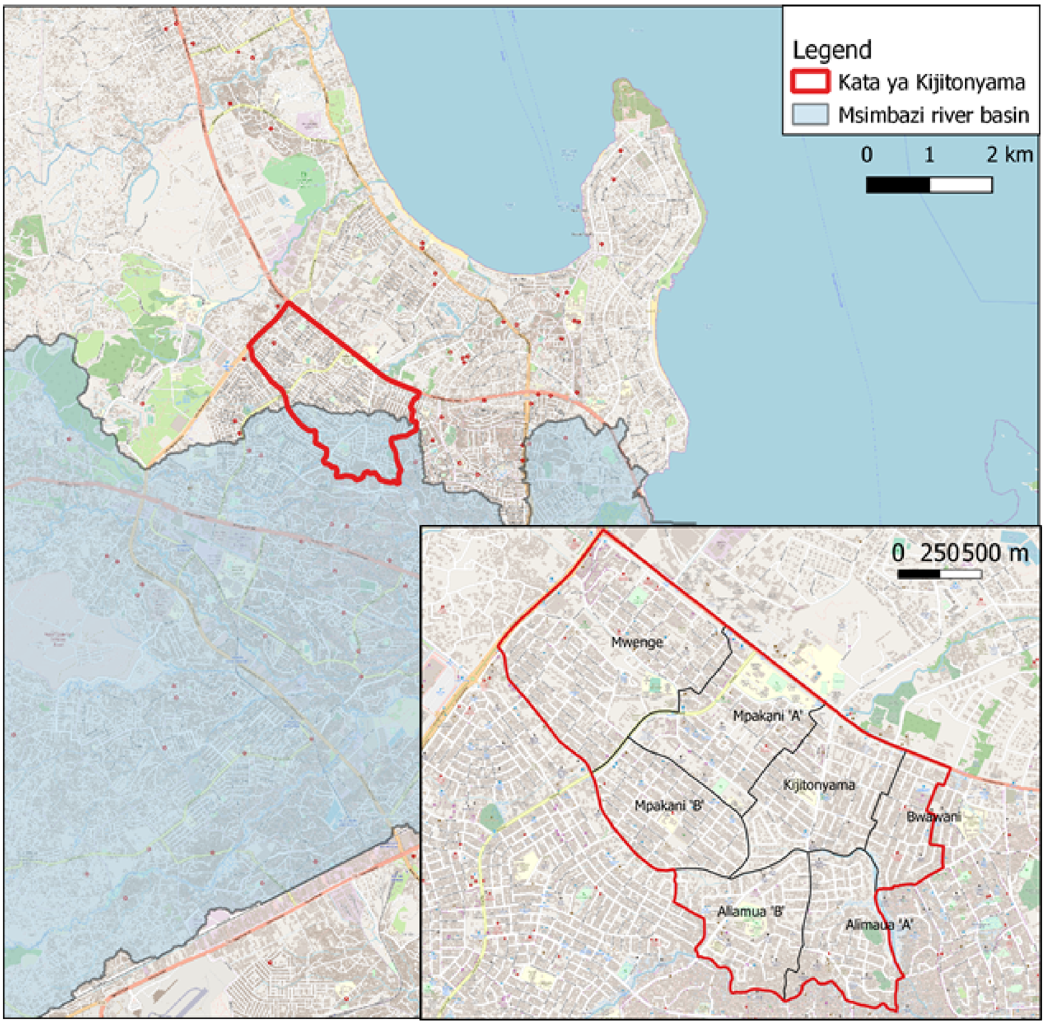

Figure 3.8: Location of *kata ya* Kijitonyama in Dar es Salaam and the Msimbazi river basin.

Kijitonyama is approximately 4 km² and consists of seven *mitaa*; Mwenge, Mpakani A, Mpakani B, *mtaa wa* Kijitonyama, Bwawani, Alimaua A and Alimaua B. The drainage mapping supervisor of *Ramani Huria*, Elia Dominic, applied for permission to perform the flood extent and blockage surveys in this thesis (see section 4.2.1 and 4.2.2) and received permission in Mpakani A, Mpakani B, *mtaa wa* Kijitonyama, Alimaua A and Alimaua B. There is, however, no drainage system in Mpakani B, and this area is therefore not included in the model setup. On the other hand, Bwawani is included in the model, as it is very interconnected with *mtaa wa* Kijitonyama in terms of drainage. Hence, the study area of this thesis consists of the *mitaa* Mpakani A, *mtaa wa* Kijitonyama, Bwawani, Alimaua A and Alimaua B, see Figure 3.9. The study area is approximately 2.3 km².

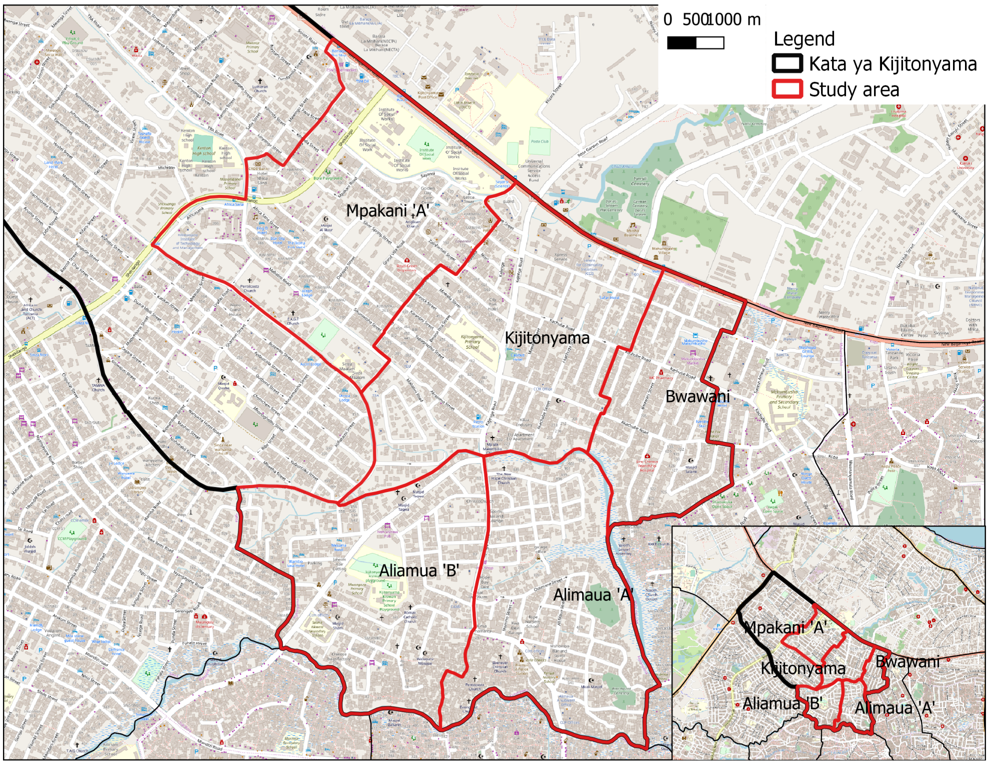

Figure 3.9: Study area outline.

No major solid waste accumulation in the drainage system was encountered during fieldwork in Kijitonyama. Figure 3.10 shows the situation at Africa Sana in 2015 compared to 2019, indicating an improvement of solid waste management in Kijitonyama in recent years.

Figure 3.10: Drain at Africa Sana, in the crossroad Shekilango road/Mabatini road. Left image: 28 September 2015, http://ramanihuria.org/mapping-drainage-in-dar-es-salaam/. Right image: 6 March 2019, photo by the author.

Chapter 4

Data

This chapter presents the data sets that constitute the model setup developed in chapter 5. It will also introduce the flood extent survey that is used to validate the model, and the data on blocked drain segments that is used in scenario 3a (see section 5.3). First, the applied data sets are described, followed by a quality analysis of the applied drainage data. Then, the data sets collected by the author, i.e. the flood extent and blockage survey, are described. Figure 4.1 provides an overview of the data sets in the model setup.

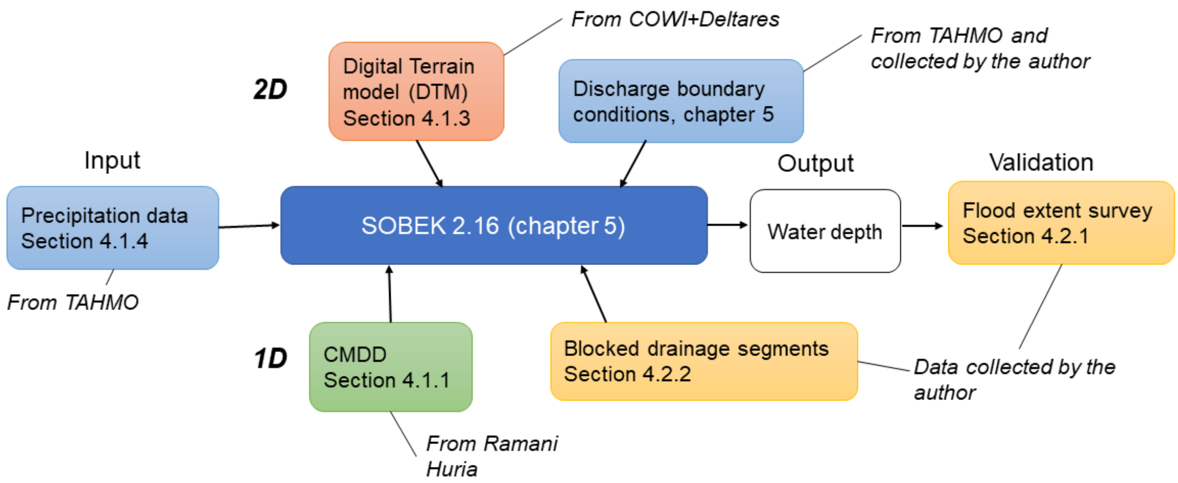

Figure 4.1: Overview of data sets and their relation in the model setup.

4.1 Applied data sets

This section introduces the data sets that are collected by external actors. First, the community mapped drainage data recorded by *Ramani Huria* is described, followed by a quality analysis of the drainage data. Then descriptions of the Digital Terrain Model (DTM) and precipitation are presented.

4.1.1 Drainage

The drainage data applied in thesis was obtained directly from employees at HOT in Dar es Salaam in February 2019, but it can also be downloaded from OSM with the HOT export tool[1]. Only the features of the drainage data within the study area is presented and analysed here. A description of all features of the drainage data recorded by *Ramani Huria* is found on the *Ramani Huria* OSM wiki[2]. This section describes the drainage data in the state that it was when it was received from *Ramani Huria*. How the

[1]https://export.hotosm.org
[2]https://wiki.openstreetmap.org/wiki/Dar_es_Salaam/Ramani_Huria

data was adapted for flood modelling will be described in chapter 5.

The drainage in *kata ya* Kijitonyama was mapped during 20 days between 4 September 2017 and 24 April 2018. It was collected with the ODK application as described in section 3.2.2. Figure 4.2 shows which dates the drainage was mapped. Note that only the drainage in the study area is depicted, which is five of the seven *mitaa* in *kata ya* Kijitonyama, as explained in section 3.3. Most of the surveying took place in October 2017. Mpakani A was mainly mapped on 16-18 October, eastern *mtaa wa* Kijitonyama, Bwawani and south-western Mpakani A on 19 October, and Alimaua A and B on 20 October, 2017. The other mapping dates are not highlighted. The drainage along New Bagamoyo road, that is the road that borders *kata ya* Kijitonyama in the north, was mapped on 4 and 6 September, 2017. The remaining drainage (19 segments) was mapped after 20 October 2017, and it is expected that this was to correct errors that appeared in the data cleaning process after the mapping campaign in October. These segments are mainly along New Bagamoyo road in Mpakani A. There are 532 drainage segments in the study area, and 805 in *kata ya* Kijitonyama in total. The mapping was carried out by 33 people, which was concluded by counting how many different SIM serial numbers (mobile phones) that contributed to the data set.

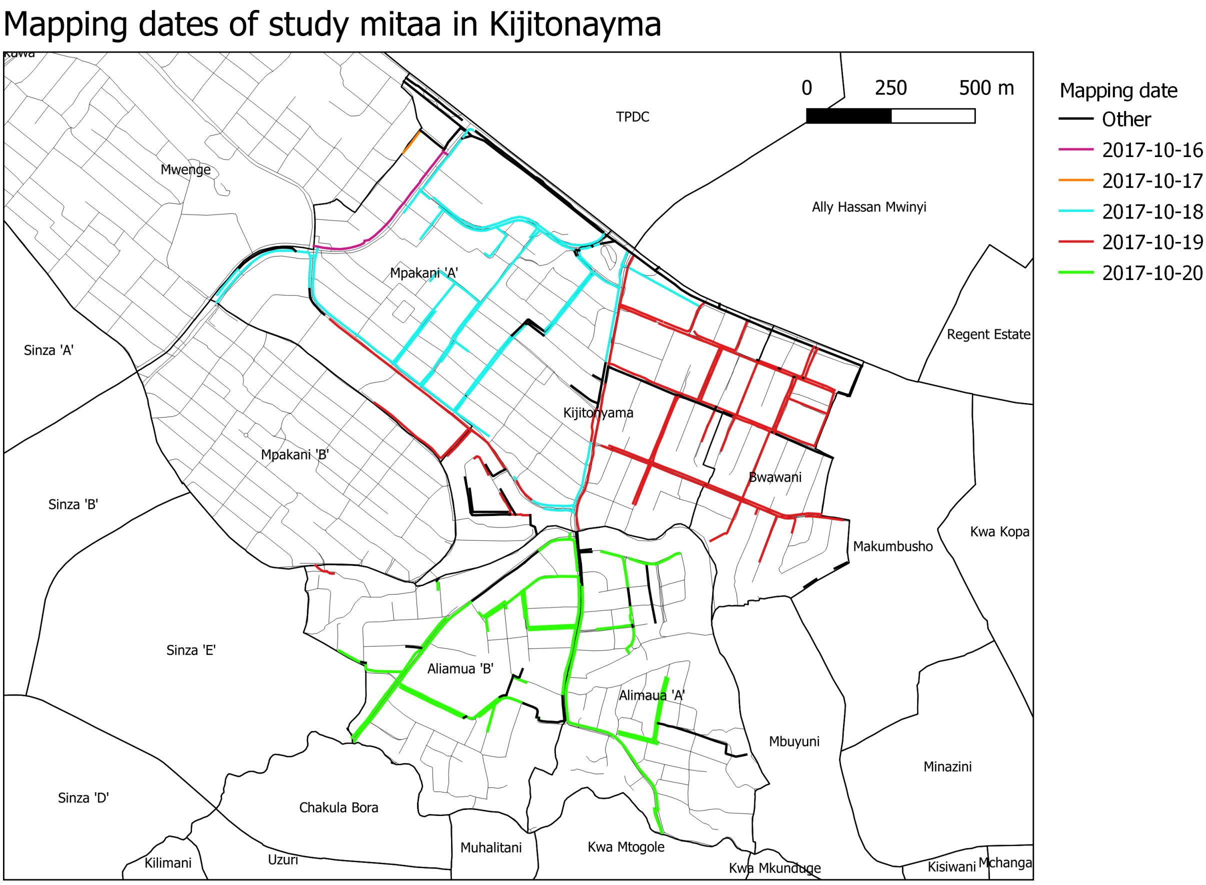

Figure 4.2: Mapping dates of the drainage data in the study area.

This section continues with describing the features of the *Ramani Huria* drainage data that are relevant for flood modelling; location, cross sections and friction.

Location

As described in section 3.2.2, the ODK application can record geopoints and geotraces. These records constitute the location of nodes and segments in the 2D plane. The elevation of features can, however, not yet be recorded by smartphones with sufficient accuracy. To overcome this, *Ramani Huria* is now measuring the *depth* and *elevation* of drainage segments to calculate their bed level and surface level in relation to the DTM. The depth is the distance between the bottom of a segment and the ground, and the elevation is measured as the distance between the bottom and the nearest road (*reference road*), see Figure 4.3.

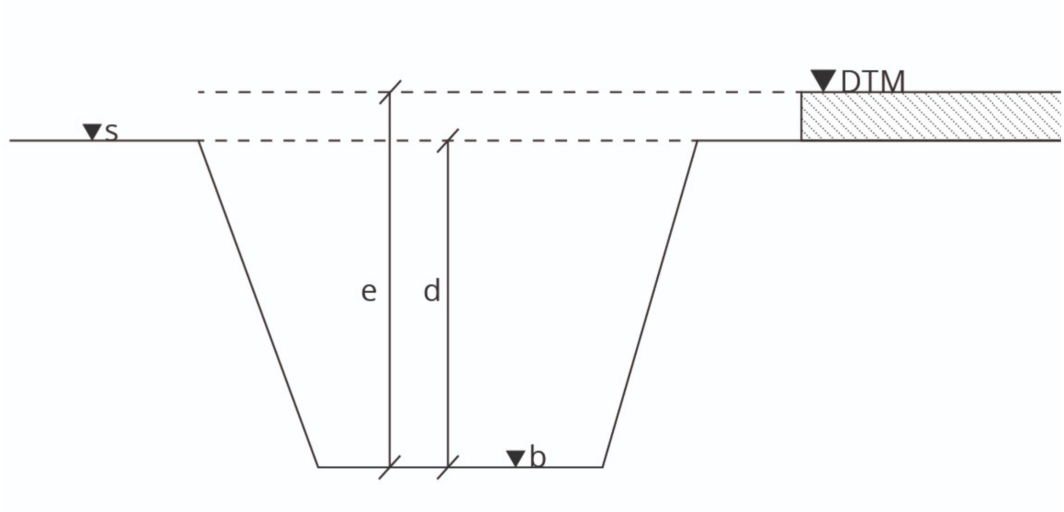

Figure 4.3: Relation between surface level s and bottom level b of a drain and DTM level.

The bed level b of a segment is calculated as

$$b = DTM - e \tag{4.1}$$

where DTM is the elevation of the reference road according to the DTM and e is the measured distance from the bottom of the segment to the tangent line of the reference road. The surface level s is found as

$$s = DTM - e + d \tag{4.2}$$

where d is the measured distance from the bottom of the drain to the tangent line of the ground level.

The elevation and depth is measured after the geotrace is finished. This means that these features are always measured at the upstream point of a segment, as the drainage mappers walk from the downstream to the upstream point of segments when recording the geotraces. This will be of importance in the model setup, see section 5.1.6.

Cross sections

The drainage segments in the *Ramani Huria* data set are of four types; culverts, ditches, drains and decommissioned drains. Culverts have a round or rectangular cross section and drains have a trapezoidal, rectangular or elliptical cross section. Drains are open or closed. Ditches have width and depth reported, and decommissioned drains have no dimensions reported in the data set. Table 4.1 provides an overview of the cross sections in the study area and the dimensions reported for each cross section type.

Table 4.1: Cross section types and their measured dimensions. Decommissioned drains have no dimensions reported.

Type	Cross section	Dimensions		
Culvert	Round	Diameter		
	Rectangular	Width	Depth	
Ditch	Rectangular	Width	Depth	
Drain	Trapezoidal	Top width	Bottom width	Depth
	Rectangular	Width	Depth	
	Elliptical	Top width	Depth	

Figure 4.4 depicts the study area in terms of drainage cross sections. The majority of the drainage system consists of open trapezoidal drains.

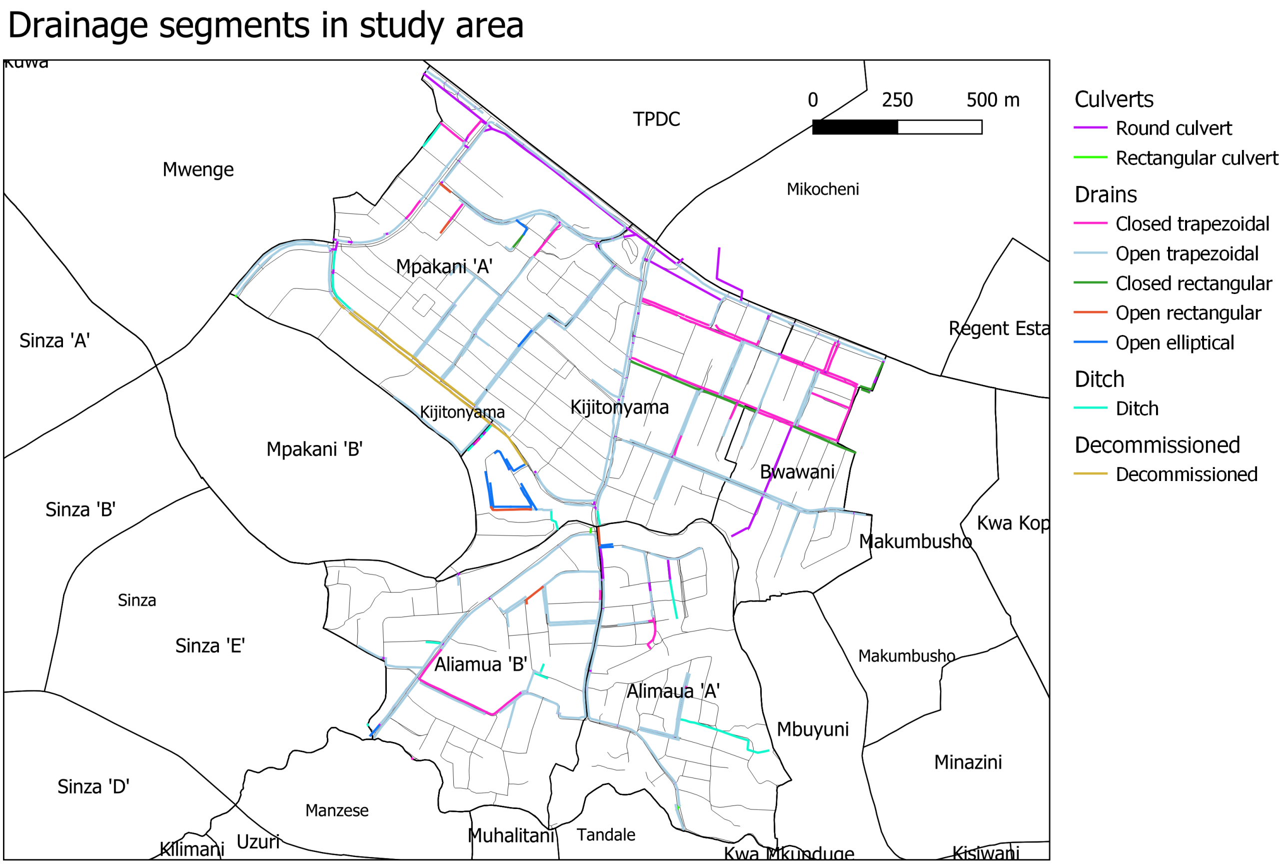

Figure 4.4: Cross sections of drainage segments in the study area.

Friction

Ramani Huria is recording the material of each segment; concrete, steel, plastic, sand or other material with free text entry. If the segment is made of concrete, they also assess the hydraulic roughness (friction) of the segment. This attribute is called *smoothness* in the *Ramani Huria* data set. The smoothness can have three different values, see Table 4.2. These values will be converted to friction values in the 1D schematisation of the model, see section 5.1.5.

Table 4.2: Smoothness of concrete segments.

Smoothness	Description
1	Normal concrete, in good repair
2	Rough, with noticable holes or cracks
3	Very rough, with loose material, broken areas and/or large cracks

4.1.2 Quality analysis of *Ramani Huria* drainage data

The *Ramani Huria* drainage data is analysed by data cleaners in a freely available Python script[3] before being uploaded to OSM. The Python script performs data quality checking for hydraulic modelling and the generation of a topologically correct 1D network. The quality check contains:

- Checking of the tagging data model; for example, if all cross sections have the dimensions in Table 4.1 recorded
- Checking of the connectivity of the network, identifying disconnected parts in the network
- Checking crossings of waterways and roads; checks if crossings of waterway and road elements are either reported as bridges or culverts.

The following sections provide an additional analysis of the drainage data in the study area in terms of completeness and accuracy.

Completeness of segments

It is difficult to assess the completeness of the *Ramani Huria* drainage data, due to the absence of a comparable data set. For future research, it is recommended to compare *Ramani Huria* drainage data with data from Tanzania Rural and Urban Road Agency (TARURA), the governmental body in charge for construction and maintenance of roads and drainage. As shown in section 2.2.5, Iliffe [50] found OSM road data to be more complete than road data held by the Dar es Salaam city council. It can, hence, be expected that the *Ramani Huria* drainage data is more extensive than data held by the authorities, but this must be further examined. It is not known if TARURA has information on ditches and decommissioned drains, which is present in the *Ramani Huria* data set. Research has shown that a considerable provision of drainage in Dar es Salaam is made by individuals, especially in informal settlements [80]. Figure 4.5 depicts a drainage ditch in Dar es Salaam.

Positional accuracy

The positional accuracy of geopoints and geotraces is dependent on the accuracy of the GPS device that records them. It is possible to set an accuracy threshold in the ODK application, so that only locations with a certain accuracy can be recorded. It is not known if such a threshold was used when recording the drainage segments in Kijitonyama in 2017. The author joined the *Ramani Huria* drainage mapping team when they mapped *mtaa wa* Gongo la Mboto, 28 February 2019, and then the accuracy threshold was set to 5 meters. The positional accuracy is inspected in the data cleaning process, where *Ramani Huria* data cleaners compare the recorded geotraces with aerial imagery. This process aims to remove errors in the records and adjust the geotraces to form a connected network.

[3]https://github.com/openearth/hydro-osm

Figure 4.5: Example of a drainage ditch recorded by *Ramani Huria*. Photo by Ivan Gayton. https://wiki.openstreetmap.org/wiki/File:Drain_ditch_open.jpgfilehistory

Additional inspections of the positional accuracy of the drainage data was performed by the author in the data processing. Three different types of errors were encountered, that here will be labelled *tracing errors*, *disconnected ends* and *double segments*. These were found through visual inspection, and when building the flood model in SOBEK (see chapter 5). The errors yield a disconnected network in the modelling software, and introduce simulation errors. A tracing error appears when a drainage segment has an unrealistic reach, see figure 4.6. Three segments like this were encountered in the study area.

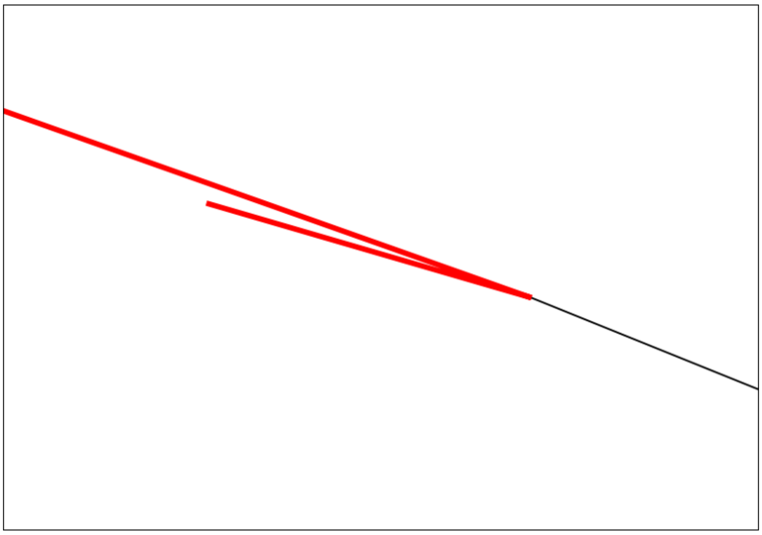

Figure 4.6: Example of a tracing error.

Figure 4.7 shows an example of a disconnected end. Five disconnected ends were found in the study area.

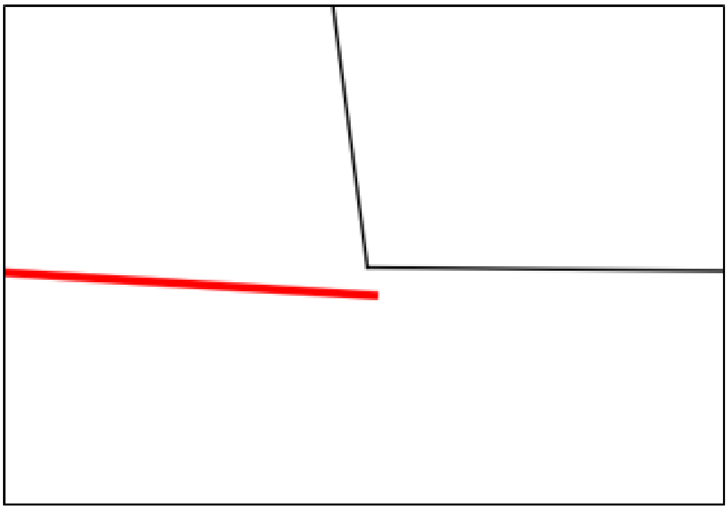

Figure 4.7: Example of a disconnected end.

A double segment appears when two segments have the same, or very similar reach, and the same properties. Then it is expected that this segment was recorded twice. This error was found four times in the study area.

The positional accuracy of the drainage data is assessed to be high, as only 12 out of 532 segments have evident positional errors. Again, the data can be compared with data from TARURA to further investigate this aspect.

Completeness of cross sections

As mentioned, the tags of the *Ramani Huria* drainage data is quality checked by a Python script before being uploaded to OSM. An additional inspection was performed with filters in the attribute table of the drainage data in QGIS, to see if any segments were missing dimensions of their cross sections. Only one segment in the study area is missing one feature; an open trapezoidal drain has no depth recorded. Hence, the cross section data is perceived as complete.

Completeness of material

The material of each segment must be known to assess its hydraulic roughness. The decommissioned drains and most of the ditches are missing material data, constituting 5% of the total data set. The assumptions made to account for this is described in section 5.1.5.

4.1.3 Digital Terrain Model

Elevation measurements still pose a challenge to resource-strained environments, as it requires expensive technology to produce results with sufficient accuracy. Elevation is an important component in hydrodynamic modelling to estimate hydraulic energy slopes. In urban areas, where flood impacts are high, it is crucial to have high resolution of elevation measurements to allow for accurate modelling of flood risks [81]. *Ramani Huria* are currently developing a methodology to measure elevation using dynamic differential barometry[4]. These efforts are ongoing, and it is recommended to evaluate and apply their results in forthcoming hydrodynamic models.

This thesis makes use of a DTM delivered by the consultancy firm COWI. Access to this DTM was acquired from Deltares research institute in Delft, the Netherlands, which have used this DTM to develop a hydrodynamic model of the Msimbazi river basin at catchment scale. The DTM has a resolution

[4] http://ramanihuria.org/developing-elevation-tools/

of 5 meters and has been produced through photogrammetry with aeroplane. The quality of the DTM has been assessed by Deltares. They draw the conclusion that noise from vegetation and buildings is removed in the DTM, and that it hence represents the bare-earth terrain or street level. Furthermore, they note that there is a structural offset between the DTM and river cross section elevation points from ground measurements performed by COWI. The ground measurements are systematically lower than the DTM, but the datum of the ground measurements is not known. Deltares can, therefore, not conclude how the DTM refers to mean sea level. They note that the DTM values show no flooding at all of the wetland area in the most downstream part of the Msimbazi river basin, and field work performed by Deltares confirmed that the inter-tidal zone indeed remains nearly dry in wet conditions, even during spring tide. They also observe that the elevation levels in the thalweg and wetland area seem realistic. Therefore, Deltares assume that the DTM zero datum is correct in their simulations. Despite these uncertainties, this thesis will make use of the DTM as it offers higher resolution than any other accessible data set. Figure 4.8 shows the elevation in the study area.

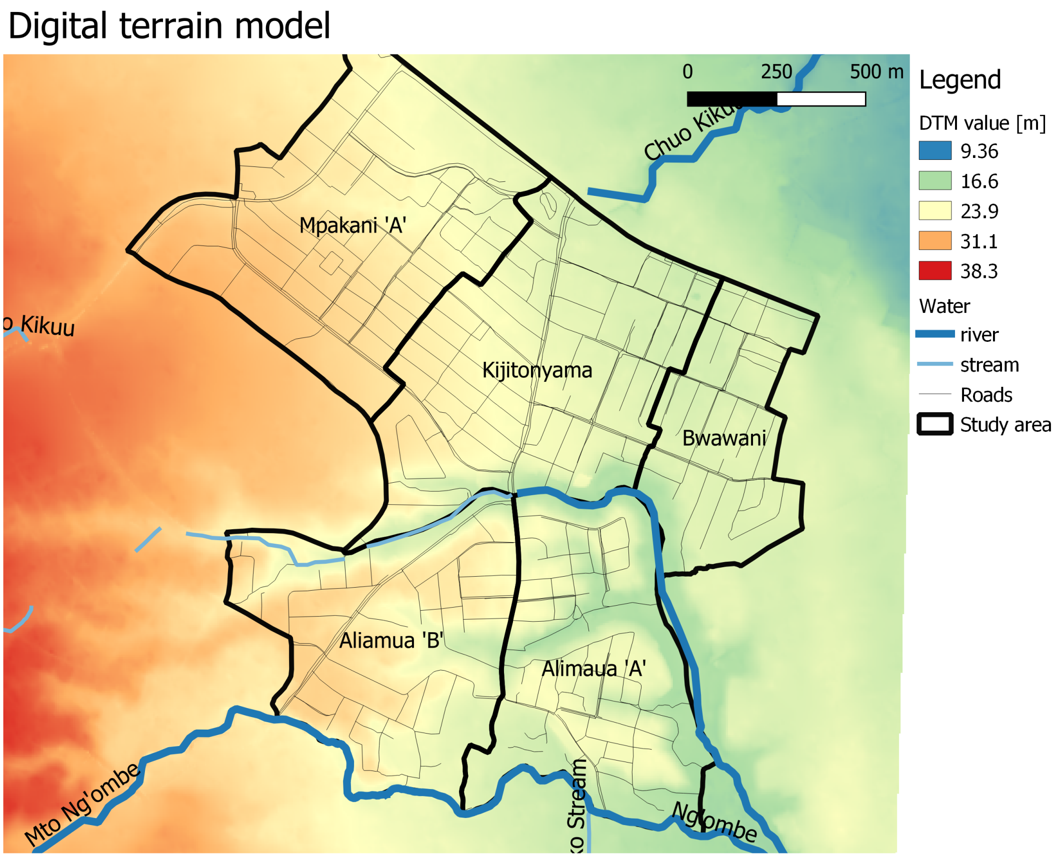

Figure 4.8: Elevation in the study area.

4.1.4 Precipitation

The precipitation data serving as forcing to the model developed in chapter 5 is recorded by the TransAfrican HydroMeteorological Observatory (TAHMO[5]). TAHMO is aiming to build a dense network of hydro-meteorological monitoring stations in sub-Saharan Africa. These stations are developed to be inexpensive and robust against dust and insects, making them suitable for sub-Saharan conditions. They record rainfall using acoustic disdrometers, which have been proven to record accurately during heavy storm events, but are less capable to capture low intensity events[6]. Figure 4.9 depicts the installation of a TAHMHO weather station in Ifakara on 21 February, 2019.

[5]www.tahmo.org

[6]https://tahmo.org/weather-stations/

Figure 4.9: Installation of a TAHMO weather station in Ifakara on 21 February, 2019. Photo by Markus Pleij.

There are 7 TAHMO weather stations installed in Dar es Salaam. The location and data quality of these stations influenced the selection of Kijitonyama as study area, see section 3.3. Figure 4.10 depicts the locations of the stations and an assessment of their data quality. The recorded time series were visualised in graphs, showing that all weather stations have recorded consistent data, capturing the rain seasons in March, April and May and October-November. The exception is Pugu, that showed an inconsistent pattern of the rainfall records and mostly measured 0 mm rainfall in the rain seasons.

The longest time series are available from the Ardi and BRT weather stations, recording consecutively since September 2017. Kijitonyama is located approximately 2 km from Ardhi, and 4 km from BRT, see Figure 4.11.

The forcing to the model is a rain event recorded by Ardhi weather station in the early morning of 3 March 2019, see figure 4.12. The event started at 00:10, had two peaks at 01:00 and 06:00, and stopped around 9:00. This event was selected as it was preceded by five dry weeks, which means that the drainage system was initially dry and the flow in natural water courses was at the base flow. Hence, the initial conditions for this rain event is known. The peak intensity was 9.5 mm rain in five minutes, which is expected to have impact in Kijitonyama, even if the majority of the study area is uphill from the rivers. The flood extent survey described in the following section was recorded a few hours after the event, which is anticipated to yield reliable results.

Discharge data from a TAHMO hydro station will be applied as boundary condition in the model setup, see section 5.2.1.

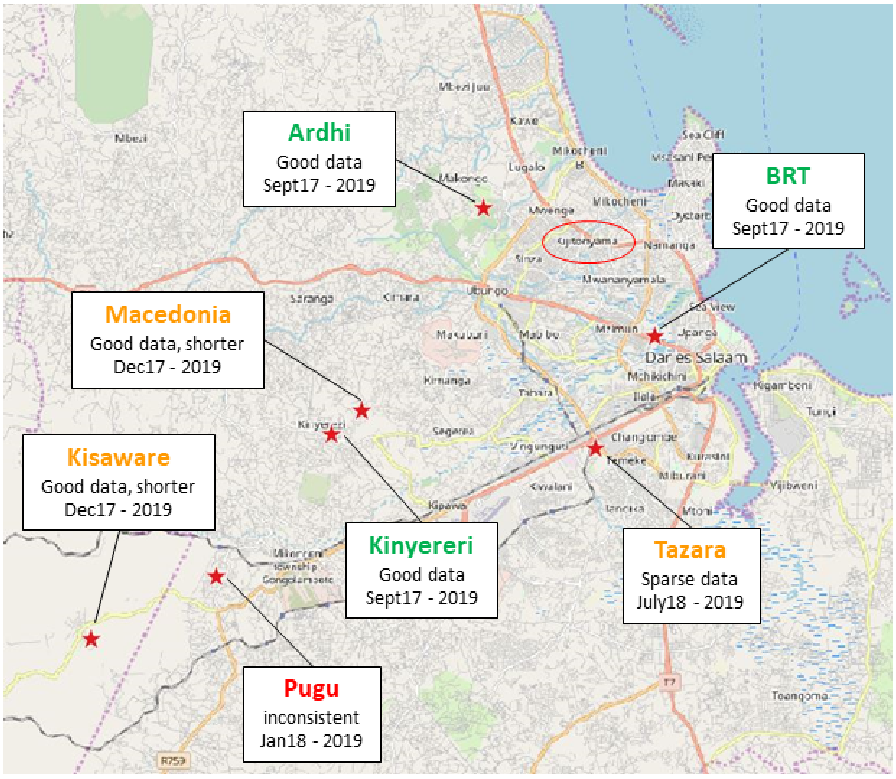

Figure 4.10: Locations and data quality of TAHMO weather stations in Dar es Salaam. The study area is highlighted with a red ellipse.

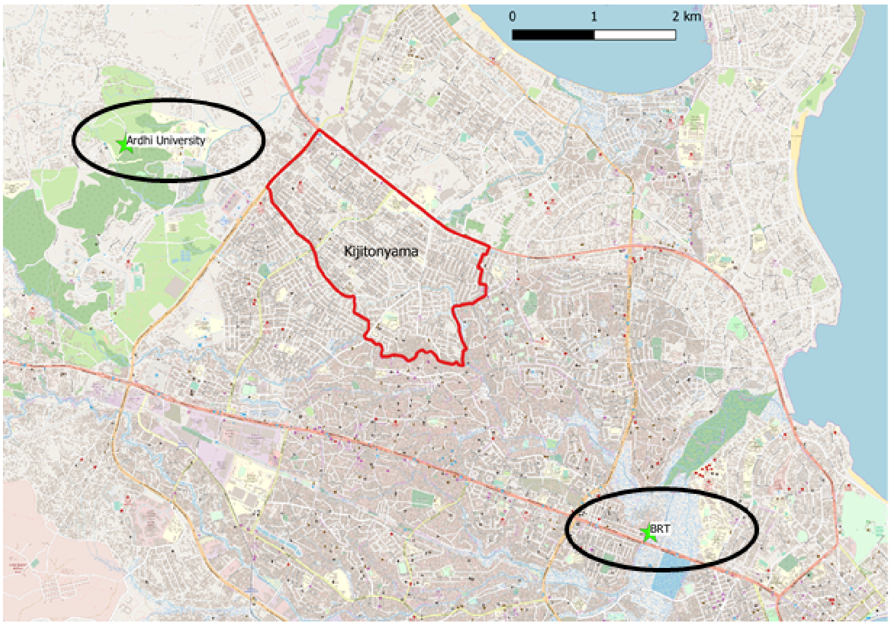

Figure 4.11: Locations of Ardhi and BRT weather stations. The study area is highlighted in red.

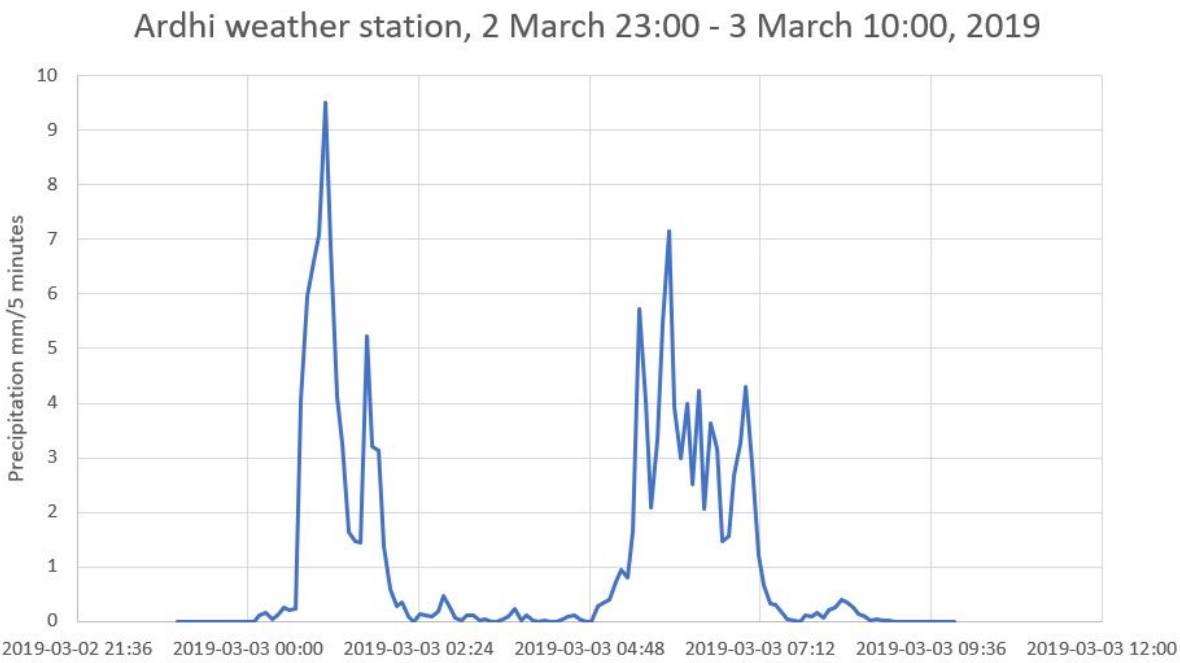

Figure 4.12: Precipitation data that serve as forcing to the model.

4.2 Collected data sets

This section describes the surveys conducted by the author to collect data on flood depth and solid waste blockages in the study area. The survey was performed around noon on 3 March 2019 in Alimaua A, Alimaua B, Mpakani A and *mtaa wa* Kijitonyama. The survey could not be carried out in Bwawani, as no survey permission was obtained from the *mtaa* office there. Eight mappers participated in the survey, including 6 experienced drainage mappers, HOT Tanzania's driver, and the author. The mappers were guided by field maps (see appendix B) that show which streets to prioritise in the survey. The aim of this priority was to focus on areas only exposed to pluvial flooding. This was concluded by examining the topography in the DTM and verified by a "threats and assets" report[7] written by *Ramani Huria*, that indicate which areas that are exposed to fluvial floods. Fluvial floods are mainly a problem around the streams in Alimaua A and B. The surveys were recorded using XLSForms, KoBo Toolbox and the ODK application as described in section 3.2.2.

4.2.1 Flood extent survey

Community reports on flood depth can be used to validate model outputs. A flood extent survey was performed in Kijitonyama based on the methodology applied by *Ramani Huria*, which first will be described briefly. *Ramani Huria* performed flood extent surveys in the Msimbazi river basin in 2017 and 2018, focusing on the areas prone to fluvial flooding and flash floods. Hence, Kijitonyama was not covered in this survey. The following questions were asked by *Ramani Huria*:

- Have you ever had a flood in this area where you live now?
- What year was this flooding event?
- How deep was the water in centimetres?
- Do you know what caused the flood?
- What do you think caused the flooding?
- Have you moved settlement because of flooding?
- What year did you move settlement because of the flooding?

[7]An example of how a threats and assets report is developed is found here: http://ramanihuria.org/community-meetings-for-flood-resilience-plan/

In the data collected in 2017, the information on water depth is given in centimetres. When studying this data, it appears that it is of low quality, as many data points possibly are given in millimetres or meters instead of centimetres, and some data points have unrealistic values. The data collected in 2018 overcomes this problem, by letting the respondents referring the water depth to a person's height instead of estimating it in centimetres. As this data is consistent, with all reports being realistic values, this person's height reference system is also applied in the performed flood extent survey. Furthermore, the option "only puddles" is added, as high land areas like Kijitonyama might not get any standing water during storm events. Table 4.3 presents the person's height reference system.

Table 4.3: Person's height reference system, developed by *Ramani Huria*. The option "only puddles" is added by the author.

Reported depth	Water depth in cm	Median (cm)
Only puddles	0	0
Finger depth	0-2	1
Ankle depth	2-10	6
Mid-shin depth	10-30	20
Knee depth	30-50	40
Waist depth	50-100	75
Chest depth	100-150	125
Person's height	150-200	175
Over person's height	+200	200

Furthermore, the questions are modified to capture the effect of pluvial rather than fluvial flooding, and focus on the rain event in the morning 3 March 2019. The questionnaire of the flood extent survey is presented in appendix A.1.

4.2.2 Solid waste blockages survey

When performing the flood extent survey described above, the mappers recorded blocked drainage segments along their way. The questionnaire of the blockages survey is presented in appendix A.2, recording extent and type of blockage. Note that it was not possible to cover the whole study area to detect all current solid waste blockages with available resources.

Chapter 5

Model

The flood model developed in this chapter is built in the software SOBEK[1], version 2.16. This program is selected as it allows for coupled 1D-2D models, which is necessary to answer the research questions of this thesis. It is also of importance that it is relatively easy to implement open drains in SOBEK, as the majority of the drainage in Dar es Salaam consists of open channels. Observation points will be inserted in the 2D schematisation of the model, and it will be studied how the water depth changes when the *Ramani Huria* drainage data is implemented in the 1D schematisation. By comparing this change with the results from the flood extent survey, it will be possible to observe if community mapped drainage data can improve flood predictions on neighbourhood scale.

SOBEK is not an open source software, which is desirable when working with open source data. To the best of the author's knowledge, there is currently no open source hydrodynamic software that can perform coupled 1D and 2D computations. There are, however, open source programs that allow for 1D schematisations only, where *Ramani Huria*'s drainage data can be implemented. This is a topic for future research.

Two limitations with SOBEK has been encountered in the model setup. Firstly, it has no infiltration module. This means that soil infiltration is not taken into account, and all precipitation is assumed to contribute to surface runoff or evaporate. This might be unrealistic for the modelled event, as the soil was dry and thus had a considerable infiltration capacity at the beginning of the event. On the other hand, the event was intense, so the precipitation rate might have exceeded the soil infiltration rate. Secondly, SOBEK only allows for spatially uniform rainfall. This is not considered to be a problem as the study area is small. Ardhi weather station is situated approximately 2 km away, and the study area is around 2.3 km^2. This offers sufficient accuracy, given the exploratory character of this research.

This chapter describes the development of the 1D schematisation, followed by the 2D schematisation. The chapter ends with a presentation of the scenarios that will be run with the model to answer the research questions.

[1] https://www.deltares.nl/en/software/sobek/

5.1 1D schematisation

This section explains how the *Ramani Huria* drainage data is prepared and processed to become suitable for hydrodynamic modelling. A detailed description of this process is provided in appendix C. After performing the additional data cleaning described in section 4.1.2, the drainage network is imported as a shapefile in SOBEK. The location of the drainage is represented by the geotraces recorded with the ODK application. The segments are connected with *flow connection nodes* added by SOBEK. When the drainage data was imported in SOBEK by the author, it was noted that many segments were disconnected from the rest of the network, despite the efforts to make a connected network in the data cleaning process. Upon further inspection in QGIS, it was concluded that what here will be called *T-junctions* are perceived as disconnected by the modelling software. This section starts with explaining how to solve the problem with T-junctions.

5.1.1 Adjustment of T-junctions

A T-junction occurs when a geotrace is passing the end of another segment, where the geotrace in fact should have been split in two parts to be perceived as connected to the other segment by modelling programs with GIS network standards. In figure 5.1 a disconnected segment (in yellow) is shown to the left. To the right, a functioning junction is shown; the red, yellow and black segments are three different geotraces.

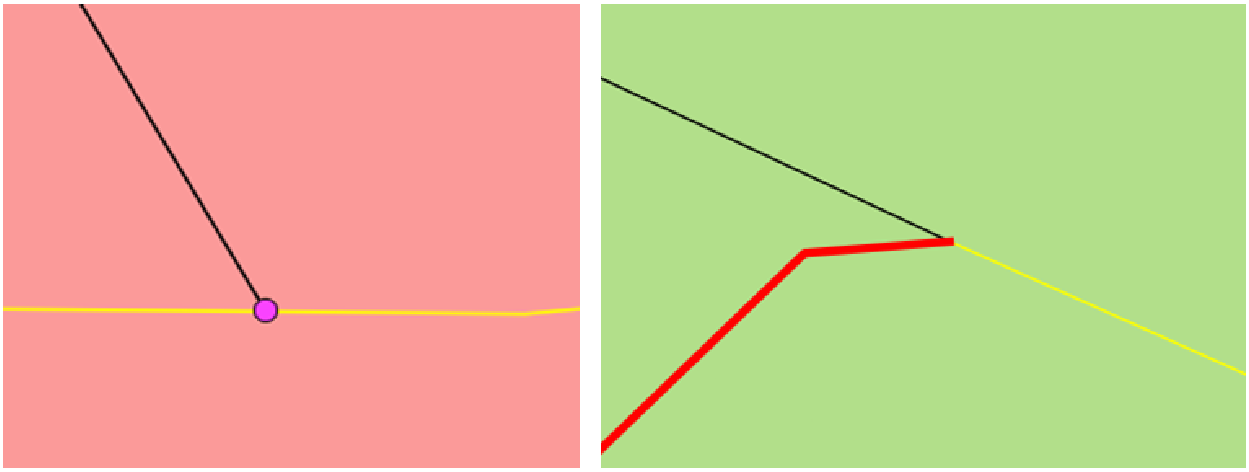

Figure 5.1: A disconnected T-junction (to the left) and a connected junction.

This is a common problem in the data set. 36 T-junctions were found in the study area, see figure 5.2. For this thesis, the problem is solved manually by splitting the segments at T-junctions with *split features* in QGIS. For future drainage mapping surveys, a new geotrace should be started every time a segment intersects with another segment. If this is not done in the field, it can be corrected in the data cleaning process. When all T-junctions had been connected, the number of segments in the study area had increased from 532 to 560 segments.

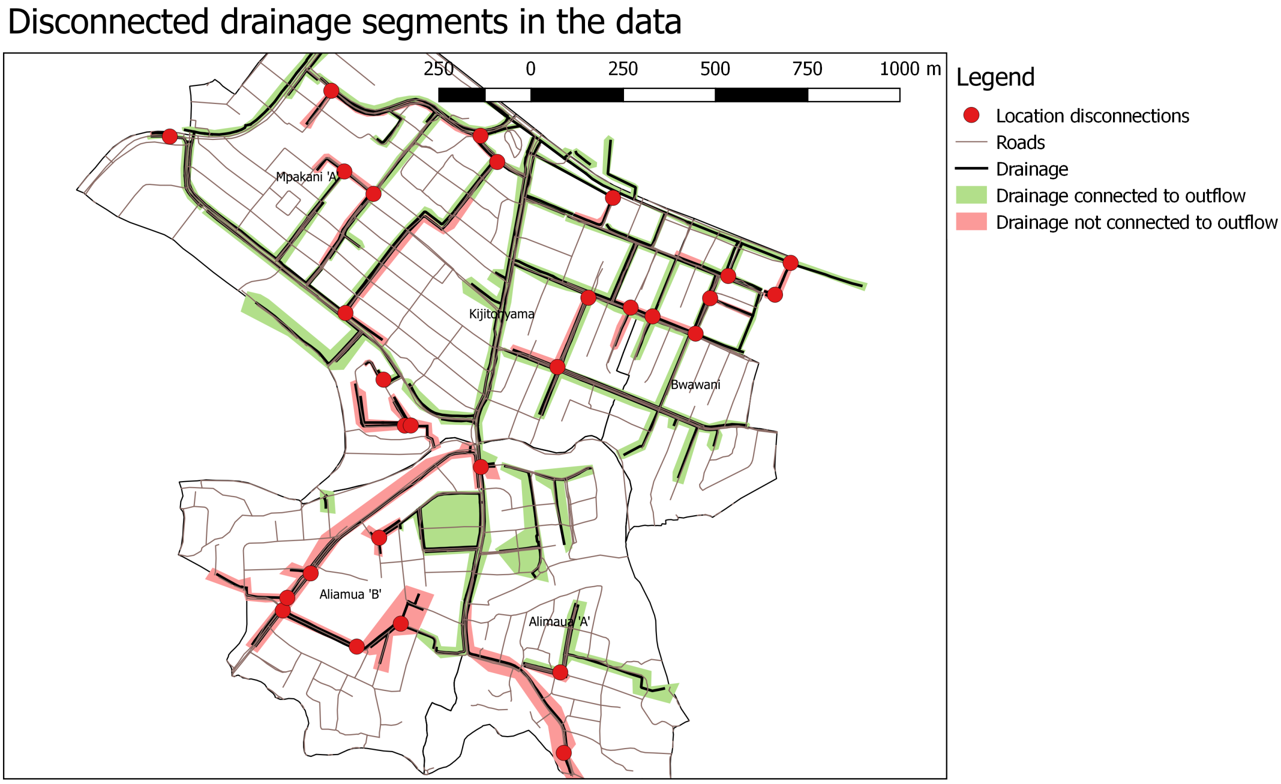

Figure 5.2: Disconnected segments due to T-junctions.

5.1.2 Location of cross sections

After assuring that all junctions consists of at least 3 geotraces, the drainage network is imported as shapefile in SOBEK. The first step is to implement the cross sections of the segments at the correct location, which later will be assigned with data on cross section profile and friction. The drainage network in Dar es Salaam consists mainly of open drains, that are often interrupted by culverts or small bridges to let pedestrians and vehicles cross over. This constant change of cross section type poses a challenge to SOBEK, as the program can not interpolate hydraulic energy slopes between two different cross section types. This means that each segment must have two cross section locations assigned. Figure 5.3 shows an example of a culvert located between two open drains in SOBEK. The pink circles are flow connection nodes between the segments, and the blue symbol represents a cross section location. As can be seen, each segment has been assigned with two cross sections, one at each end.

Each cross section has an unique ID, that is the ID of the segment that it is assigned to, plus the suffix "*_ds*" or "*_us*", depending on if it is at the downstream or upstream point of that segment. The cross section locations are prepared as a shapefile in QGIS, and then imported as *reach elements* in SOBEK. How to prepare this shapefile in GIS is described in appendix C.3. This operation was performed with ArcGIS. The necessary geo-processing tools are available in QGIS as well[2], but unfortunately QGIS fails to perform the task with sufficient accuracy.

[2]QGIS is an open source software, whereas ArcGIS is not.

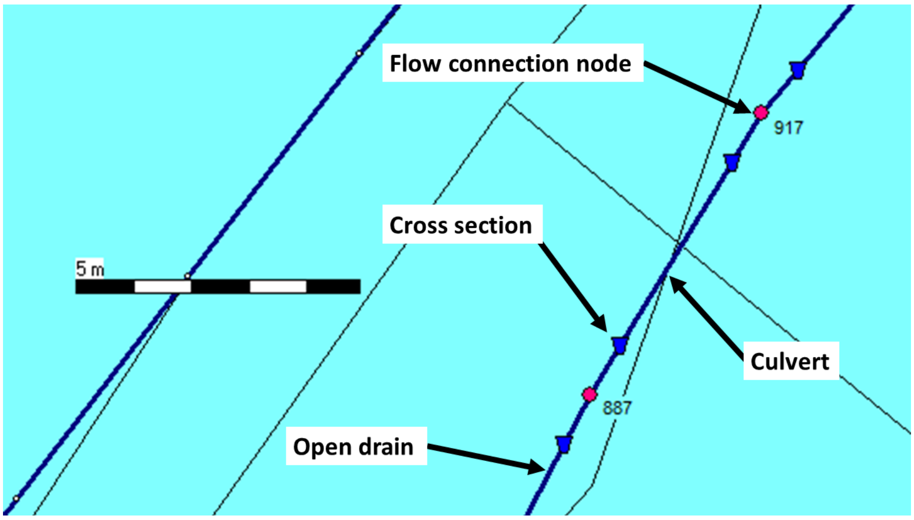

Figure 5.3: Imported drainage segments in SOBEK.

5.1.3 Representation of cross sections

The next step is to assign a cross section profile to each cross section location. This operation is dependent on the requirements of the modelling software that is used, and no general methodology for this step can be proposed here. For this thesis, the preparation is done with a macro activated Excel sheet (*.xlsm*) that was accessed from Deltares research institute. The *Ramani Huria* drainage data is exported as *.csv*-file from QGIS, opened in Excel and then saved as a *.xlsx*-file. Then the data is copied from this file to the *.xlsm*-file. Each segment ID is pasted twice, and given the suffix "*_ds*" or "*_us*", representing the cross section located at the downstream and upstream end of the segment. Then the bed level, surface level and dimensions of the segment are assigned. Appendix C.4 explains how to derive the bed level and surface level for each upstream and downstream point from the digital terrain model. Figure 5.4 show the attributes needed to describe round cross sections, here culvert 223 and 225, in the *.xlsm*-file.

General				Parameters		
ID	Name	X	Y	Bed level	Surface level	Diameter
223_ds				24.06	24.96	0.5
223_us				24.07	24.97	0.5
225_ds				24.79	25.49	0.8
225_us				24.80	25.50	0.8

Figure 5.4: Preparing cross section profiles for culverts in Excel.

All other cross sections, i.e. rectangular, trapezoidal and elliptical, that can be either open or closed, must be described as tabulated profiles. The cross section is constructed in table form by inserting rows with the width at the bed level and the surface level. If the segment is closed, this is described with an extra level added 1 cm above the surface level, where the width is set to 0. It is assumed that the flow width equals the total width, i.e. that the water can flow through the whole cross section of the segment. Figure 5.5 shows an example on how to describe an open trapezoidal (ID 222) and closed trapezoidal (ID 224) cross section as tabulated profile.

The Excel sheet writes SOBEK datafiles (*.dat*) that are moved to the work folder of SOBEK. In this way, the IDs of the cross section locations are matched with the IDs in the *.dat*-file, and each cross section location is assigned with its correct cross section profile.

ID	X	Y	Surface Level	Bed Level	Total Width	Flow Width
222_ds			26.46	25.86	0.5	0.5
222_ds			26.46	26.46	1	1
222_us			27.41	26.21	0.5	0.5
222_us			27.41	27.41	1	1
224_ds			23.76	22.96	0.5	0.5
224_ds			23.76	23.76	1	1
224_ds			23.77	23.77	0	0
224_us			24.96	24.06	0.5	0.5
224_us			24.96	24.96	1	1
224_us			24.97	24.97	0	0

Figure 5.5: Preparing open and closed tabulated profiles in Excel.

5.1.4 Dimensions of decommissioned drains

There are 14 drainage segments along Mabatini road in Kijitonyama that are reported as *decommissioned* in the *Ramani Huria* data set, with no dimensions recorded. The location of these segments is shown in Figure 5.6.

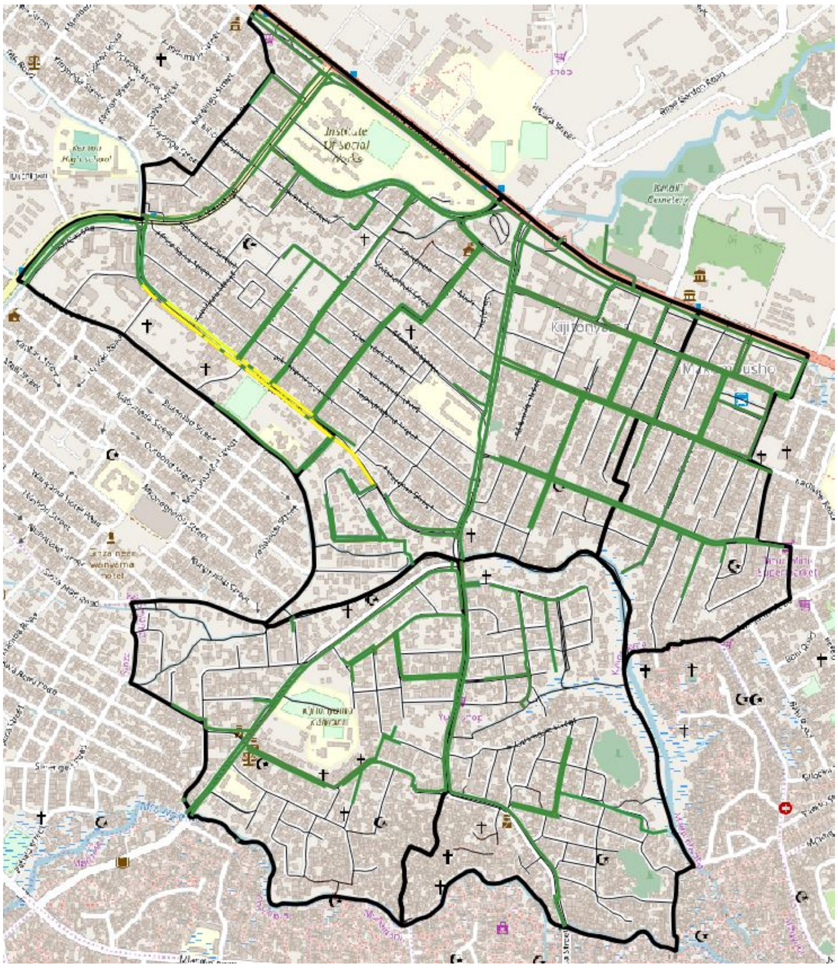

Figure 5.6: Decommissioned drains along Mabatini road in Mpakani A, highlighted in yellow.

It is not known why the segments were reported as decommissioned. Fieldwork showed that these drainage segments are ditches that have a considerable conveyance capacity that can not be neglected in the 1D schematisation. Hence, the dimensions of these segments were measured manually. The 9 segments on the south side of the road were recorded as trapezoidal ditches. This cross-section type is not applied in the *Ramani Huria* survey, but was considered as the most realistic representation of the segments. Due to time constraints, only the top width and depth were measured of each segment, and the bottom width was assumed to be 20% of the top width. One ditch on the north side has a rectangular cross section and was, hence, added to the other ditches in the *Ramani Huria* data set. The 4 remaining segments on the north side were kept as decommissioned, as these ditches are full of vegetation. This distinction was done as the drain types *ditches* and *decommissioned drains* are given different friction values in the model setup, see below.

5.1.5 Friction of segments

Each segment is assigned with a friction value corresponding to the material reported by *Ramani Huria*. As mentioned above, the decommissioned drains are lacking material data, but it was observed during field work that they are ditches with abundant vegetation. Most of the ditches are also lacking material data, but 3 ditches are reported as *sand*. Hence, it is assumed that the remaining ditches are also made of sand. In total, 8 different segment materials are present in the study area. These materials and their assigned friction value are shown in table 5.1. Manning roughness values are assigned, as this is widely applied with empirically derived values for many different materials. A Chézy coefficient is then calculated in the computation by SOBEK, see section 2.3.3.

Table 5.1: Assigned manning roughness coefficients for reported materials. From [71]. A qualitative description of the concrete classes is found in table 4.2.

Reported material	Amount (%)	Manning roughness coefficient s/m$^{1/3}$
Concrete class 1	428 (77%)	0.02
Concrete class 2	79 (14%)	0.025
Concrete class 3	19 (3%)	0.03
Rock	38 (0.5%)	0.04
Decommissioned (with abundant vegetation)	4 (0.7%)	0.1
Sand	23 (4%)	0.02
Steel (corrugated)	1 (0.2%)	0.02
Plastic (assuming it is PVC)	1 (0.2%)	0.01
Other (assumed to be concrete class 1)	2 (0.4 %)	0.02

The allocation of friction values was done with a Python script. An example of how this can be done is shown in appendix C.6. Figure 5.7 shows the distribution of building materials of the drainage in the study area.

5.1.6 Adjustment of bed levels

When inspecting side views of the drainage segments in SOBEK, it was noted that the bed level of the network, over all, is irregular. Many jumps in the bed levels are present, see figure 5.8. Recalling section 4.1.1, the bed level of a segment is calculated by subtracting the measured elevation from the DTM value, and the surface level by adding the measured depth to the bed level. This is done for each downstream and upstream point of a segment, see C.4. The drainage mappers measure the elevation after they have recorded a geotrace. As they trace the segments from the downstream to the upstream point, the elevation is measured at the upstream point of each segment. This elevation difference between the bed level and the reference road might not be constant along the whole segment, especially not if the segment is long. The bed levels seen in figure 5.8 are calculated from the same DTM value, that is sampled where the segments connect. Apparently, the recorded elevation of the left drain is lower than the one for the right drain, which introduces a gap. However, the elevation of the left drain was not measured at the connection displayed in the picture, but at the upstream point of the left drain. Maybe the elevation of the left drain, in fact, is higher at the connection displayed in the picture, which would have been captured if the elevation was measured before the geotrace was recorded.

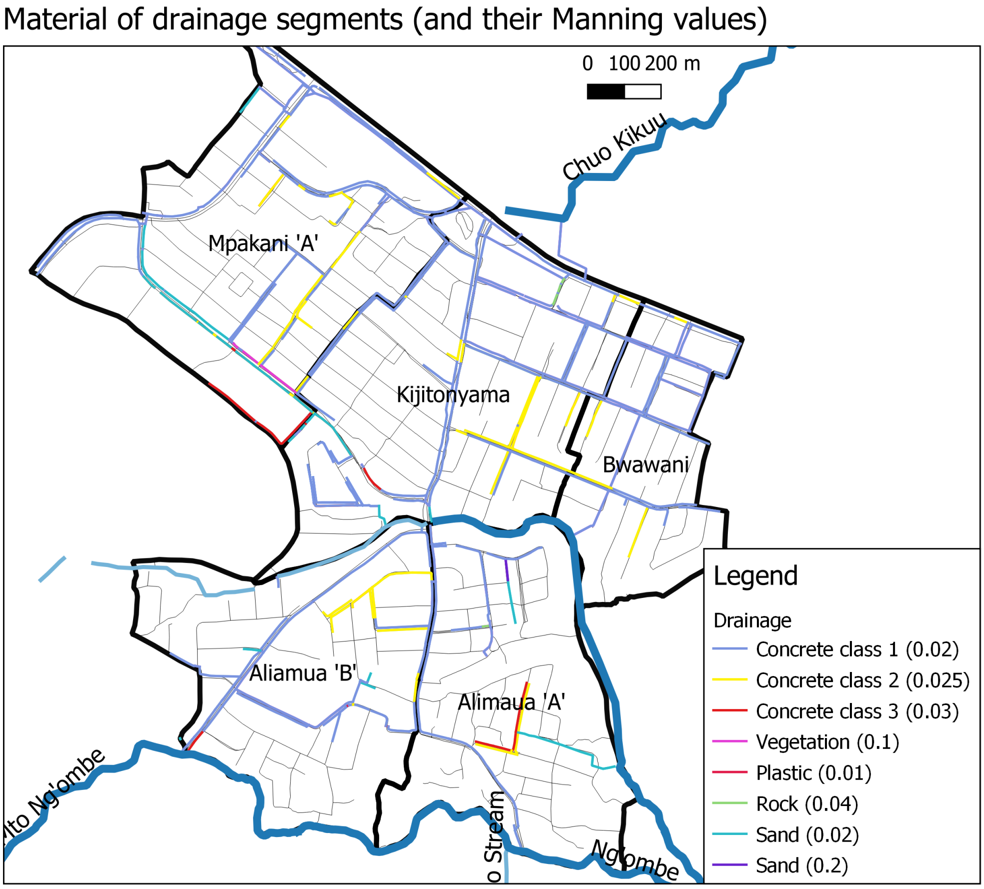

Figure 5.7: Drainage materials and Manning values.

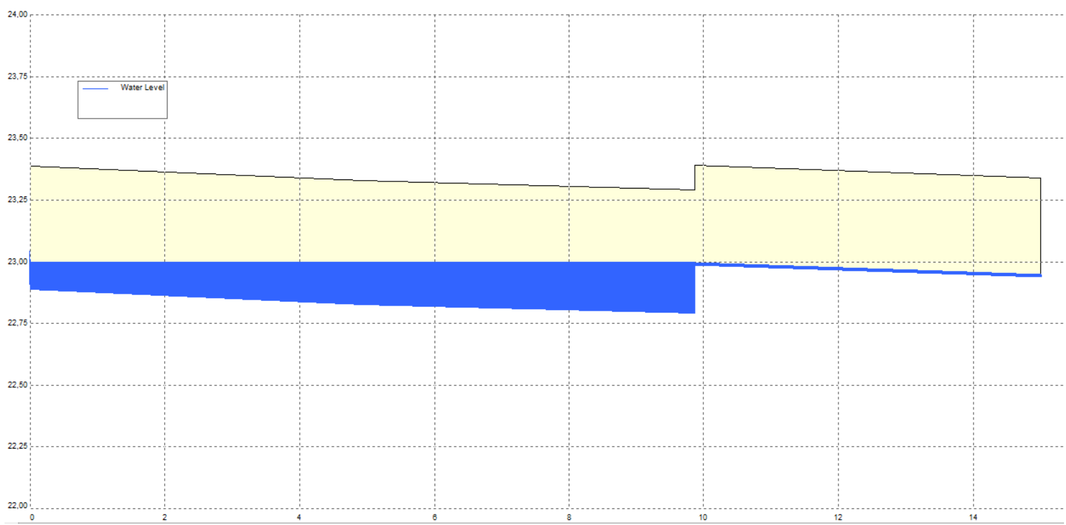

Figure 5.8: Example of irregular bed levels.

The gap shown in figure 5.8 might represent reality, but given that these gaps are present at almost every connection in the whole data set, it is expected that the elevation measurements introduce a systematic error when assuming that the elevation is constant along the whole segment. It seems more realistic to assume that the bed level is smooth at each connection point. As the elevation is measured at the upstream point of each segment, the upstream bed levels are most likely to represent the actual bed levels. Hence, a Python script was written that adjusts the downstream bed level of each segment to the upstream bed level of the segment that is downstream of it[3], see appendix C.5. In figure 5.8, this means that the downstream bed level of the left drain is being set to the upstream bed level of the right drain. This result is shown in figure 5.9.

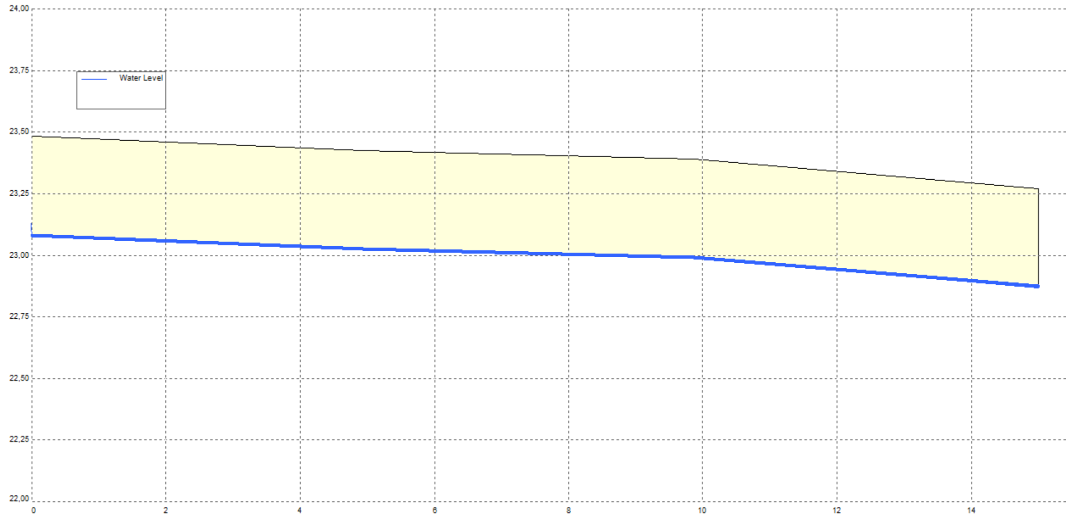

Figure 5.9: The same segments as in figure 5.8, after adjusting the bed levels.

This approach works satisfactory for long drains, but it was noted that culverts systematically have a slope against the direction of flow when the adjustment described above have been done, see figure 5.10.

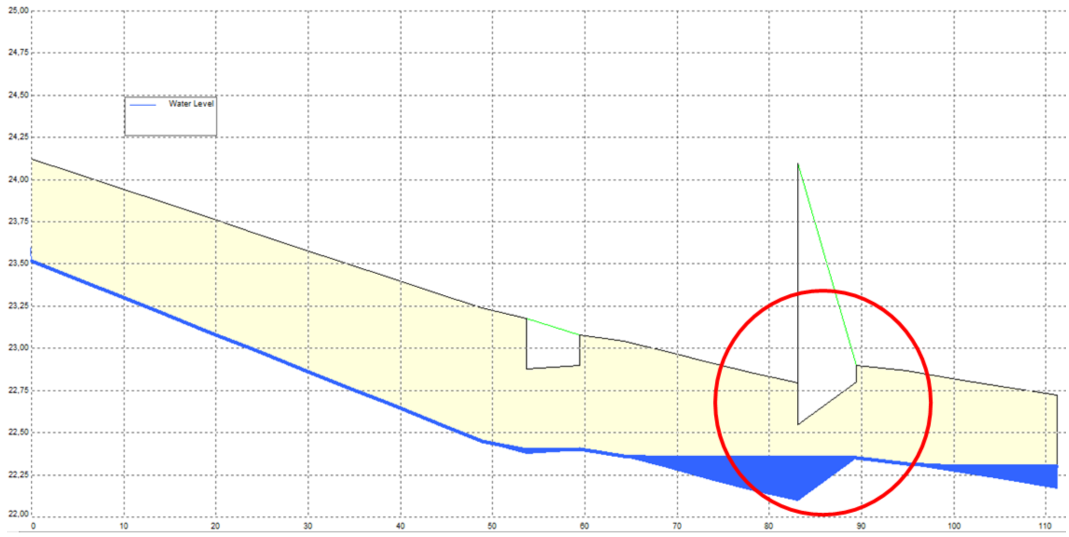

Figure 5.10: A culvert with slope against the direction of flow after adjusting the bed levels, due to a local depression in the DTM.

This behaviour probably occurs because most culverts are around 5 meters long, which is also the resolution of the DTM. If the drainage segments span over several grid cells in the DTM, the likelihood increases that the general slope of the ground is captured, but the culverts are very sensitive for local depressions in the DTM as it only spans over one or two grid cells. Therefore, it was decided to perform another step in the adjustment of the bed levels; to assume that culverts are almost straight, with a slope of 0.2%. This seems realistic to assume, as the culverts usually are situated below roads that pass over open drains. An example of this adjustment is shown in figure 5.11. A few very long culverts in the study area were removed from this operation by setting their drain type to *drain* instead of *culvert*.

[3] Yes, this is confusing.

The segments that have been shifted upwards in the adjustment, and is recorded as deeper than their downstream segments, now have their downstream surface level above ground. This is checked by subtracting the surface level value from the DTM value at each downstream point, and this occurs 100 times. The majority of the surface levels are, however, only a few centimetres above the ground level. In these cases, the downstream surface level is set to the DTM value. An example of this is shown in figure 5.11.

In 6 cases, the surface level is more than 1 meter above the ground level. It was also controlled if any downstream bed levels has a higher elevation than the upstream bed level of the same segment. This appears 77 times. In 7 cases, the elevation difference was more than 1 meter. These 13 locations were inspected, and it could be concluded that extreme elevation errors are caused by:

1. *Local depressions in the DTM.* The ground level in the study area is, on average, higher in the west and lower in the north east. Some segments do, however, transport water against this direction, and these local variations can not be captured with a resolution of 5x5 meters in an urban environment.
2. *Segments that are bordering thalwegs.* The ground slope is steep close to natural water courses, which make segments in these areas prone to errors when deriving the bed levels from the DTM.
3. *Wrong mapping direction.* In a few cases, it appeared that the drainage mappers had recorded the geotrace against the direction of flow, which explained why the downstream bed level had a much higher elevation than the upstream bed level.

A few extreme errors were changed manually. It was prioritised to avoid local depressions close to outflow points in the network, to avoid unrealistic back water effects in the model simulation. It was also controlled that all segments connected to an outflow point, i.e. discharging into a natural watercourse, did not have local depressions. Figure 5.12 shows the outflow points in the study area where the drainage network connects to a natural water course or flows out of the model space.

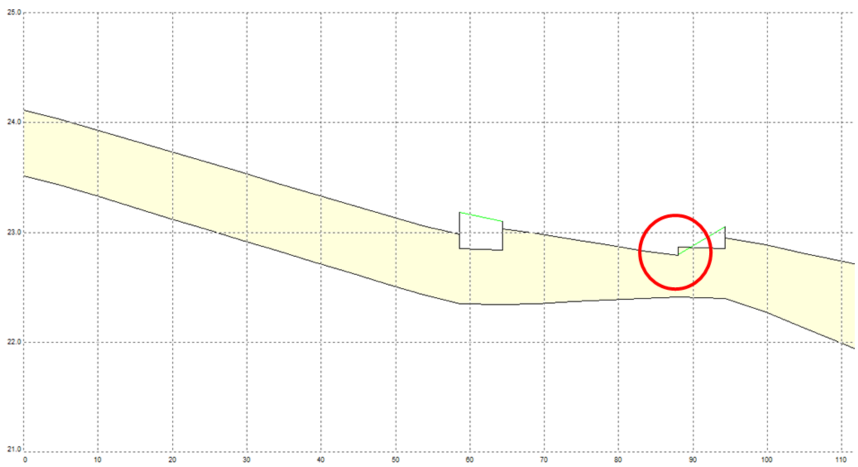

Figure 5.11: The same segments as in figure 5.10, after assuming that all culverts have a slope of 0.2%. The red circle shows an example where the downstream surface level have been adjusted to the DTM value. Compare with the local depression in figure 5.10.

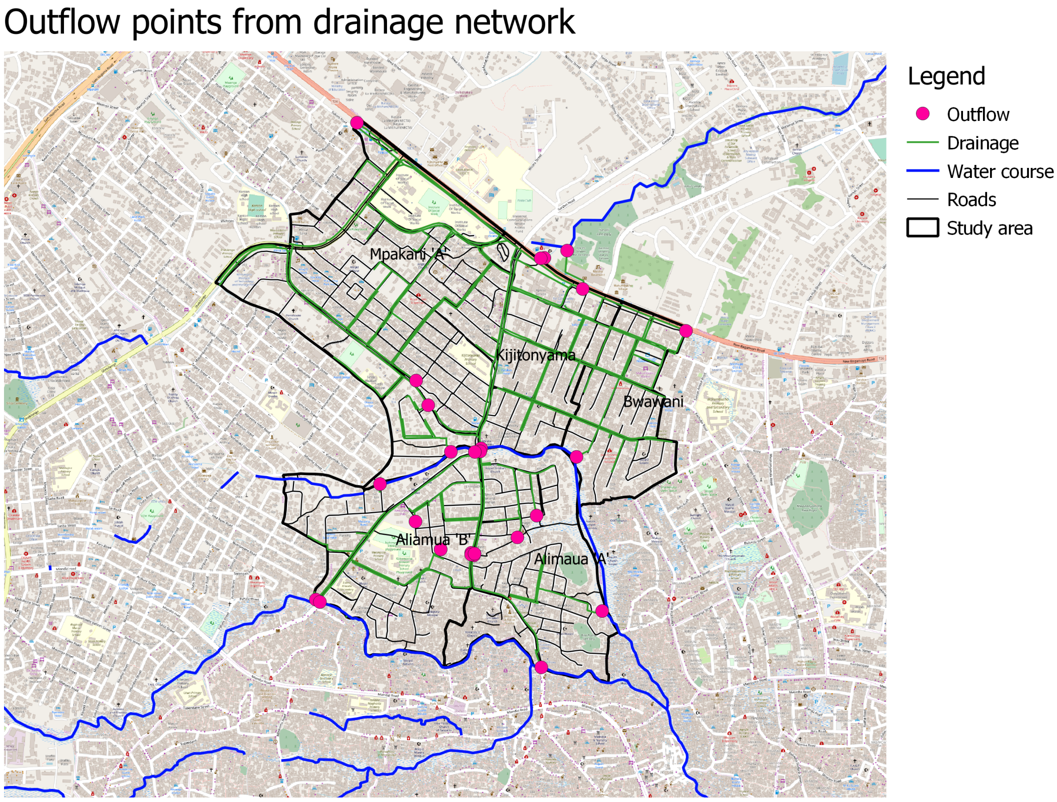

Figure 5.12: Outflow points were the drainage network connects to a natural water course or flows out of the model space.

5.1.7 Settings for 1D module in SOBEK

This section summarises the settings in for the 1D schematisation in SOBEK.

- As Ardhi weather station records precipitation with 5 minutes resolution, the computational time step is set to 5 minutes. The simulation period equals the duration of the modelled event, see section 4.1.4.
- The output time step is set to 15 minutes, saving water depth, velocity and discharge for each output time step.
- The initial condition is set to *completely dry system*, as the modelled storm event was preceded by five weeks without rain.
- The calculation grid is set to 5 meters.
- The runtime parameters is set to a typical *rural schematisation*. This is chosen because it is suitable for hydrodynamics in open water systems, whereas the *urban schematisation* is developed for closed sewer pipes[4].

[4] SOBEK user manual, version 1.00

5.2 2D schematisation

This section explains the components in the 2D schematisation of the model.

5.2.1 Boundary conditions

Two upstream discharge boundary conditions are implemented in the 2D schematisation of the model. The discharge data is taken from TAHMO's hydro station at Ubungo bridge. The measured discharge during the modelled event is shown in figure 5.13.

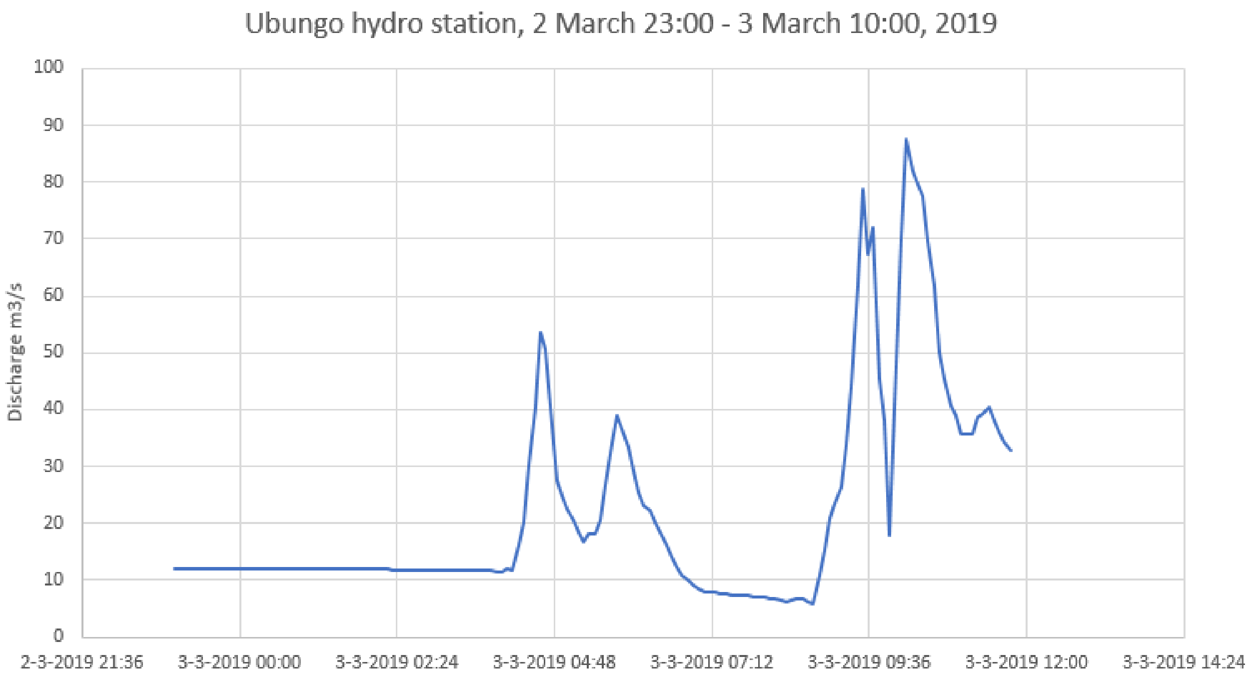

Figure 5.13: Discharge data from Ubungo bridge during the modelled event.

The locations of the hydro station and the boundary conditions in relation to the study area are shown in Figure 5.14. At upstream boundary condition 1, the discharge from the Ubungo hydro station is applied. The discharge at upstream boundary condition 2 was estimated by the author around noon 2 March 2019, before the modelled event. This was done using a float and stop watch and multiplying the surface water velocity with the estimated cross section area of the water course [82]. The flow was estimated to be very low, around 0.05 m^3/s. This was assigned as the initial value of the flow at boundary condition 2, and then the discharge data from Ubungo hydro station was re-scaled to this initial value, keeping the variance constant. The downstream boundary conditions were both set to a constant water level of 0.5 m, meaning that the runoff flows out of the model space when the water depth exceeds 0.5 m in the grid cells at the boundary condition.

5.2.2 Land roughness

For this thesis, a constant land roughness is assumed for all grid cells. Deltares research institute has built a flood model of the Msimbazi river basin on catchment scale, where they defined land roughness values based on land use data that was downloaded from OSM. They set the Manning roughness coefficient to 0.2 $s/m^{1/3}$ for *buildings*, which is selected for this model as it is assessed to be the most common land use type in the study area. For future models, it is recommended to derive land roughness values per grid cell from land use data from OSM.

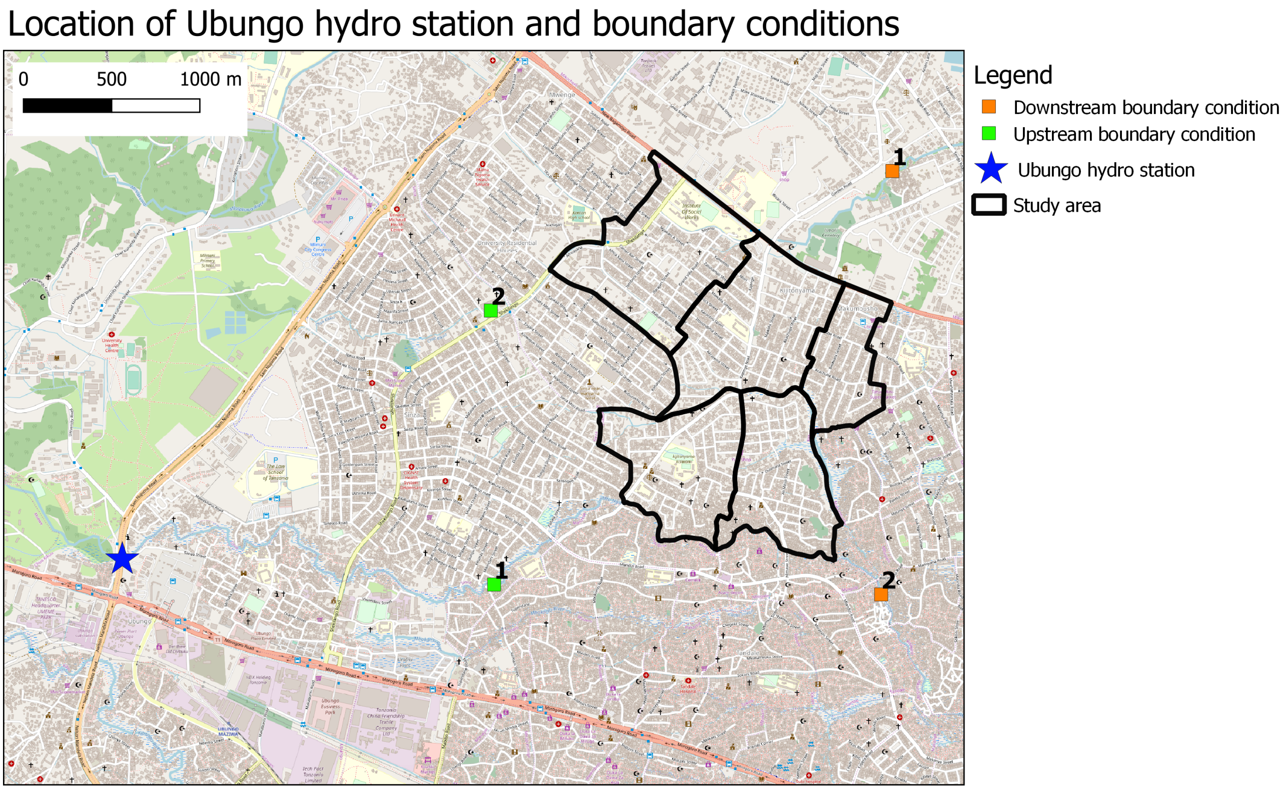

Figure 5.14: Locations of Ubungo hydro station and boundary conditions.

5.2.3 Observation points

Observation points are inserted in the 2D schematisation to record how the simulated water depth changes for the different scenarios presented in section 5.3. The locations of the observation points are identical with the 44 geopoints that were recorded in the flood extent survey, see section 4.2.1. In this way, it will be possible to compare how the water depth in the simulations correlates with community members' reports on flood depth. The locations of the observation points and their labels are shown in figure 6.4 in chapter 6.

5.3 Scenarios

This section seeks to explain the scenarios that will be run with the model in SOBEK to answer the research questions of this thesis. All scenarios are run with the precipitation data presented in section 4.1.4 as forcing. Furthermore, the wind speed is set to 0 m/s and the evaporation to *long-term average* in the *Meteorological data* task block in SOBEK.

5.3.1 Scenario 1

Scenario 1 is run with only the 2D schematisation as described in section 5.2, without the *Ramani Huria* drainage network. The output will be used as bench mark to the result of scenario 2c (see below), to assess the impact of community mapped drainage data on flood predictions.

5.3.2 Scenario 2

Scenario 2 aims to investigate the contribution of community mapped drainage data to flood predictions on neighbourhood scale. The 2D schematisation is identical with scenario 1, but now the 1D schematisation is implemented as well. The scenario is divided into three sub-scenarios, to examine the effects of adjusting the bed levels, and assigning distributed friction values.

Scenario 2a

Scenario 2a is run with the drainage network in its original state, before adjusting the bed levels as described in section 5.1.6. Here, all segments are assumed to have the same friction value. As 76% of all segments are reported as concrete class 1, see table 4.2, it seems most realistic to assign this friction value to all segments, i.e. 0.06 $s/m^{1/3}$. Scenario 1 ans 2a will be compared to see how the implementation of the 1D network influence the model output, see section 6.2.2.

Scenario 2b

This scenario is run with adjusted bed levels, including straight culverts, as described in section 5.1.6. The friction value is constant for all segments, as in scenario 2a. Scenario 2a and 2b will be compared to see how the adjustment of the bed levels influence the model output, see section 6.2.3.

Scenario 2c

Scenario 2c investigates the added value of distributed friction values in the 1D schematisation. It is run with adjusted bed levels as scenario 2b, but each segment is assigned a friction value that corresponds with its recorded material, as explained in section 5.1.5. Scenario 2b and 2c will be compared to examine how distributed friction values influence the model output, see section 6.2.4.

5.3.3 Scenario 3

Once the model built with *Ramani Huria* drainage data is developed and validated with scenario 1 and 2, it will be applied to investigate the impact of solid waste in the drainage system on floods. This will be done with two sub-scenarios. The model is run with the 2D schematisation described in section 5.2, and the 1D schematisation with adjusted bed levels and distributed friction values.

Scenario 3a

This scenario is run with the same 1D schematisation as scenario 2c, but the segments that were reported as blocked in the blockage survey, see section 4.2.2, are closed according to the results of the survey. This aims to investigate the impact of solid waste accumulation on floods. The blockages were recorded around noon the day after the simulated event, 3 March 2019. The mappers reported blockages along their way, see field maps in appendix B. It was not possible to cover all blockages in the study area with available resources. The segments that were reported as 100% blocked were removed from the model schematisation. For the segments that were reported as 50% or 75% blocked, the cross sectional area was reduced to 50% and 25% of the original cross section area, respectively. For round culverts, the diameter was adjusted, and for all other cross sections, the depth was decreased. The results of scenario 3a will be compared with scenario 2c, see section 6.3.1.

Scenario 3b

During fieldwork in Kijitonyama, it was noted that culverts often get blocked by solid waste. Figure 5.15 shows an example.

The final scenario is of experimental character, and investigates how blocked culverts affect flooding. A third of all segments in Alimaua A and B, 17 culverts, were selected randomly and removed from the 1D schematisation. Figure 5.16 show the culverts that are simulated to be 100% blocked in this scenario. As Alimaua A and B are hydraulically disconnected from the rest of the study area, it seems reasonable to limit this research to only these two *mitaa*. The result is presented in section 6.3.2.

Figure 5.15: Culvert blocked by plastics the morning after the simulated event.

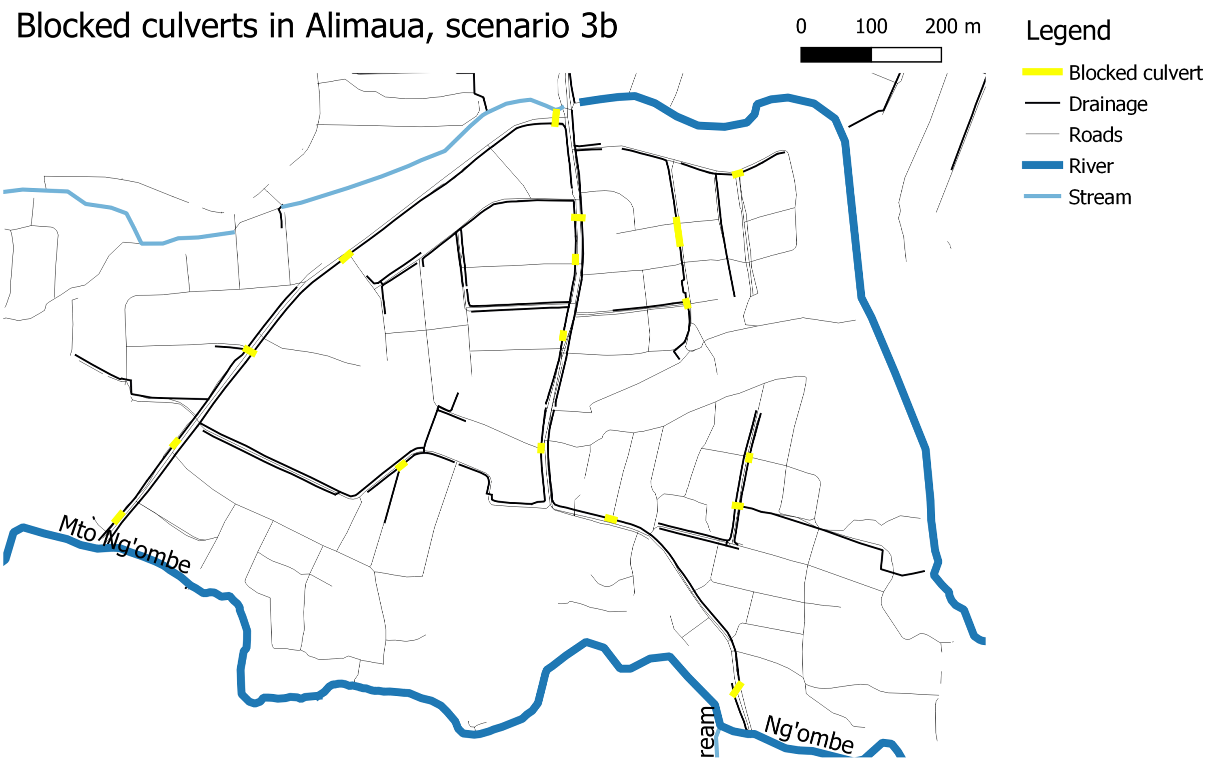

Figure 5.16: Culverts, selected randomly, that are 100% blocked in scenario 3b .

Chapter 6

Results

This chapter presents the results of the simulations presented in section 5.3. It begins with the outcome of the flood extent- and blockages surveys, see section 4.2.1 and 4.2.2. Then follows the results of scenario 1-3 with additional analyses.

6.1 Survey results

This section presents the results of the flood extent- and blockages survey, carried out in the study area around noon on 3 March 2019. The questionnaires used in these surveys are shown in appendix A.

6.1.1 Results flood extent survey

Figure 6.1 shows the flood depth as reported by 44 respondents during the flood extent survey. Most respondents report that there was *only puddles* on the street the same morning. Not surprisingly, respondents along streets without drainage report a deeper flood depth. In general, the water is reported as deeper towards the north end of Mpakani A, *mtaa wa* Kijitonyama and Bwawani. This is expected, due to the ground slope towards north east. In the middle of Alimaua, there is a cluster of respondents that report a deeper flood depth. The consistency of these reports indicate that it indeed were considerable water levels here. It should be noted that there is a small stream flowing from west to east in the middle of Alimaua, that is not mapped on OSM.

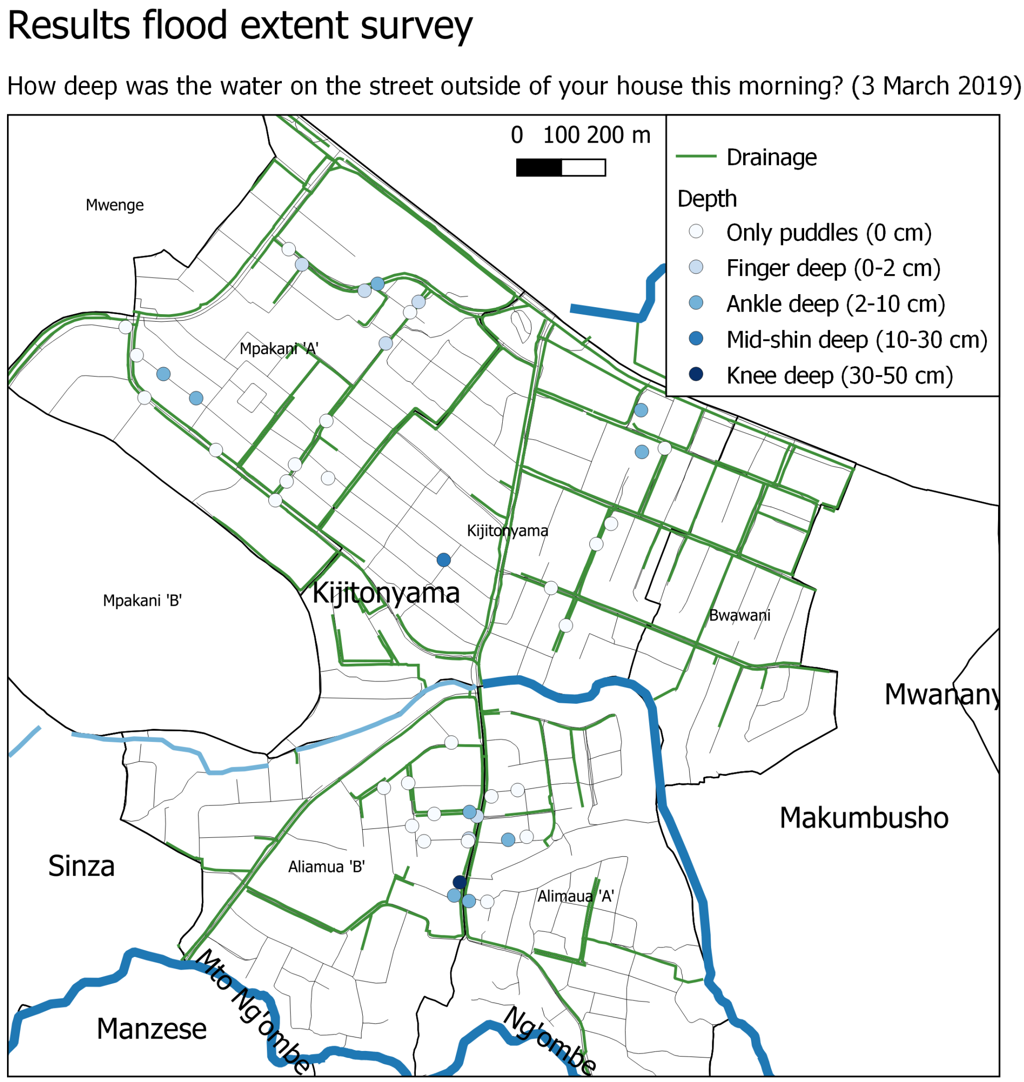

Figure 6.1: Answers to the question: How deep was the water on the street outside of your house this morning (3 March 2019)?

6.1.2 Results solid waste blockages survey

Figure 6.2 show the types of blockages in drainage segments that were reported 3 March 2019. Note that it was not possible to cover the whole study area to detect all current solid waste blockages with available resources. The survey form only included *solid waste* and *sand* as predefined blockage types. The drainage mappers identified the following other types of blockages:

- Broken drain
- Building materials and vegetation
- Tree roots
- Vegetation

Different types of blockages, and how these potentially influence the conveyance capacity of the drainage, is a topic for future research. For this thesis, only the degree of blockage is taken into account. Figure 6.3 show to what extent the drainage segments were blocked.

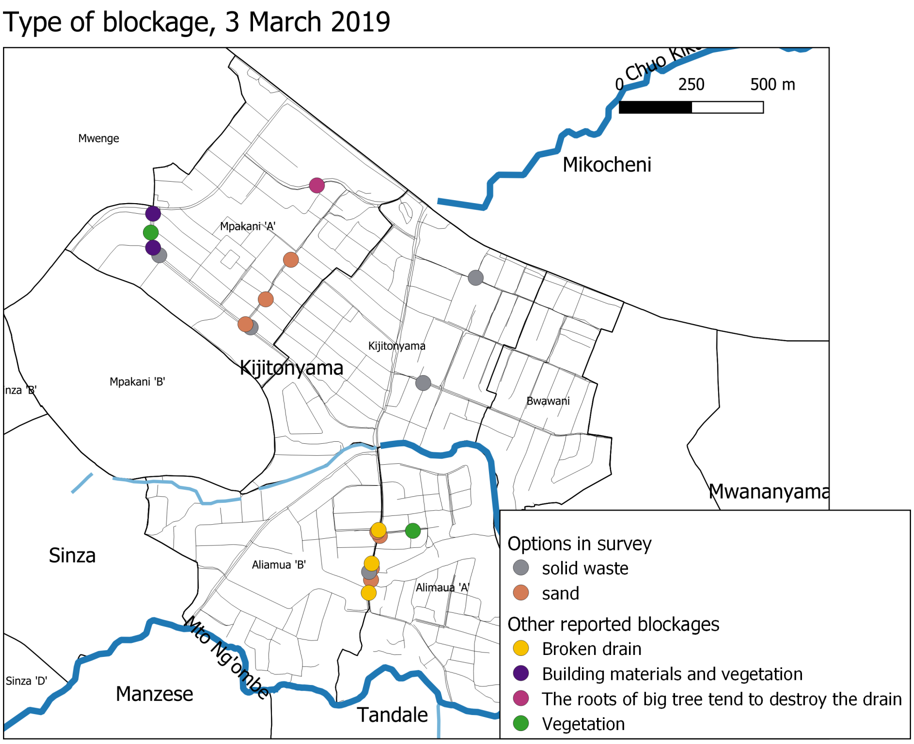

Figure 6.2: Type of blockages recorded in the survey.

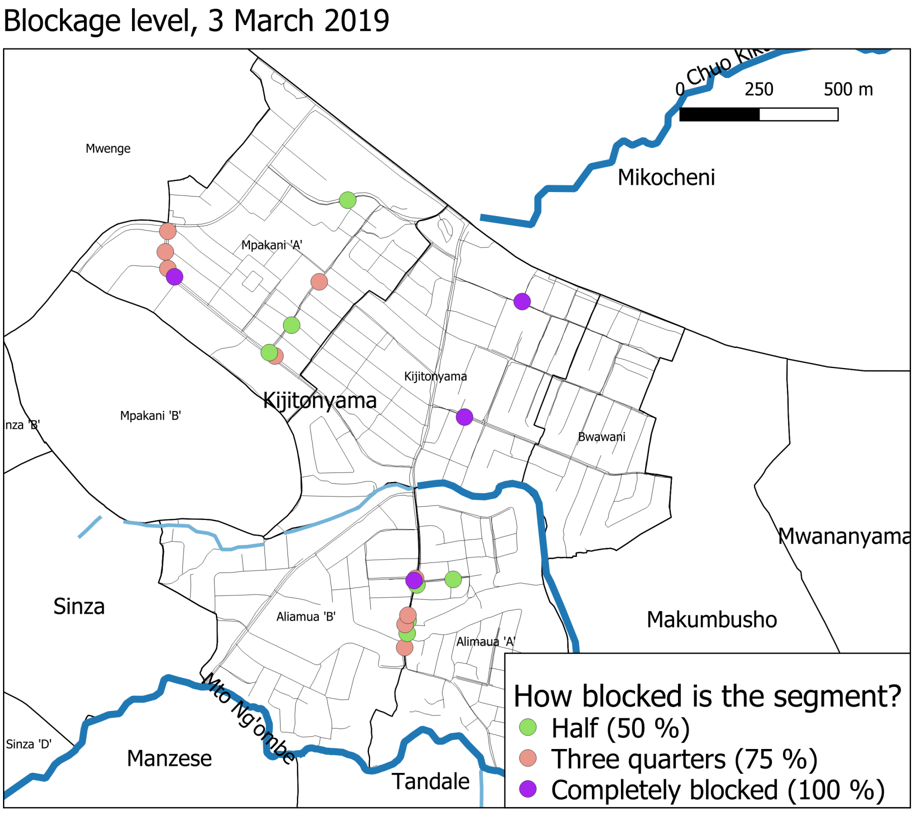

Figure 6.3: Blockage levels recorded in the survey.

6.2 Results of model development

This section analyses the results of scenario 1 and 2, that aims to build a flood model with community mapped drainage data and investigate its contribution to flood predictions on neighbourhood scale. As described in section 4.2.1, the community members' reports on flood depth were recorded in relation to a "person's height reference system", see table 4.3. This reference system contains several classes with high resolution. For shallow water depths, the classes are *only puddles*, *finger depth*, *ankle depth*, *mid-shin depth* and *knee depth*. However, concerning the high uncertainties in people's estimates of water depth, it was decided to lump several classes in the model validation. No deep water occurs in the study area, which is expected due to its elevated location, but makes it more difficult to make a reliable validation of the model output. It is considered to be most valid to work with a few, wide validation classes. It should be noted that the thresholds of the classes are set arbitrary, and no research has been performed on how well this reference system represents reality. Nevertheless, the classes give an indication of the flood depth at each observation point. Table 6.1 shows the lumped water depth classes that are used in the model validation.

Table 6.1: Lumped water depth classes used in the model validation.

Reported depth	Water depth in cm
Only puddles and finger depth	0 - 5
Ankle depth	5 - 20
Mid-shin and knee depth	>20

As explained in section 5.2.3, observation points are inserted in the 2D schematisation to record how the simulated water depth changes for each scenario. The location and labels of the observation points are shown in figure 6.4.

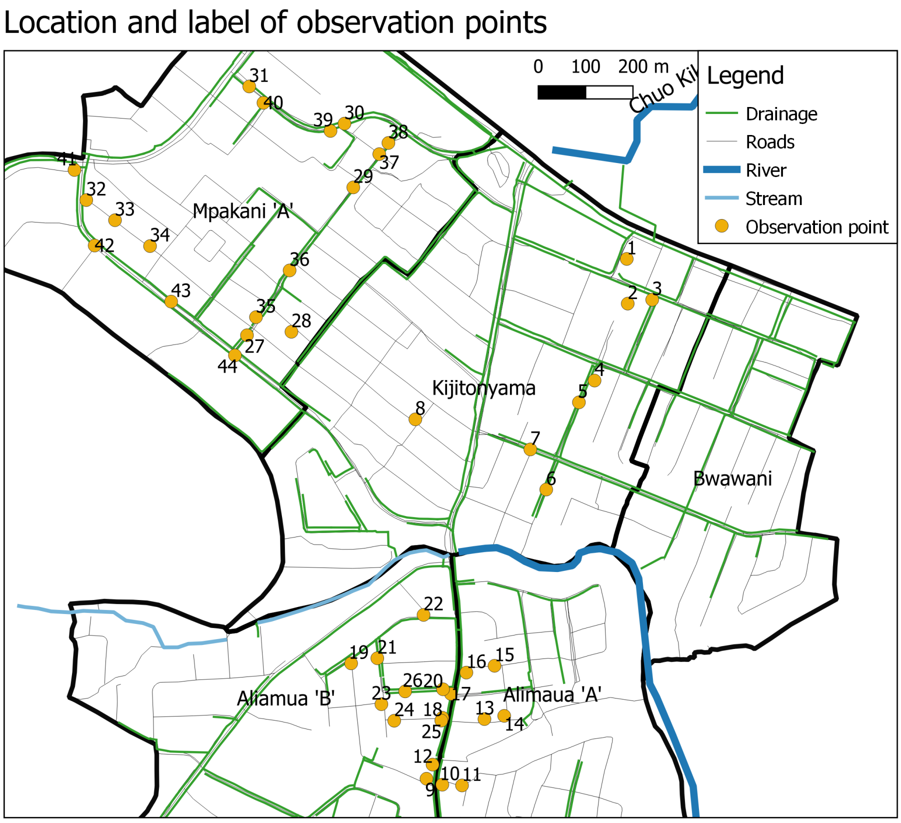

Figure 6.4: Location and label of observation points in the 2D schematisation, corresponding with geopoints recorded in the flood extent survey.

6.2.1 Scenario 1 - only 2D schematisation

Figure 6.5 shows a flood map of the study area for scenario 1, with the maximum simulated water depth per grid cell. This result seems reasonable when comparing with the elevation in the area, see figure 4.8. Figure 6.6 shows the deepest water recorded in each observation point during the simulated event. Note that these depths do not necessarily occur simultaneously, but it seems reasonable that the respondents were recalling the deepest water on the street during the storm event in the flood extent survey. Hence, the deepest simulated water in each observation point will be compared with the reported water depths. Ten observation points record less than 1 cm of water, and ten more than 10 cm. As expected, the simulated water depth increases towards the north eastern part of the study area. In Alimaua, there is less than 10 cm of water in all observation points, except for number 12, that records 45 cm of water.

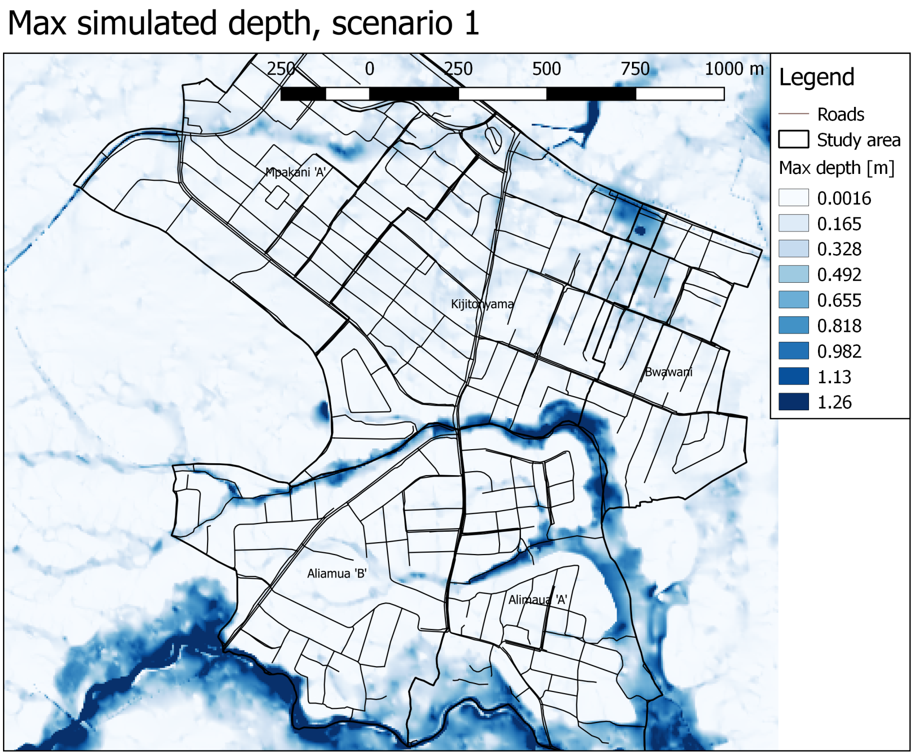

Figure 6.5: Flood map of scenario 1, max simulated water depth per grid cell.

Figure 6.7 depicts how the simulated water depth relates to the reported water depth in each observation point. In 12 cases, the simulated water depth is lower than the reported, in 19 cases it falls within the class, and in 13 cases it is above the results of the flood extent survey. The majority of the results in Alimaua falls within the reported class. In the northern *mitaa*, the majority of the results are overestimating the water depth in relation to the reported values.

Max simulated water depth in observation points, scenario 1

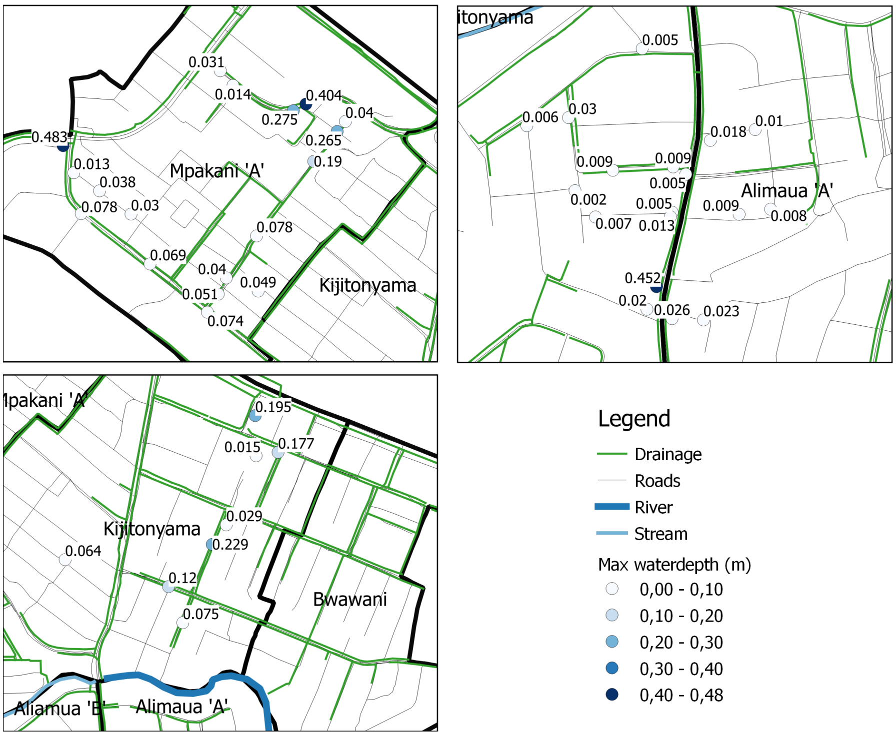

Figure 6.6: Max simulated water depths in observation points, scenario 1.

Simulated depth related to reported water depth, scenario 1

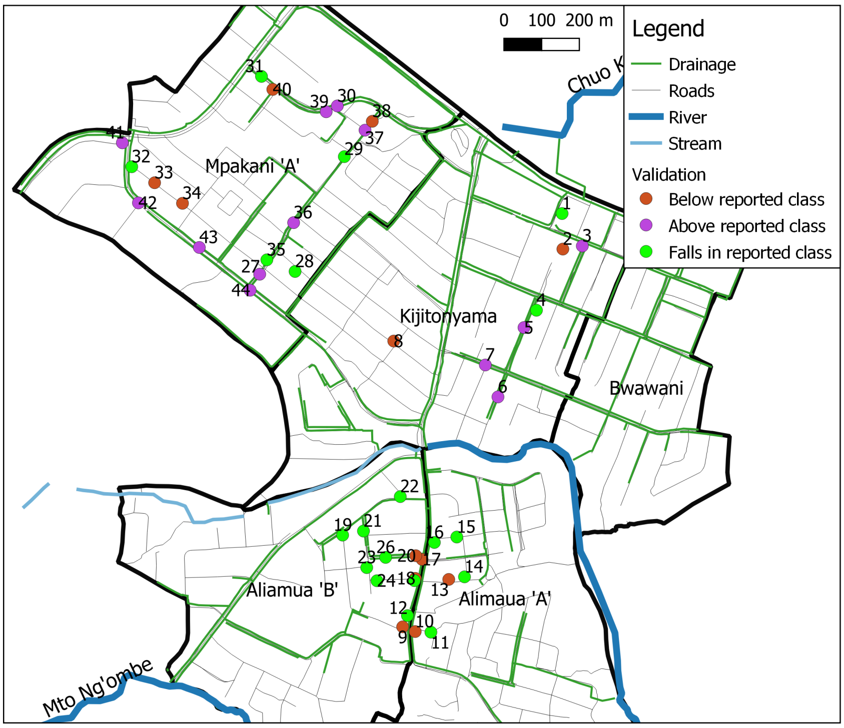

Figure 6.7: Simulated water depth related to reported water depth, scenario 1. The observation points are labelled with their ID to allow for comparisons with other figures.

6.2.2 Scenario 1 and 2a - Impact of implementing 1D network

Scenario 2a is run as a coupled 1D-2D model, with the 1D schematisation without adjusted bed levels, and a constant Manning roughness coefficient of 0.02 for all segments. No flood map of this result is shown here, as it is very similar to the result displayed in figure 6.5. The maximum water depth decreases in all observation points compared to scenario 1, which is expected when introducing a drainage network. Figure 6.8 shows how much the simulated water depth decrease in the observation points when introducing the drainage in the model schematisation. Not surprisingly, it decreases most in the points located on drainage segments. The biggest difference in maximum water depth is found in observation point 5, where it decreases from 23 cm to 0 cm of water. The impact of the drainage network appears to be bigger in the northern *mitaa* compared to Alimaua in the south. Only observation point 21 record a considerable water level difference of 3 cm when introducing the drainage network in Alimaua. This will be further examined below.

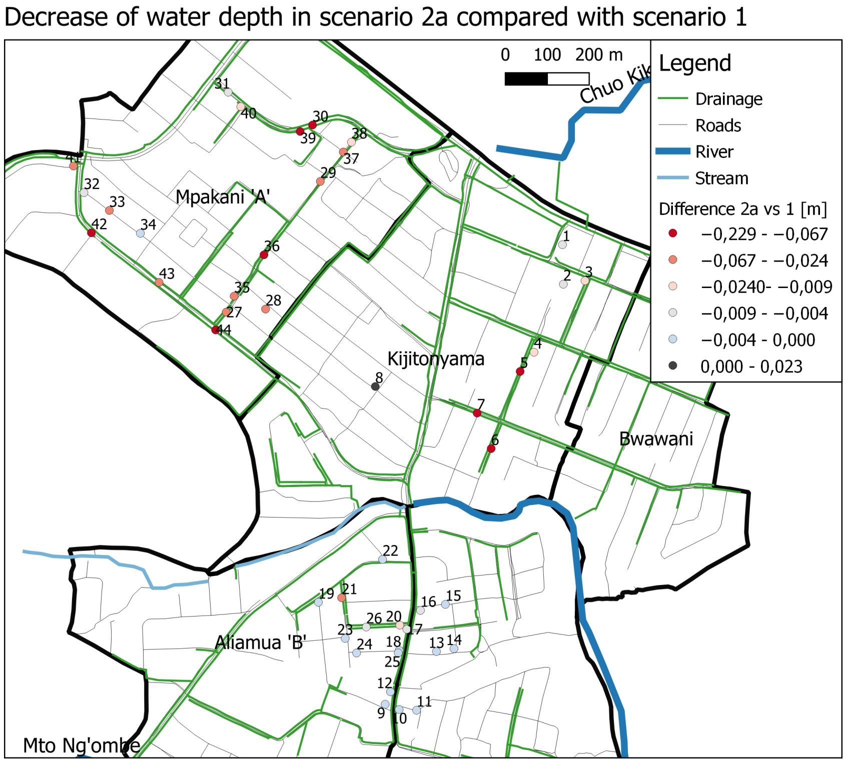

Figure 6.8: Decrease of water depth when introducing the drainage network. The water decrease in all observation points, except number 8. The difference is larger in the northern *mitaa* compared with Alimaua in the south.

The simulated water depth is still lower than the reported depth in the same cases as in scenario 1, except for in observation point 17 and 20, where it increases and falls within the reported class. The simulated water depth decreases in location 5, 6, 7, 27, 36, 39, 42, 43 and 44 in Mpakani A and *mtaa wa* Kijitonyama, so that these results fall within the reported class. No observation point falls out of the reported class when introducing the 1D network. Hence, the number of observations corresponding with the reported flood depth increases from 19 to 30 when comparing scenario 1 and 2a, see figure 6.9.

A few examples of observation points that fall within the reported class in scenario 2a compared with scenario 1 are shown in figure 6.10.

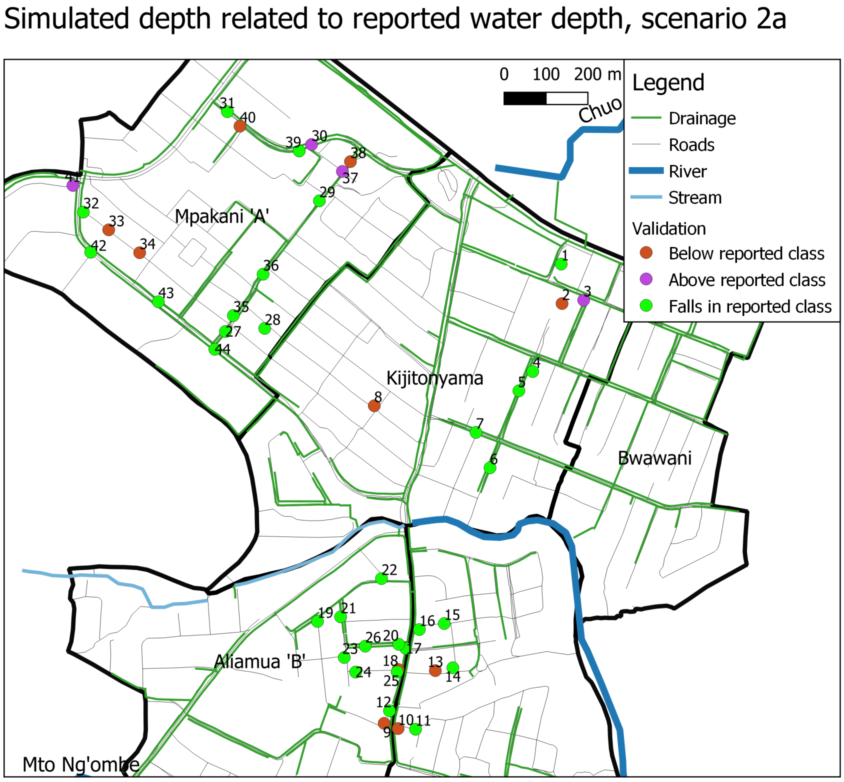

Figure 6.9: Simulated water depth related to water depth, scenario 2a.

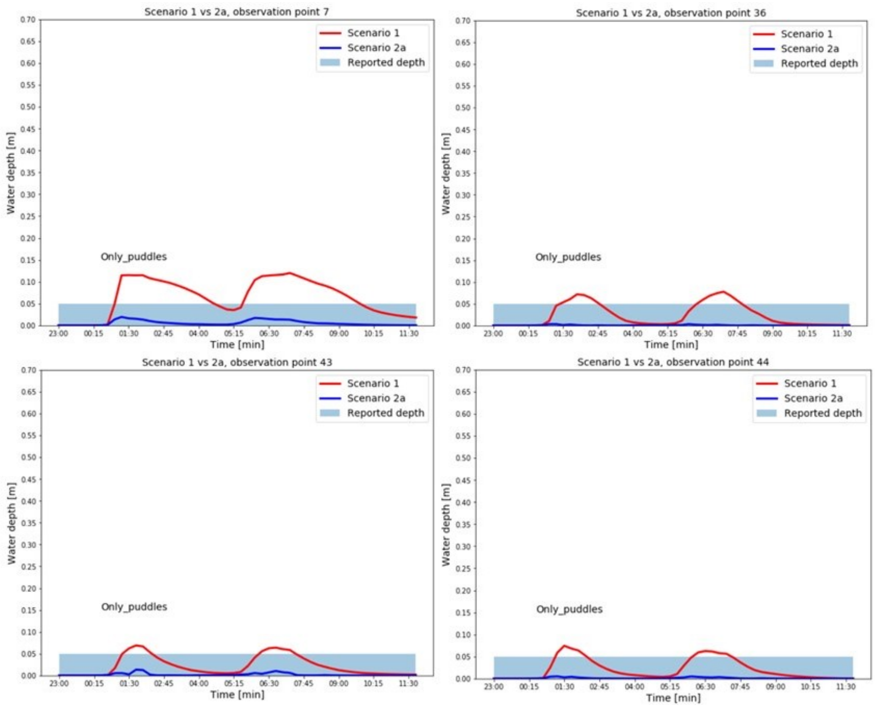

Figure 6.10: Examples of observation points that fall within the reported class, when introducing the drainage network in scenario 2a.

6.2.3 Scenario 2a and 2b - Impact of adjusted bed levels

In scenario 2b, the bed levels have been adjusted as described in section 5.1.6, with constant friction values. However, gaps in the bed levels are still present in 14 locations in the model. This problem appears in junctions where the downstream point of a segment is connected to the upstream point of more than one other segment. In these situations, a choice has to be made about which upstream bed level to adjust the downstream bed level to, see appendix C.5. It seems reasonable that this choice can be done randomly, as the elevation of the bed levels should be very similar, given that they are connected to each other in their upstream ends. Apparently, this assumption is not true, as the cross sections are not overlapping in 14 junctions, even after adjusting the bed levels. An example is shown in figure 6.11.

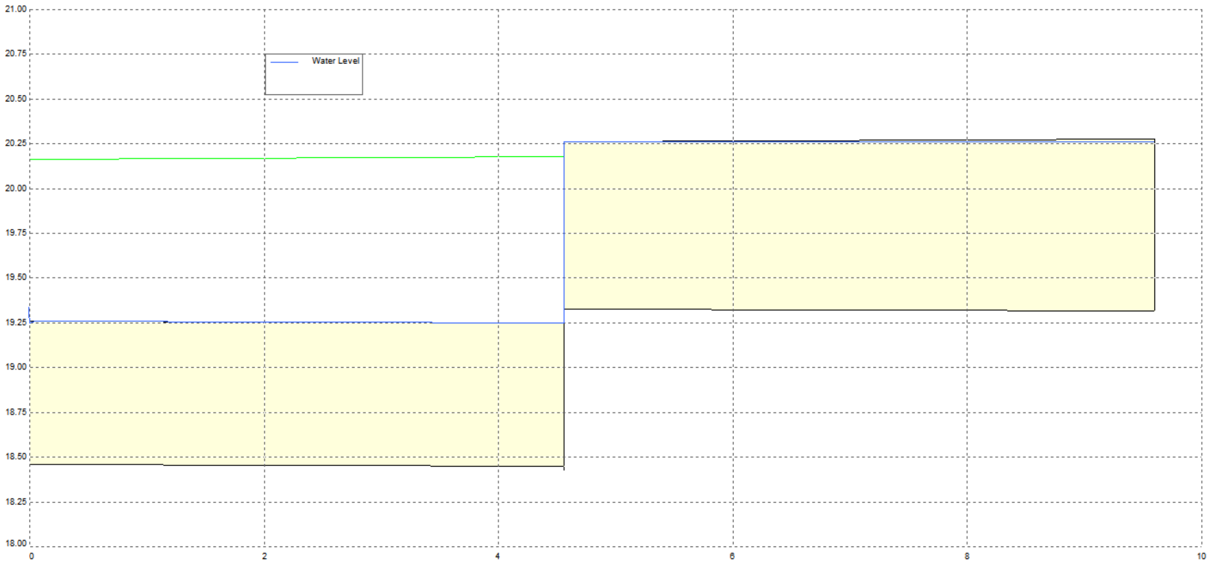

Figure 6.11: Example of segments in a junction that do not overlap, when the bed levels have been adjusted in a script. This is due to big differences in the elevation measurements in this junction. The problem appears 14 times in the model applied in scenario 2b-3b.

When studying the resulting water depths, it is revealed that they do not differ more than 1 cm i any observation point, compared with scenario 2a. The simulated depth relates to the reported water depth in the same way as scenario 2a in all observation points. Hence, the validation result is the same as shown in figure 6.9. No flood map of this result is shown here, as it is very similar to the result displayed in figure 6.5. As no difference is detected in the observation points, the maximum water level is studied in a sample of the drainage segments instead. Five inspection reaches are selected for further inspection, see figure 6.12. These reaches are also used to examine the results of scenario 2b and 2c, see below.

The maximum water level in the calculation nodes along these segments are studied for scenario 2a and 2b. The segments have 590 calculation nodes in total, constituting approximately 10% of all calculation nodes in the model. Figure 6.13 shows how the maximum water level change when comparing scenario 2b with 2a, that is, when adjusting the bed levels as described in section 5.1.6. The percentages represent the share of the total number of calculation nodes in the inspection reaches.

The adjustment leads to an increase of maximum water level in 56.8% of the observation points, and a decrease in 43.2%. In 50% of the calculation nodes, the difference is less than 1 cm. No spatial trends of these results can be detected, and no conclusion can be drawn from this about if or how the adjustment of bed levels improve the model output. Nevertheless, it is argued that the 1D schematisation in scenario 2b provides a more realistic model, as it avoids gaps in the drainage bed levels. Hence, the remaining scenarios are run with adjusted bed levels as described in section 5.1.6. Figure 6.14 shows an example of how a segment reach is changed when adjusting the bed levels. The displayed water level is the deepest recorded water in the segment reach.

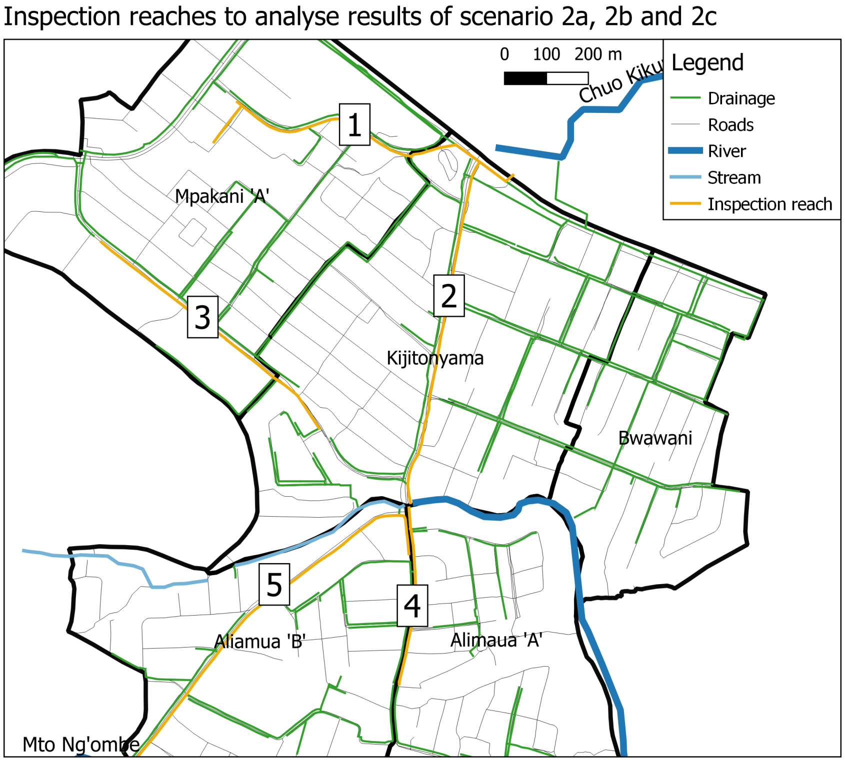

Figure 6.12: Selected inspection reaches of the drainage network to analyse results of scenario 2a, 2b and 2c.

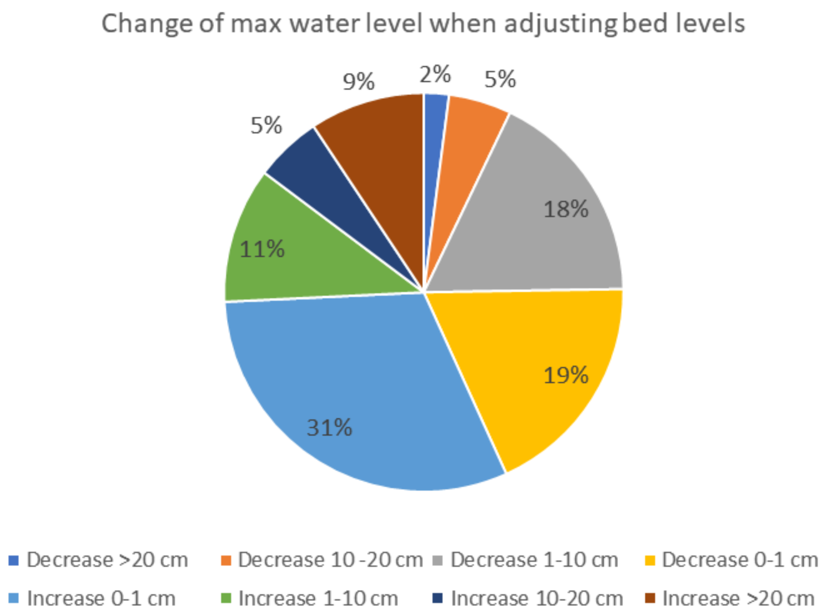

Figure 6.13: Change of maximum water level in inspection reaches when adjusting the bed levels. The percentages represent the share of the total number of calculation nodes in the inspection reaches.

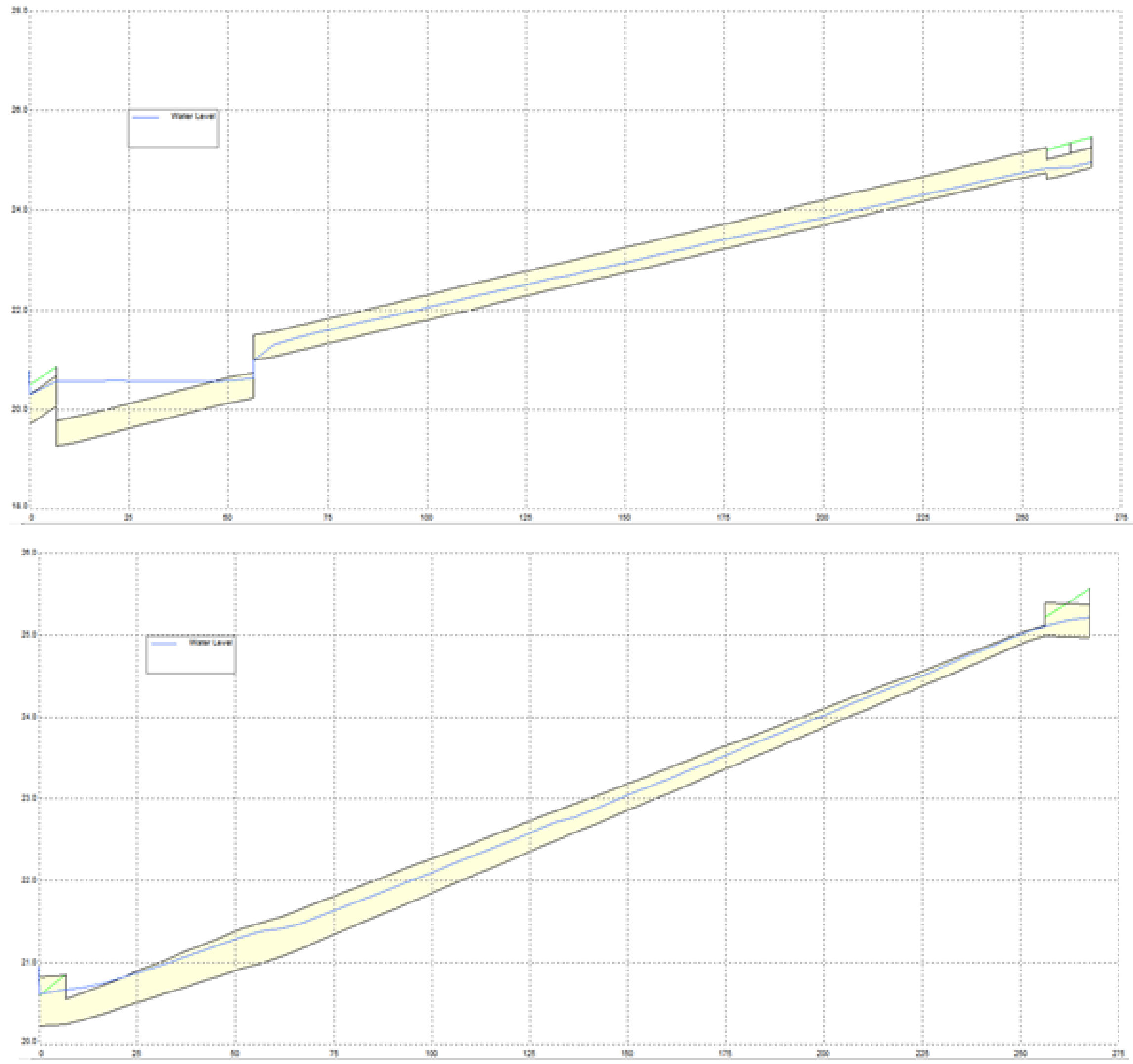

Figure 6.14: Example of how a segment reach is changed when adjusting the bed levels.

6.2.4 Scenario 2b and 2c - Impact of distributed 1D friction values

Scenario 2c is run with adjusted bed levels, and with distributed friction values as explained in section 5.1.5. No flood map of this result is shown here, as it is very similar to the result displayed in figure 6.5. The simulated water depth relates to the reported depth in the same way as the results for scenario 2a and 2b. Hence, the validation result is the same as shown in figure 6.9. The difference in maximum water depth is smaller than 0.5 cm in all observation points when comparing with scenario 2b. Instead, the maximum water level is studied in the same inspection reaches as in section 6.2.3. The result is shown in figure 6.15. The majority of the calculation nodes, 69%, record a difference smaller than 1 cm when comparing scenario 2c with 2b. The water level increase in 53% of the nodes, decrease in 40% and remains unchanged in 7% of the nodes. No spatial correlations in these results can be detected.

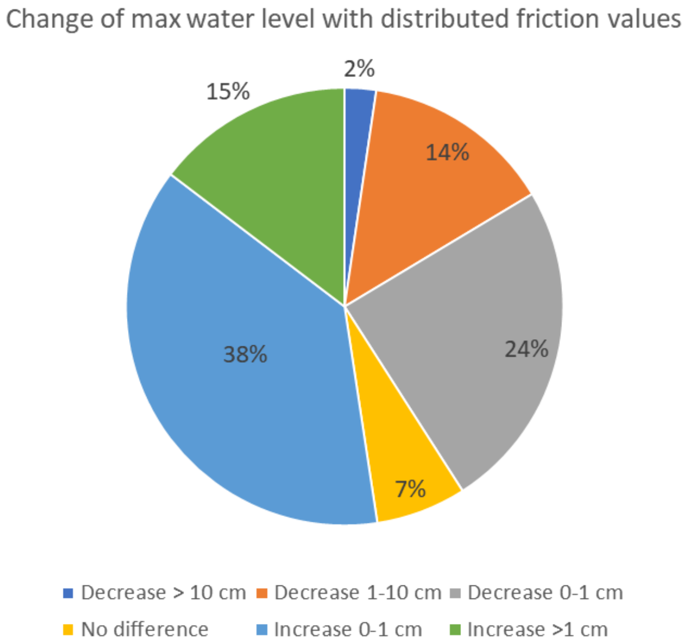

Figure 6.15: Change of maximum water level in inspection reaches when applying distributed friction values, compared with constant friction values. The percentages represent the share of the total number of calculation nodes in the inspection reaches

6.2.5 Summary results of model development

Table 6.2 shows a summary of the validation of the model development scenarios. When implementing the 1D schematisation, the model performance increases, as more observation points fall in the reported water depth class. Efforts to refine the 1D schematisation, by adjusting bed levels and assigning distributed friction values, does not contribute to further improvement of the model.

Table 6.2: Summary of model development results. Number of observation points (and percentage).

	Scenario 1	Scenario 2a	Scenario 2b	Scenario 2c
Below reported class	12 (27%)	10 (23%)	10 (23%)	10 (23%)
In reported class	19 (43%)	30 (68%)	30 (68%)	30 (68%)
Above reported class	13 (30%)	4 (9%)	4 (9%)	4 (9%)

This section has analysed the development of the model built with community mapped drainage data, by investigating the impact of the 1D schematisation, and adjusted bed levels and distributed friction values. The following section analyses the results when applying the model to examine the impact of solid waste blockages in the drainage network.

6.3 Results of model application

Recalling section 5.3, two scenarios, number 3a and 3b, are run to investigate the impact of solid waste blockages. Scenario 3a contains blockages that were recorded the morning after the simulated event, and scenario 3b is of experimental character and investigates the impact of blocked culverts. The scenarios will be run with the 1D schematisation applied in scenario 2c. It is argued that scenario 2 a-c perform equally well, and that scenario 2c is most likely to represent reality, due to the distribution of friction values. The 1D schematisation from scenario 2c will, hence, be used in the model application.

6.3.1 Scenario 3a - Solid waste blockages

This scenario is run with the 1D schematisation of scenario 2c, with adjusted bed levels and distributed friction values. 20 segments are blocked according to the blockages survey, see section 5.3. It is expected that the water would increase in observation points situated upstream of blockages, so that the simulated water depth increase above the reported class, but the validation of the model yields the same result as for scenario 2a-2c. Perhaps surprisingly, the water depth is very similar in all observation points, when comparing scenario 2c and 3a. There are many blockages reported along the main road in Alimaua, see figure 6.16, and the simulated water depth does not increase in any of the observation points here compared with scenario 2c, as would have been expected. A more intense rainfall might be needed to detect changes in the observation points. Most observation points in Alimaua record less than 5 cm of water.

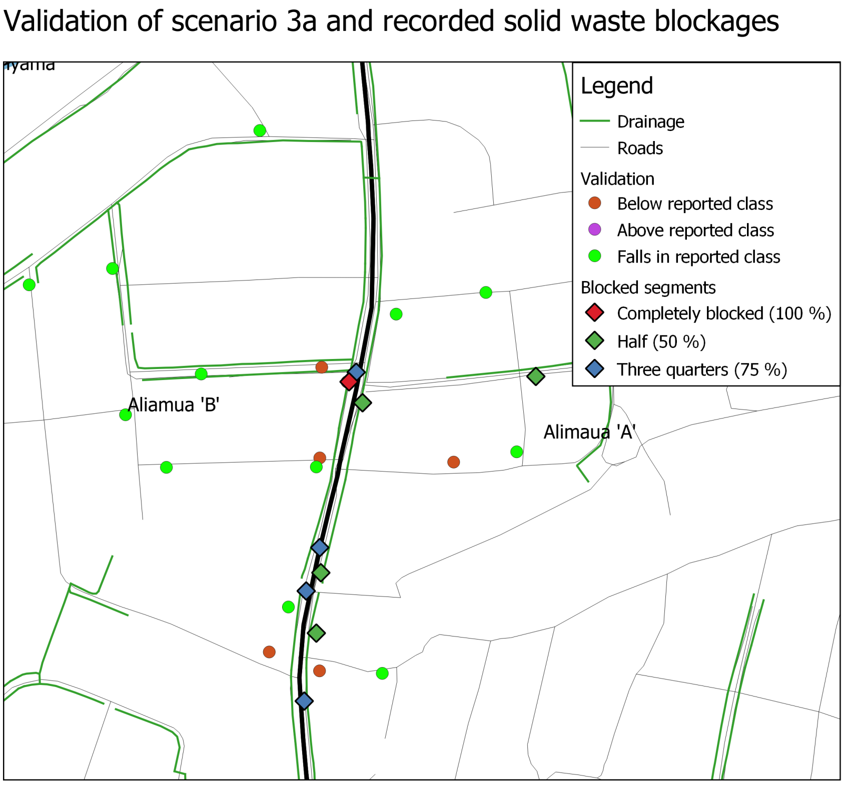

Figure 6.16: Validated water depths and recorded blockages in Alimaua, scenario 3a. Despite the blockages recorded here, the water depth does not increase in any observation point when comparing with scenario 2c, that is run without blockages.

Instead, the behaviour of the drainage segments blocked by solid waste is examined in calculation nodes on the segments upstream of the blockages. In this way, it can be examined how the water level varies over time at certain locations in the drainage system during the event. The inspection points are shown in figure 6.17. A distinction is made between main and secondary transport routes, as the impact is expected to be larger on main transport routes. The light blue arrows indicate the direction of flow in the segments.

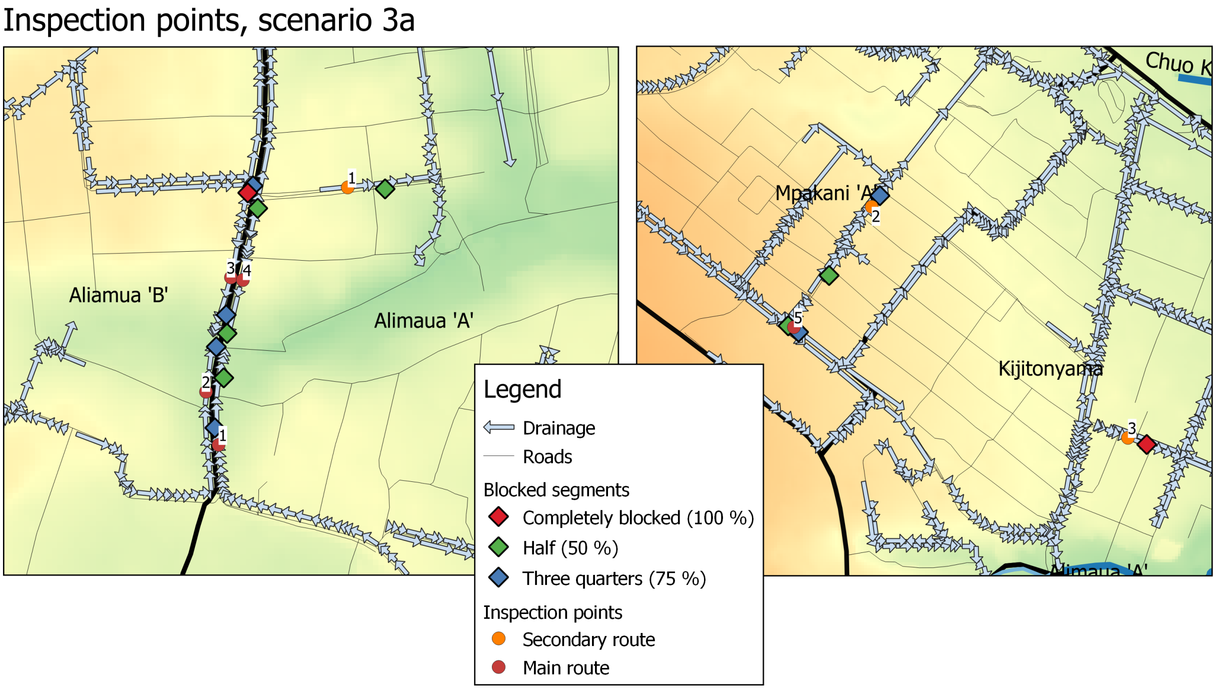

Figure 6.17: Locations inspected in scenario 3a and their labels.

Figure 6.18 compare the maximum water depth in the inspection points on main transport routes for scenario 2c and 3a. Quite unexpectedly, the water depth *decrease* in point 1, 2 and 5. Point 1, 3 and 4 record very little water during the event, which makes it difficult to assess the validity of these results.

Figure 6.19 compare the maximum water depth in the inspection points on secondary transport routes for scenario 2c and 3a. Point 1 record a small increase in water depth, but the depth is over all small in this point. A more significant increase is observed in point 2 and 3. Here, it should be noted that the water depth decrease to almost zero between the flow peaks in scenario 2c, which is not the case in scenario 3a. This indicates that the drainage capacity is insufficient in these locations when introducing solid waste blockages.

Table 6.3 summarise how the maximum water depth changes in the inspection points when comparing scenario 3a with scenario 2c. The water decrease considerably in the studied main transport routes, and increase in the secondary routes.

Table 6.3: Change of maximum water depth in inspection points when comparing scenario 3a with scenario 2c.

Point	Main route	Secondary route
1	- 4 cm	+ 3 cm
2	- 12 cm	+ 4 cm
3	+ 0.7 cm	+ 32 cm
4	+ 0.4 cm	
5	- 18 cm	

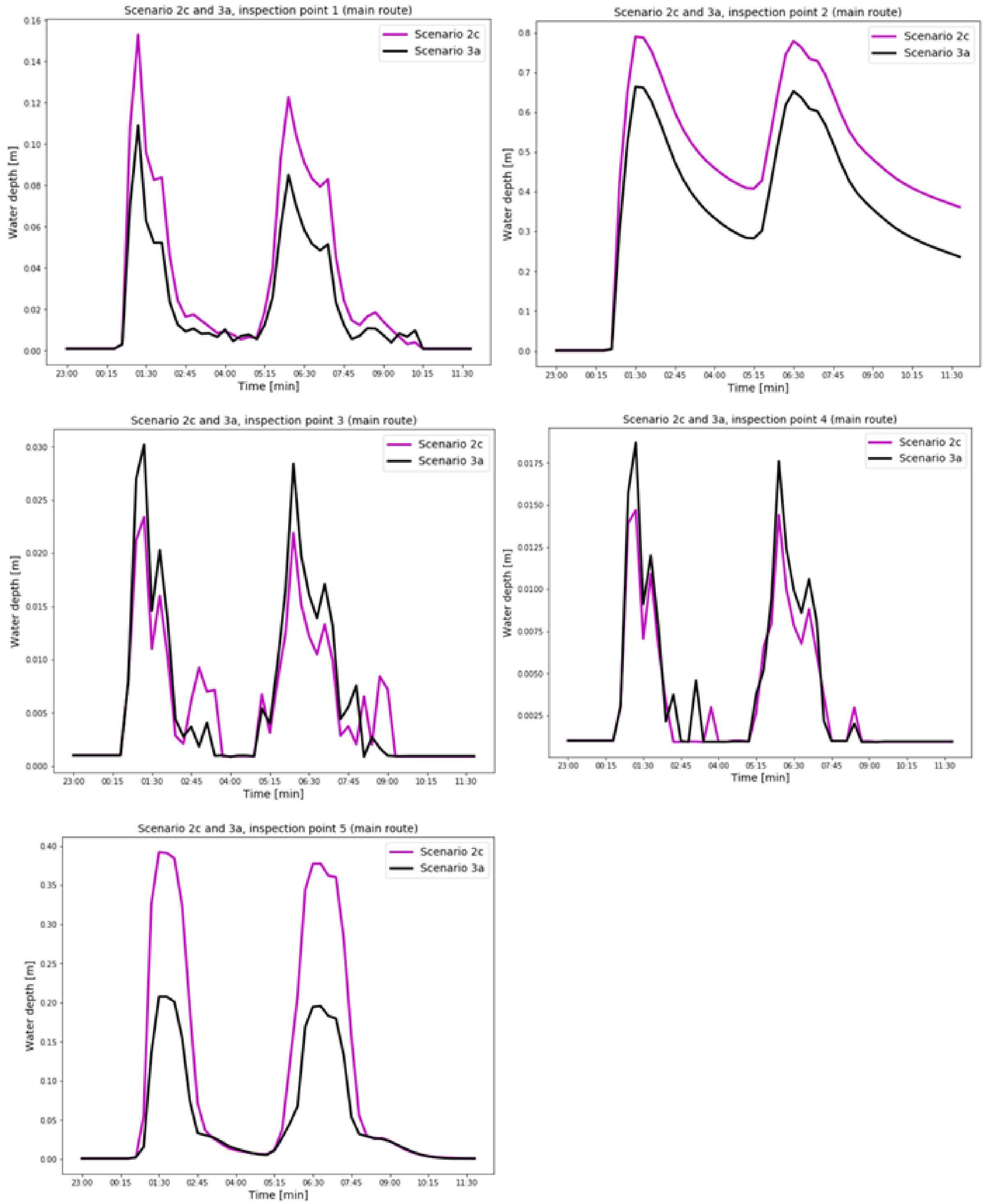

Figure 6.18: Differences in maximum water depth in main transport routes, scenario 2c and 3a.

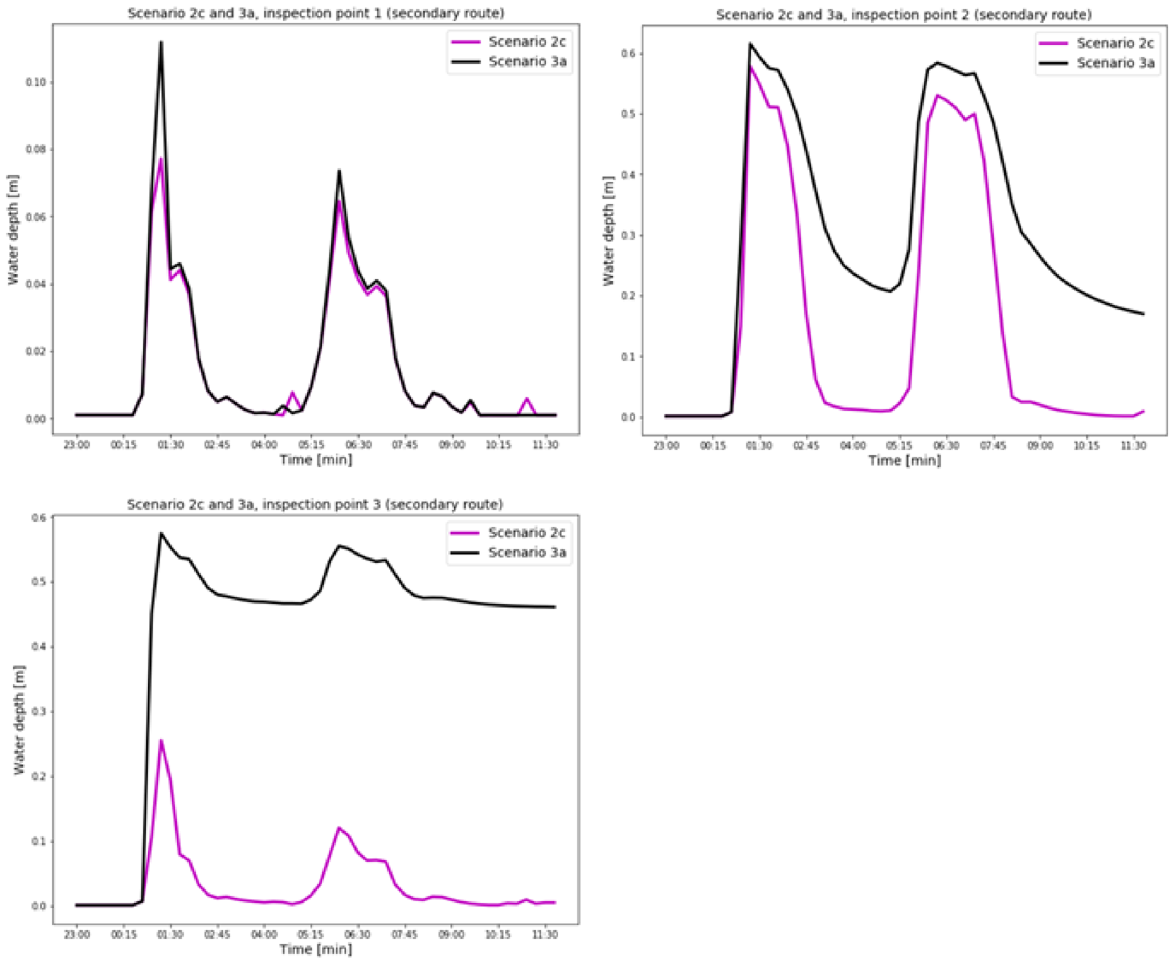

Figure 6.19: Differences in maximum water depth in secondary transport routes, scenario 2c and 3a.

Figure 6.20 and 6.21 relate the hydrograph of each inspection point to its location in the northern and southern *mitaa*, respectively. The yellow arrows indicate the direction of flow in the drainage segments and the flood map displays the deepest water recorded in each 2D grid cell. No spatial difference can be detected in the impact on main and secondary transport routes.

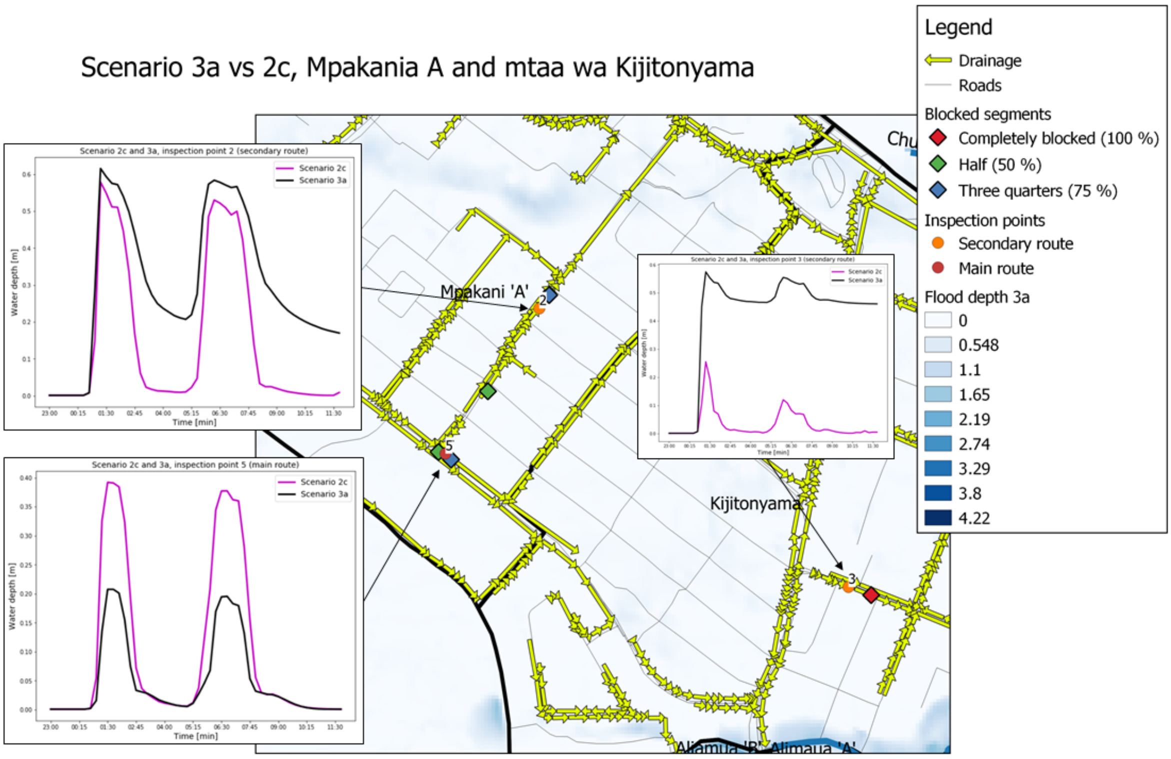

Figure 6.20: Impact of blockages on inspection points in Mpakani A and *mtaa wa* Kijitonyama.

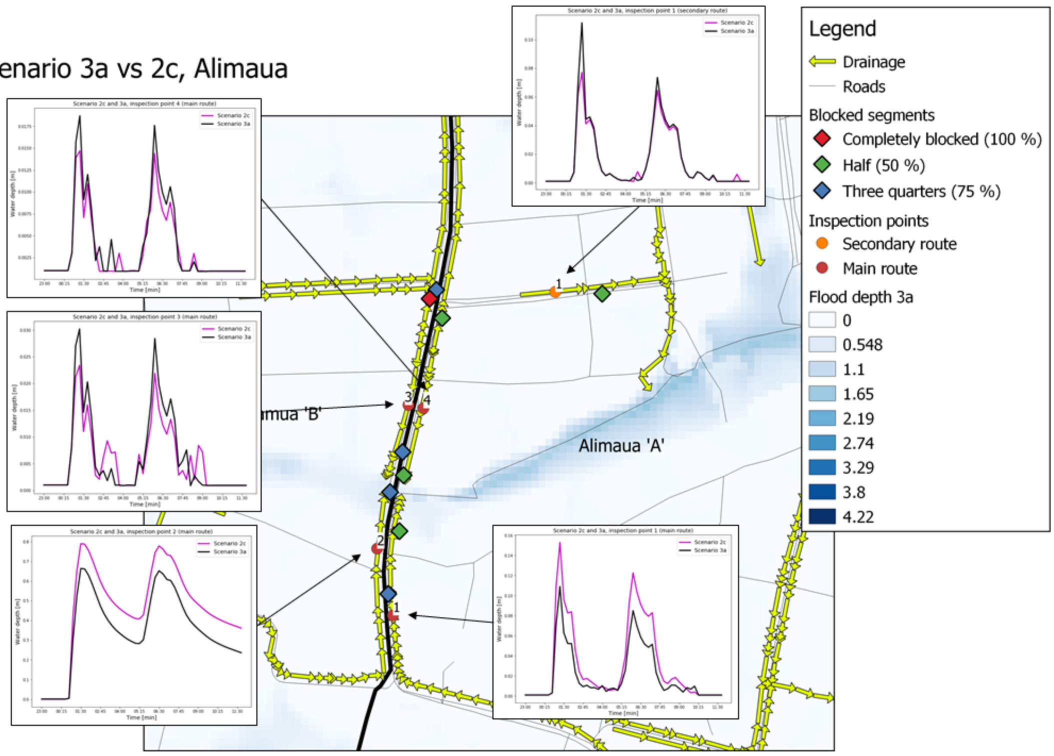

Figure 6.21: Impact of blockages on inspection points in Alimaua.

6.3.2 Scenario 3b - Blocked culverts

Scenario 3b is run with 33% of the culverts in Alimaua removed from the schematisation, see figure 5.16. This is intended to represent culverts blocked by accumulated solid waste. When comparing the maximum simulated water depth in scenario 3b with scenario 2c, there is no considerable difference in any observation point. It should be noted that all observation points record no or very little water during the simulated event in Alimaua, which holds for all scenarios. When plotting flood depth of the two scenarios as a function of time for all observation points, the plots show almost identical results for all locations. An example is shown in figure 6.22.

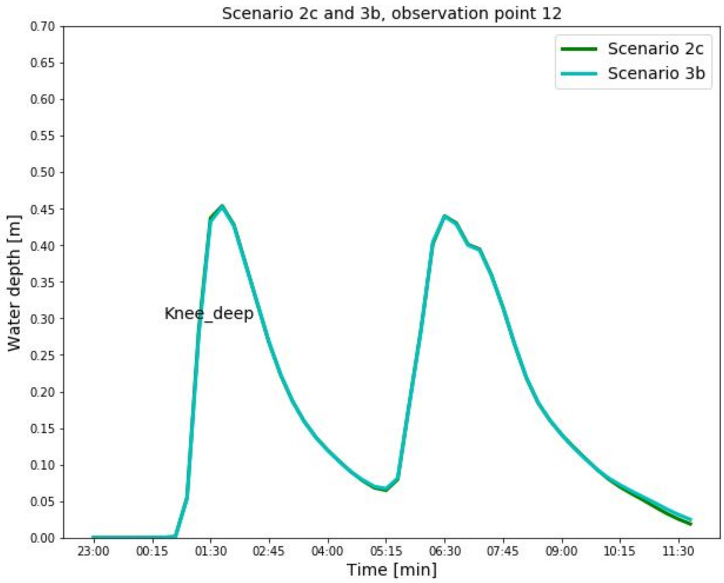

Figure 6.22: Comparison between scenario 2c and 3b. No difference is detected in any observation point, when blocking a third of the culverts in Alimaua.

Instead, the change in water level is studied in the drainage segments upstream of the blocked culverts. Figure 6.23 show the locations that are inspected.

Figure 6.24 compare the maximum water depth in the inspection points on main transport routes for scenario 2c and 3b. Inspection point 1 and 3 behaves similarly to inspection point 3 and 4 on main routes in scenario 3a - there is a small increase of maximum water depth when introducing blocked segments, but the inspection points record too little water to detect any significant effect. The maximum water depth increase with 10 cm in point 2, and similarly to point 2 and 3 on secondary routes in scenario 3a, this segment can not convey enough water between the flow peaks. A similar, but much less significant, tendency is shown in point 4. The water *decrease* in point 5, which is unexpected when blocking a downstream culvert.

Figure 6.25 compare the maximum water depth in the inspection points on secondary transport routes for scenario 2c and 3b. No difference at all is detected in point 1 and 5. The maximum water depth is very similar for the two scenarios in point 3 and 4, but again, these segments fail to reduce the water level after the first flow peak when blocking downstream culverts. This holds for point 2 as well, but here, the maximum water depth increase with almost 1 m. Again, it is difficult to detect differences in impact on main and secondary routes. Both point 1 and 5 are situated far upstream, and are not affected at all by the downstream blockages. The impact is, however, very big in point 2, that appears to have similar spatial properties.

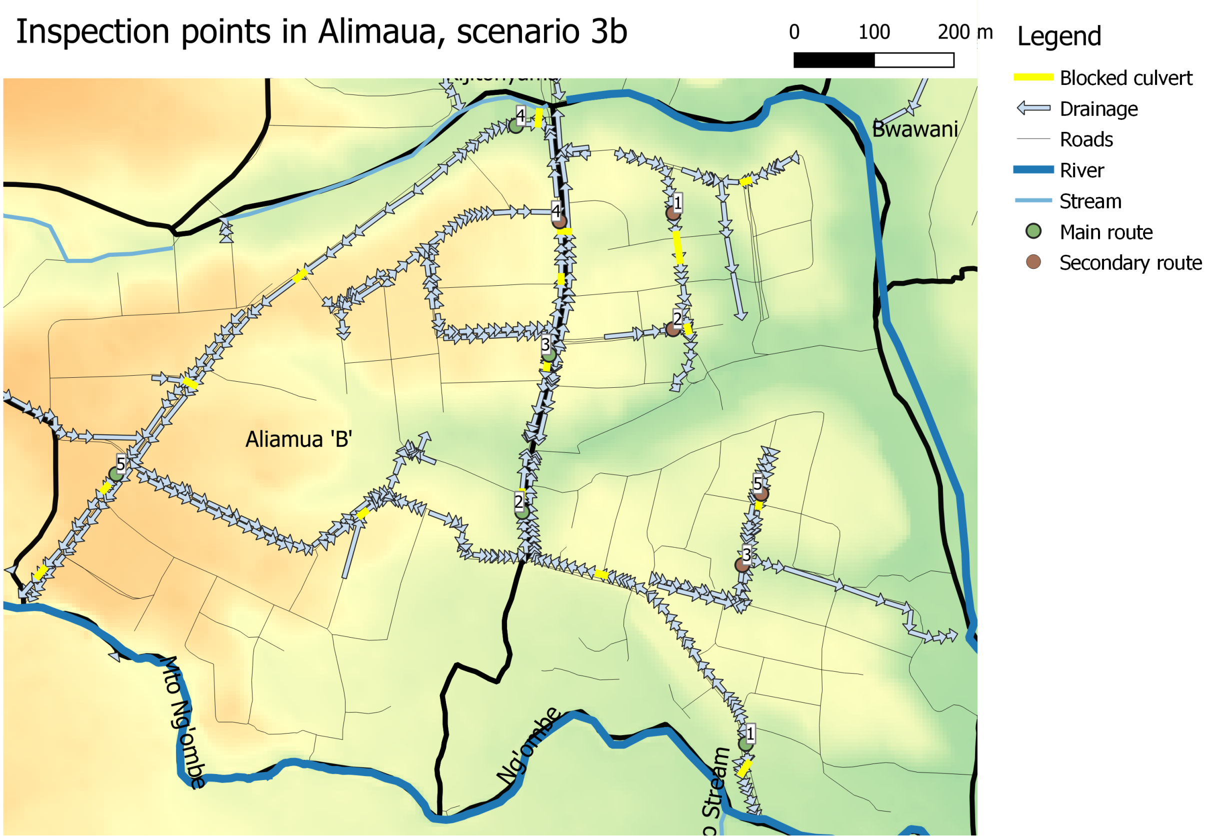

Figure 6.23: Locations inspected in scenario 3b and their labels.

Table 6.4 summarise how the maximum water depth changes in the inspection points when comparing scenario 3b with scenario 2c.

Table 6.4: Change of maximum water depth in inspection points when comparing scenario 3b with scenario 2c.

Point	Main route	Secondary route
1	+ 1.5 cm	No difference
2	+ 10 cm	+ 98cm
3	+ 0.3 cm	+ 2 cm
4	+ 0.2 cm	+ 4 cm
5	- 2 cm	No difference

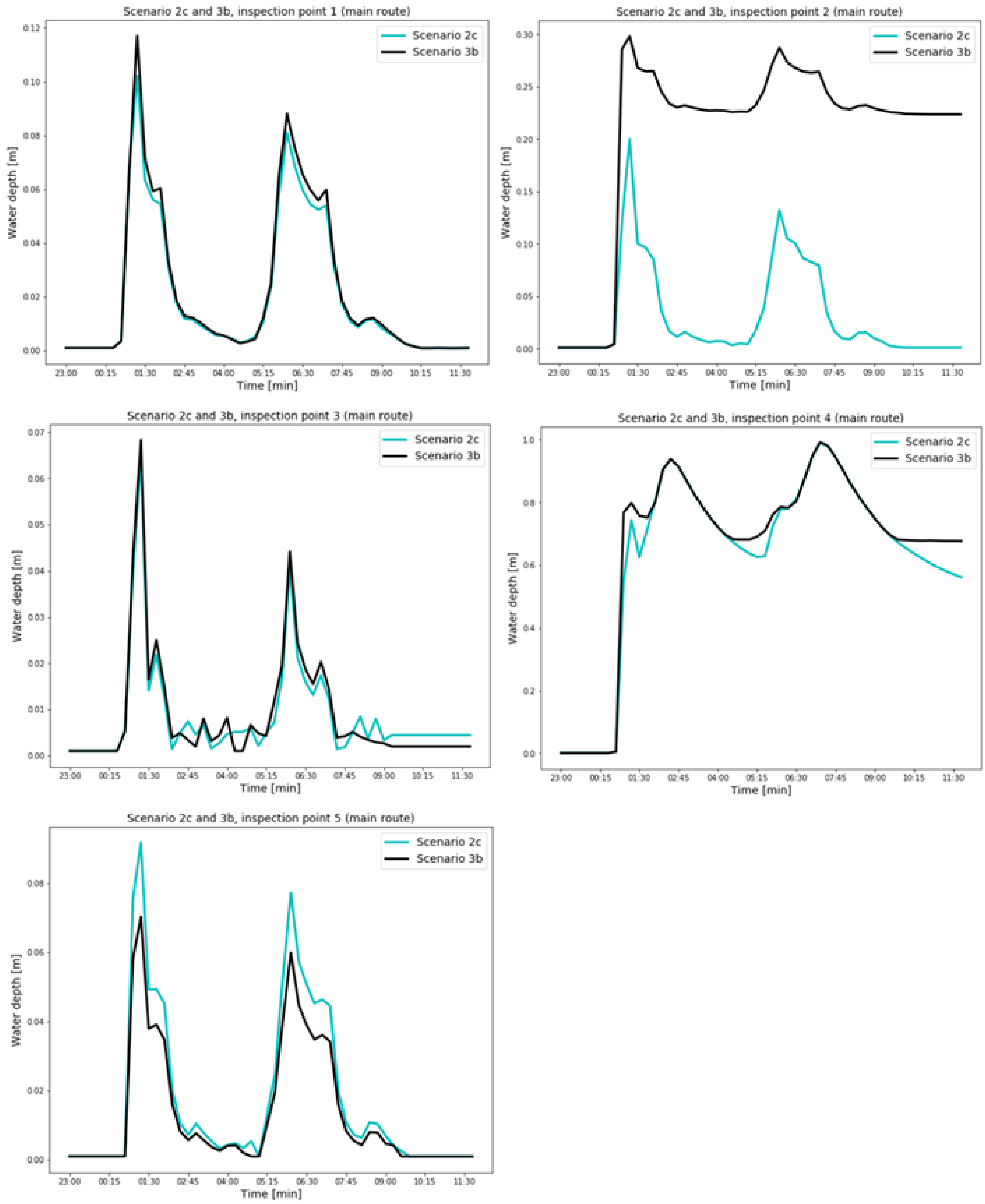

Figure 6.24: Differences in maximum water depth in main transport routes, scenario 2c and 3b.

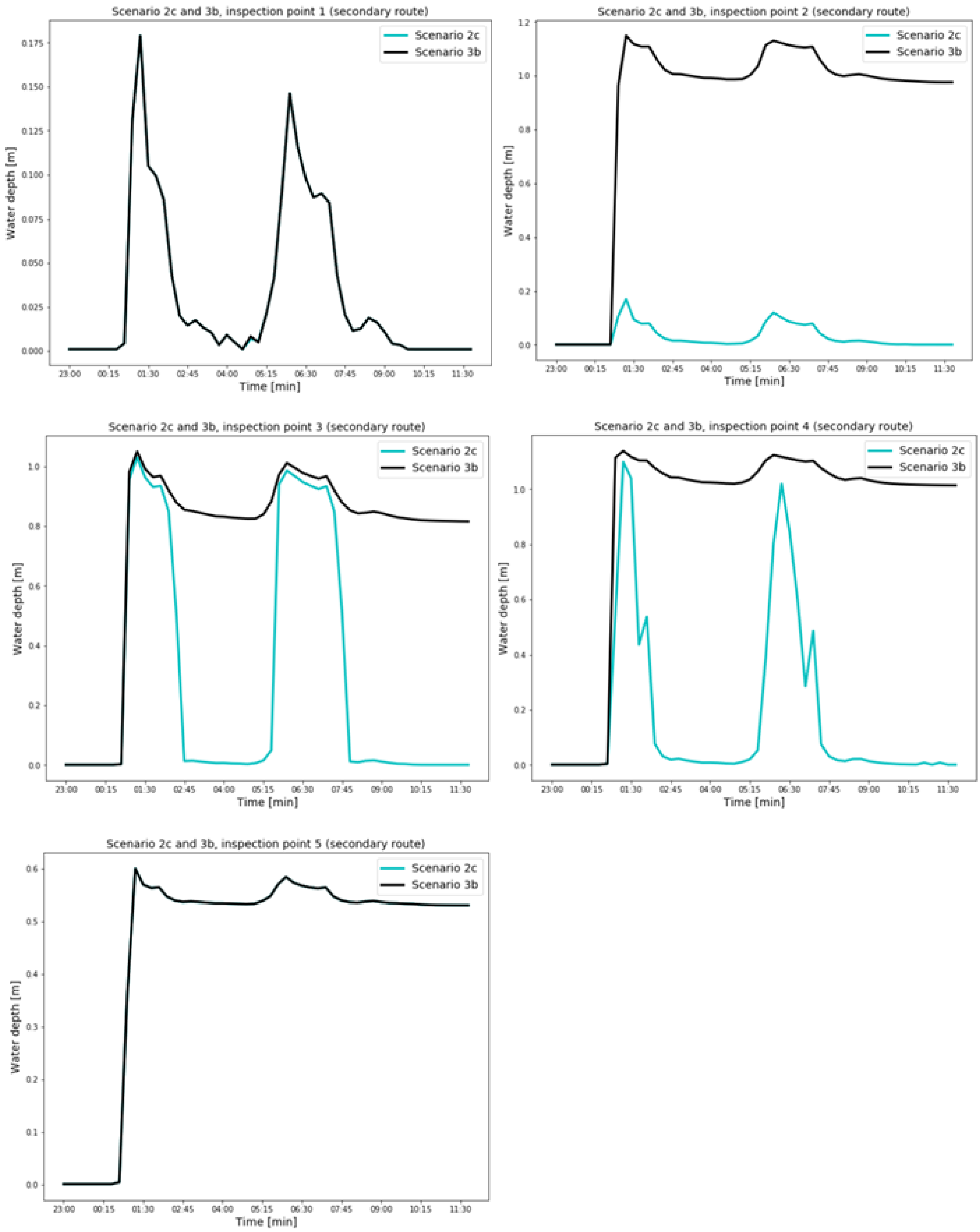

Figure 6.25: Differences in maximum water depth in secondary transport routes, scenario 2c and 3b.

Figure 6.26 and 6.27 relate the hydrograph of each inspection point to its location for main and seconary transport routes, respectively. The light blue arrows indicate the direction of flow in the drainage segments and the flood map displays the deepest water recorded in each 2D grid cell. No difference can be detected in the impact on main and secondary transport routes.

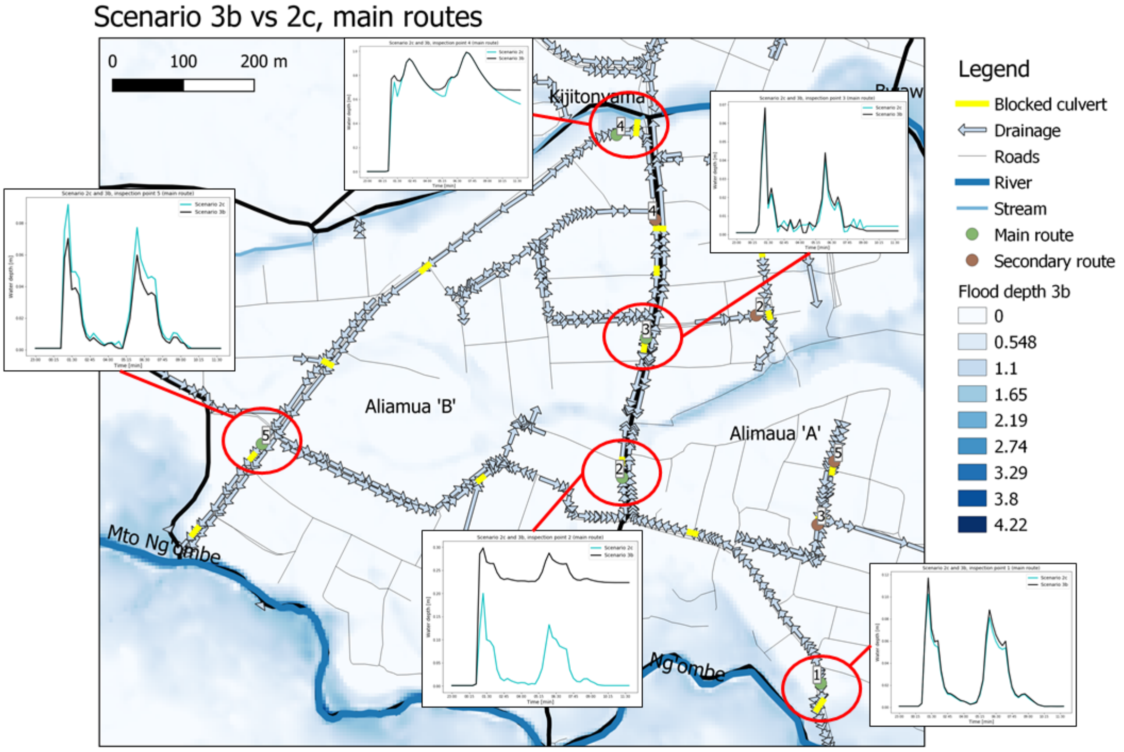

Figure 6.26: Impact of blockages on main transport routes, scenario 3b vs 2c.

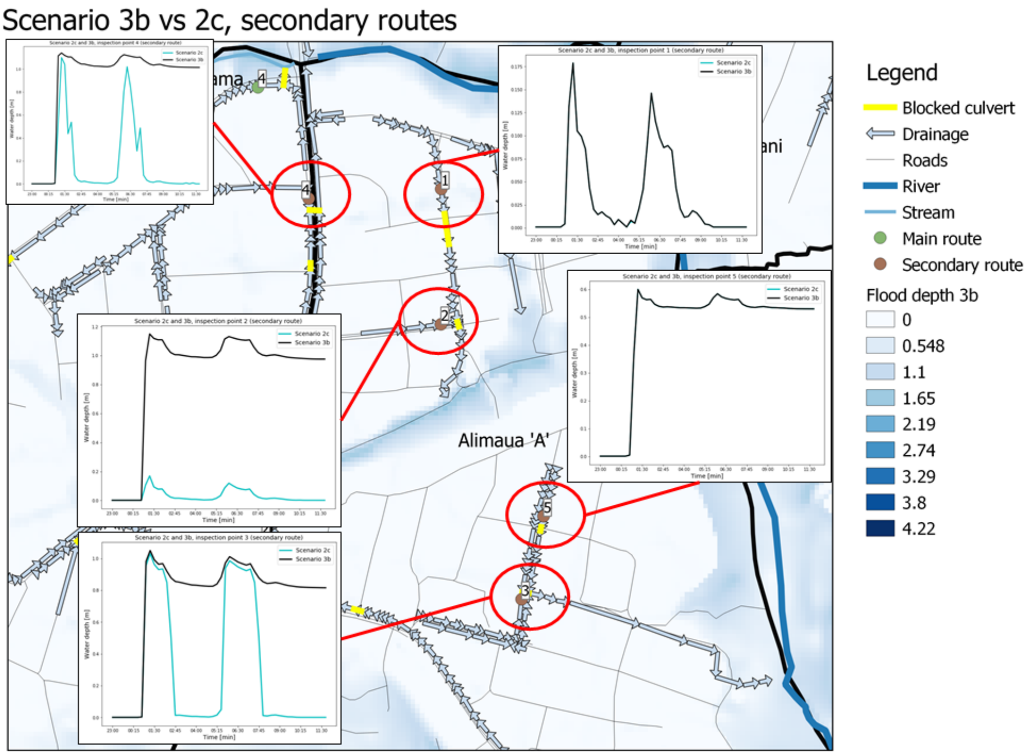

Figure 6.27: Impact of blockages on secondary transport routes, scenario 3b vs 2c.

Figure 6.28 displays the output of the coupled 1D-2D model at peak flow (07:15 in the morning) for scenario 2c and 3b. The 2D schematisation displays the simulated water depth in each grid cell at the time. The 1D network is classified according to how deep the water is on the street (in meters) at each calculation node. All green nodes can cope with the hydraulic load in the current time step, and yellow nodes record water above the surface level of the drain segment. The red circles highlight locations that get flooded when culverts downstream are closed in the model schematisation, compared with scenario 2c.

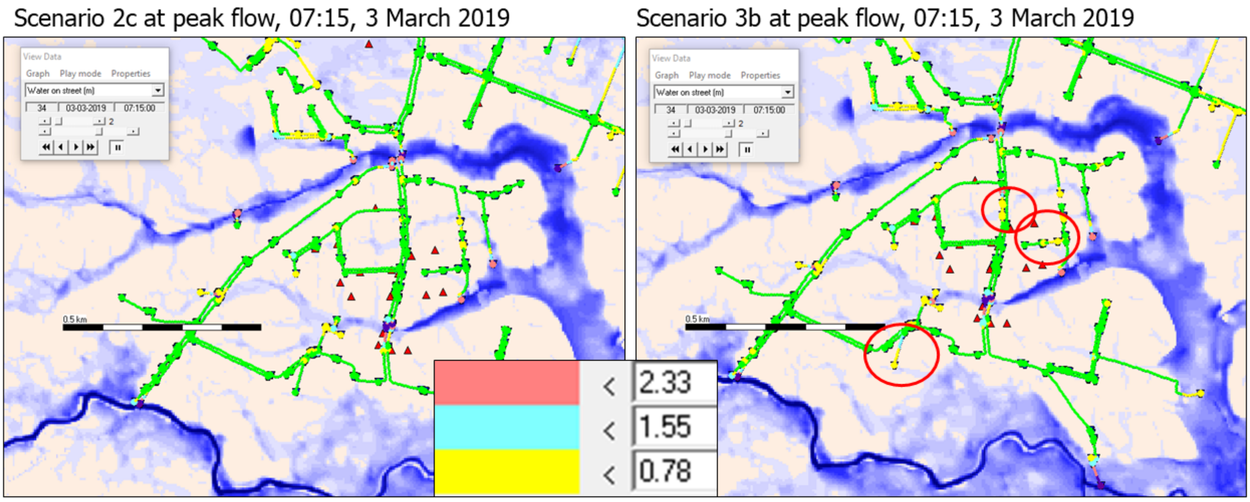

Figure 6.28: Model output at peak flow (07:15) for scenario 2c and 3b. The drainage network is classified according to how deep the water is on the street (in meters) at each calculation node. The red circles highlight locations that get flooded when culverts downstream are closed in the model schematisation.

6.3.3 Summary results of model application

In general, the water level in the examined segments behaves as expected in the locations that record a maximum water depth that is several decimetres deep. The exceptions are point 2 and 5 on main transport routes in scenario 3a, that record a considerable decrease of maximum water depth when blocking downstream drainage segments. The modelled storm event has two flow peaks, which causes drainage problems when introducing blocked culverts in scenario 3b. The segments that are loaded with deep water during the storm event (point 2 on main route and point 2, 3 and 5 on secondary routes) fail to drain the water before the next flow peak, which they would have managed to do if the drainage segments downstream were not blocked, as shown by scenario 2c. Figure 6.29 show a summary of all inspection points in both scenario 3a and 3b. No general conclusion about the impact of solid waste blockages on floods can be drawn from the results presented here. It is shown that solid waste blockages cause inundation upstream, but no spatial trend can be detected in terms of where or how the blockages appear. In some cases, the water decrease when introducing blockages downstream, which is unexpected. The results do not show any difference between main and secondary transport routes. It is recommended to investigate this further with statistical and experimental approaches.

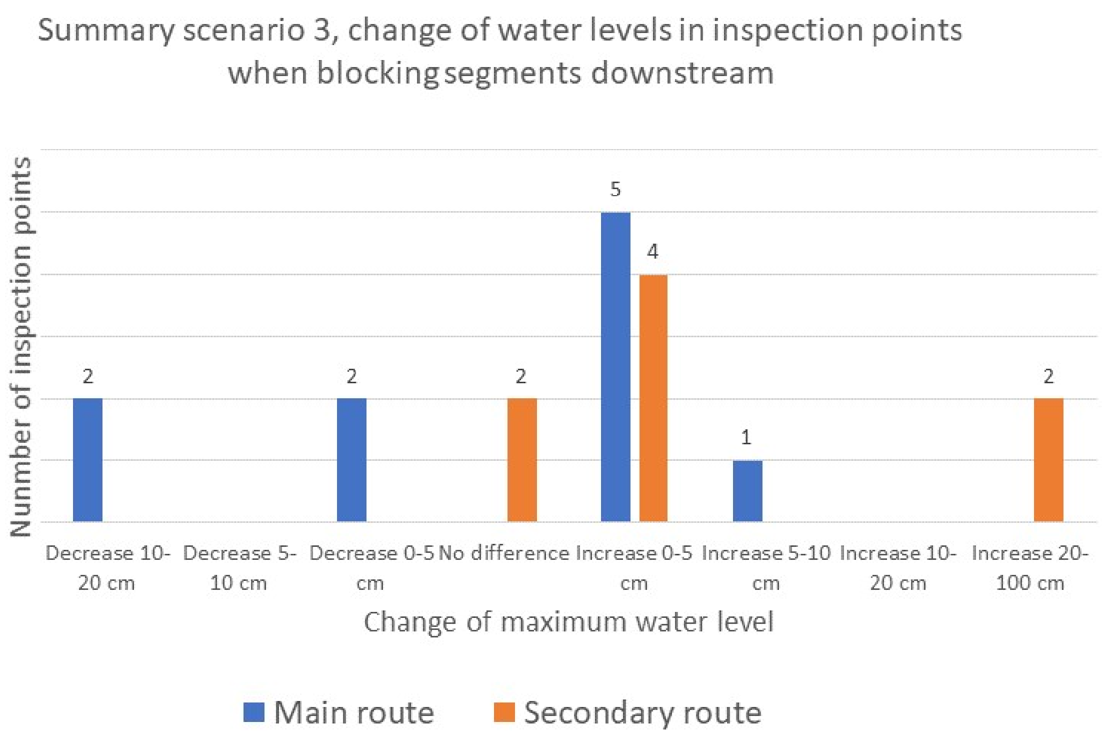

Figure 6.29: Summary of scenario 3.

Chapter 7

Discussion

This thesis has developed a flood model utilising drainage data from the *Ramani Huria* community mapping project in Dar es Salaam, Tanzania. The model has been applied to investigate the impact of solid waste accumulations on floods on neighbourhood scale. Table 7.1 repeats the scenarios that have been run to answer the research questions of the thesis.

Table 7.1: Scenarios.

Phase	Scenario	Description
Development	**1**	Only 2D schematisation
	2a	Coupled 1D-2D model without adjusted bed levels and constant friction values
	2b	Coupled 1D-2D model with adjusted bed levels and constant friction values
	2c	Coupled 1D-2D model with adjusted bed levels and distributed friction values
Application	**3a**	Coupled 1D-2D model with segments blocked according to the results of the solid waste blockages survey
	3b	Experimental coupled 1D-2D model with a third of the culverts in a part of the study area being blocked

The results show that community mapped drainage data indeed can enhance the performance of hydrodynamic models, as the model output corresponds better with the validation data when implementing *Ramani Huria*'s drainage data in the 1D schematisation, compared with a scenario run with only a 2D schematisation. However, the drainage system only has an impact on the model validation in the northern part of the study area, that consists of the *mitaa* Mpakani A, *mtaa wa* Kijitonyama and Bwawani. Here, the drainage network has an impact on the records of almost all observation points in the model. In Alimaua A and B, the southern part of the study area, the majority of the observation points does not get influenced when implementing the drainage network. Here, the difference in maximum simulated water depth is less than 1 cm for all scenarios. Also the examined drainage segments in Alimaua transport very little water during the simulated event, with a few exceptions. Most of the runoff seems to flow on the surface directly to natural water courses.

Figure 7.1 highlights how the observation points are influenced by the drainage data. The yellow points represent locations where the difference in water depth can be visually detected in a graph when implementing the drainage data, that is, that the difference in maximum simulated water depth is more than 1 cm. As can be seen, the drainage network have an impact in most of the northern *mitaa*, but to a much less extent in Alimaua. No similarities in physical properties are observed among the unaffected locations; they are located at high and low elevations of the study area, far upstream and far downstream, on flat and sloped ground, on streets with and without drainage. The only apparent property the unaffected observation points have in common is that they record less than 5 cm of water in the model simulation.

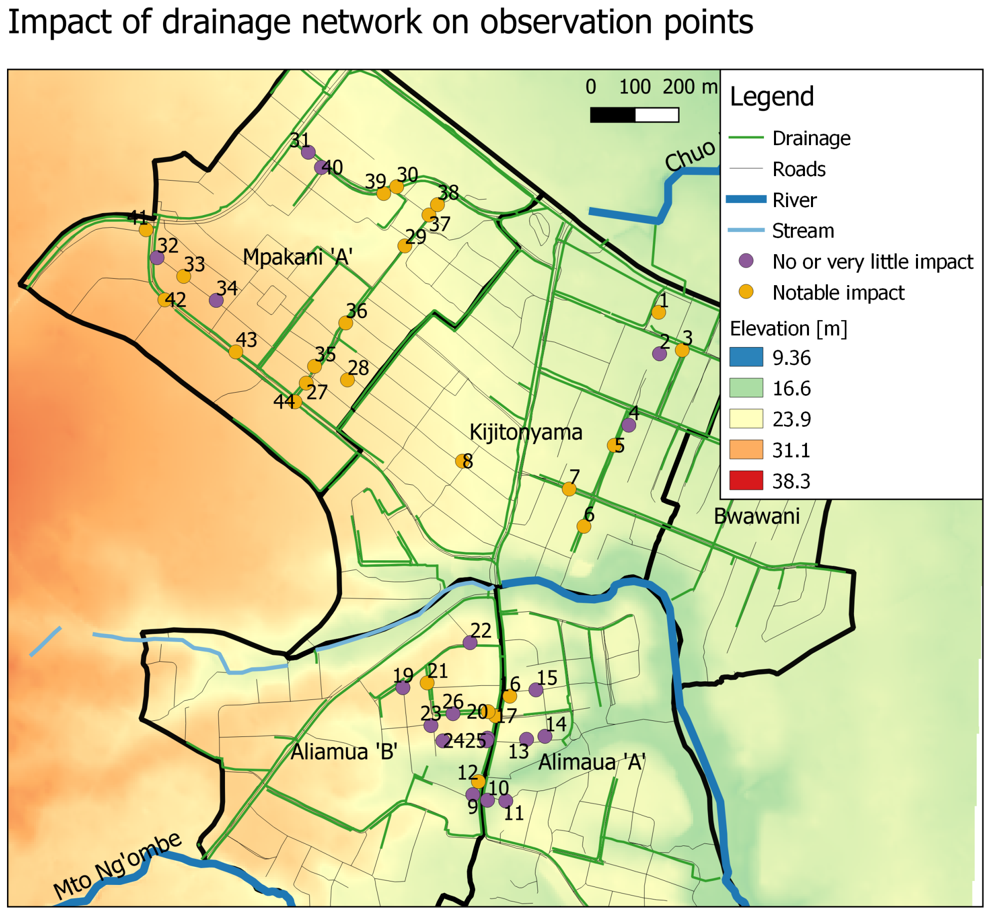

Figure 7.1: The community mapped drainage data influences the flood depth in the northern *mitaa*, but to a much less extent in Alimaua.

Most of the respondents in Alimaua reported that there was *only puddles* on the street outside of their house the morning after the simulated rain event. Six respondents in the middle of Alimaua did, however, report a deeper flood depth, and the model fails to capture this in all simulations. These reports might be wrong, but the consistency of them indicate that it indeed was considerable water depths here during the storm event. It is not known why the model generates almost no standing water in Alimaua, when the rain event, in fact, was of considerable magnitude. As the catchment in this *mtaa* is small and the distance to the nearest water course is short and the ground slope is steep, the water might not accumulate here in the same way as it does in the northern *mitaa*. This reveals limitations with the flood extent survey as validation method for pluvial flooding, as the simulated events might not cause changes outside of the drainage segments. This could potentially be improved by refining the validation method. The observation points were inserted at the exactly same locations as the recorded geopoints of the survey, which might cause validation errors as the respondents were referring to the water level on the street outside of their houses, but it was not controlled if the observation points indeed were located on streets. There might be offsets that have been caused by errors in the GPS accuracy of the smartphones that recorded the survey. For future validations, it might be appropriate to move observation points to the nearest street. Furthermore, a less precise but perhaps more reliable method might be to use a binary approach in the validation. It can be examined whether the water level exceed the surface level of the drainage at the location, and check if the community members reported a flood depth deeper than *only puddles*.

Nevertheless, the flood extent survey appears to be a promising way to validate model outputs, as a large amount of flood records can be collected with limited resources. It might, however, be more appropriate to use the method for fluvial flooding, given the high uncertainties when asking community members to assess shallow water depths. The person's height reference system can be further studied and developed, to see how well it corresponds with actual water levels.

In scenario 3, the cross section of segments are decreased or closed to simulate the impact of solid waste blockages. Again, almost no difference is detected in the observation points for these events, which is expected to be due to the shallow water depths outside of the drainage channels. This is possibly exacerbated by the relatively coarse resolution of the DTM for an urban environment, 5x5 meters, which might be too low to detect shallow water level variations on the ground level. Instead, the impact of solid waste blockages is studied inside the drainage segments, at 18 locations upstream of the blockages. A distinction is made between main and secondary transport routes, as the impact is expected to be larger on main transport routes. It is difficult to draw general conclusions from the results; two points record a considerable decrease of maximum water depth, and two a considerable increase. The remaining 14 channels show a difference of maximum a few centimetres when blocking drainage segments downstream. Nevertheless, in scenario 3b, the 1D-schematisation reports water on the street at more locations at peak flow compared to a simulation without solid waste blockages. The results do not show any difference between main and secondary transport routes. An important observation can be made from the fact that the simulated event consists of two flow peaks. Segments that are loaded with high water levels in the first peak fail to drain the water before the next flow peak, which they would have managed to do if the drainage segments downstream were not blocked, as shown by scenario 2c. This drainage problem appears even if the drainage system initially was dry in the modelled event. The effect is expected to get exacerbated in wet conditions, for example during events in the middle of the rainy season, as the drainage system then is partially full at the beginning of the event.

The research on the impact of solid waste has only started. This thesis shows that such studies must be carried out in drainage systems that are loaded with a considerable amount of runoff, to be able to detect any impact of the solid waste blockages. Experimental studies can investigate how different types and extents of blockages affect the conveyance capacity of drainage segments, and statistical approaches can be used to detect how much, and where, the blockages must occur to have a considerable impact upstream. It was noted during fieldwork that there is a high temporal variability of solid waste accumulations in drainage systems. A drain that is blocked one day, might be cleared the next day. Hence, it is considered difficult to validate models run with blockage data collected in the field. It might be more appropriate to use experimental approaches to investigate the impact of solid waste.

The quality of the drainage data collected by *Ramani Huria* has been studied in terms of accuracy and completeness. The data set is almost complete; only one segment is missing one dimension, and only a few segments are missing reported materials. The positional accuracy in the 2D plane can not be compared with a reference data set, but it is assumed to be high as it has been compared with aerial imagery in the data cleaning process. Three different types of positional errors are identified; tracing errors, disconnected ends and double segments. These errors are, however, only encountered a few times in the data set. However, the elevation of the bed levels in the drainage system is very uncertain, and is expected to decrease the positional accuracy significantly in the z-direction. When inspecting side views of the drainage data in its original state, many gaps are present in the connections between drains. In some cases, the cross sections of the segments do not overlap at all, which has a major impact on the drainage capacity of the segments in the model. This error is mitigated by adjusting the bed levels to each other, to create a more smooth network. This adjustment does, however, not influence the model validation. It would have been desirable to visualise in which locations the water increase, decrease or remain unchanged and relate it to how the bed level was adjusted at each location. This analysis was not possible to do with available resources, given the time consuming process to retrieve simulation results from calculation nodes in the modelling software. It should also be noted that it would have been more valid to examine the water *depth* instead of absolute water level when studying the impact of adjusted bed levels, as the water level difference between the scenarios might be explained by the bed level difference. On the other hand, it can be argued that it is more worthwhile to focus future research on how to make more accurate elevation measurements with limited resources, for example using dynamic differential barometry. Apparently, efforts to refine bed levels derived with the methodology presented here do not improve the model output. Hence, the results of this thesis show that the major improvement of the model performance is achieved by implementing a drainage network as recorded by the drainage mappers, and no further adjustments must be done. The only exceptions are so called *T-junctions*, that must be removed from the data set.

Distributed friction values of the drainage network do not improve the model validation, when comparing with a scenario run with constant friction values. The impact on water levels in the drainage system is also small; 69% of the calculation nodes record a difference in maximum water depth that is smaller than 1 cm. Again, it would have been desirable to visualise how the water level differences spatially correlates with distributed friction values upstream, to better understand the impact of these adjustments. The absence of impact might be explained by the fact that 76% of all segments in the study area have the same reported material. On the other hand, it can be argued that these results show that distributed friction values might not be necessary to take into account at this stage when modelling with community mapped drainage data. The increased accuracy that is achieved by assigning correct friction values is possibly overruled by other errors in the schematisation, most likely elevation errors.

The model developed in this thesis neglects infiltration and assumes a lumped value of the land roughness. As the simulated event is short and intense, it would not influence the model output significantly to take infiltration into account. It is expected that distributed land roughness would have had an impact on the model output, but it is difficult to assess how it would have redistributed the simulated runoff. The land roughness is overestimated in the model schematisation, as the study area is not only covered by buildings, but also other land use types. It might be appropriate to set a lower value for land roughness in future schematisations.

As stated in the Sendai framework [41], disaster risk reduction requires open and up-to-date data. Given the low barriers to produce community mapped data, it offers an accessible way to perform regular surveys that are up-to-date. The mapping campaign carried out by *Ramani Huria* does, however, not answer the question how this could be organised. The drainage mapping of Dar es Salaam has been carried out over the last two years, and some of the collected data is already outdated. Field work revealed that the roads and drainage in northern *mtaa wa* Kijitonyama and Bwawani have been elevated in 2018, after the applied data set was mapped. This was not taken into account in the schematisation, as the dimensions of the new drainage could not be measured with available resources. It would be desirable to develop an institutional framework that guarantees regular updates of community mapped data sets.

This thesis has scrutinised and applied community mapped drainage data to an extent that has not been done previously. The drainage data collected by *Ramani Huria* is assessed to be extensive and accurate, especially when regarding attributes and location in the 2D-plane. It is still a challenge to implement correct drainage bed levels with open source technologies, which imposes high uncertainties in the model schematisation. Despite this, the drainage data collected by *Ramani Huria* allows for modelling, planning and design on a level of detail that has not been possible previously. *Ramani Huria* demonstrates how volunteered geographic information and ICT allows for the production of high-quality, extensive data in resource-strained environments. The exploration of the potential of community mapped data for building flood resilience has only started.

Chapter 8

Conclusion

The research carried out in this thesis has been guided by two research questions. The first question aims to investigate if community mapped drainage data can improve flood prediction on neighbourhood scale. The results show that this is possible, once a work flow has been defined that can implement the data in a hydrodynamic modelling software. The output of the model is validated with community members' reports on flood depth, recorded the morning after the simulated event, and the simulated water depth corresponds better with this data when introducing the community mapped drainage data, compared to a scenario run without the drainage network. The largest contribution of the drainage data mapped by *Ramani Huria* is that it is extensive and of high quality. Very few errors are present in the data set, almost no attributes are missing, and when studying previous research, it can be expected that this drainage data is more extensive than data held by local authorities. Hence, it is proven that the mapping methodology applied by *Ramani Huria* has the potential to support decision making, flood resilience plans, risk reduction and urban development in resource-strained environments.

The second research question applies the model to investigate the impact of solid waste blockages in the drainage network on flooding. Two events are simulated, one with blockages recorded in the field the morning after the simulated event, and one experiment where a third of the culverts in a part of the study area are blocked. The results show that more locations in the model get flooded when implementing solid waste blockages, and that the drainage capacity of the system is reduced. This effect is expected to be exacerbated in heavier storm events. No conclusions can be drawn about how the locations of the blockages influence the water levels upstream. The further study of how solid waste blockages impact floods on neighbourhood scale is a topic for future research, that now can be explored with models built with community mapped drainage data.

Chapter 9

Outlook

This thesis ends with a summary of ideas which could support improvement and further understanding of flood modelling with community mapped data. The outlook includes recommendations for future drainage mapping projects and recommendations for future research.

9.1 Recommendations for future drainage mapping projects

During the work of this thesis, a few experiences have been acquired that could support future mapping campaigns utilising the ODK collect application.

- The elevation of the bed levels is still a challenge, due to the limitations of the method to derive it from a digital terrain model. As shown in this thesis, gaps are introduced in the bed levels when assuming that the elevation is constant along a whole drainage segment. This could be improved by measuring the downstream elevation before a geotrace is started, and upstream elevation when the geotrace is finished.
- Even if the quality of the *Ramani Huria* drainage data is assessed to be high, especially in terms of completeness, it can of course be further improved. The dimensions of decommissioned drains is not reported in the data set, which would be desirable. It is recommended to pay more attention to equal distances when mapping in the field, to increase the accuracy of the data. For example, if the surface level of a drain is aligned with the reference road next to it, the depth and elevation of the drain must not be recorded twice, but can be set to the same value.
- What here is labelled *T-junctions*, see section 5.1.1, must be avoided when recording geotraces. Or else, these segments will be perceived as disconnected by any modelling software. This can be done in the field, or in the data cleaning process.
- When building flood models, it is of importance to know the reaches and dimensions of natural water courses, especially when assigning boundary conditions of the model and interpreting the model output. Hence, community mapping for flood modelling could also include the surveying of small streams. The streams can be traced on aerial imagery, and additional measurements can be performed on site.
- *Ramani Huria* has assigned *width* and *depth* for rectangular drains, and *top width* and *bottom with* for trapezoidal drains. This causes a lot of extra work in the data processing. It is recommended to only make use of the *top width* and *bottom with* dimensions, and when the cross section is rectangular, they are set to the same value.

9.2 Recommendations for future research

Many research topics, of more or less technical character, can continue the study of how community mapped data can support resilience building in resource-strained environments. A few areas of research are proposed here.

- The drainage data analysed in this thesis does not contain information on who is in charge of the construction and maintenance of the drainage segments. This information could add an interesting dimension to the data, that would support the cooperation between different stakeholders in the application of community mapped data. The knowledge exchange with local authorities, for example the Tanzanian Urban and Rural Road Agency, should be examined and handled with care. Scientists must pay attention to how open source data applied in governance influence the relation between authorities and community members.
- Community mapped drainage data can be compared with drainage data held by local authorities to get a better understanding of its added value in terms of positional accuracy and completeness.
- The simulation run in this thesis is an isolated rain event of a few hours, and it could be examined how big the impact of the drainage network is when running longer time series. In this case, the infiltration capacity should also be taken into account, which can be derived from the soil sample survey performed by *Ramani Huria* in 2018. Future models could also investigate the impact of distributed land roughness values.
- Some steps in the work flow proposed in this thesis, see appendix C, is not performed with open source software. This serves as a start, but must be improved to be accessible for everyone.
- There is a lot to be done in the understanding of how solid waste blockages impact floods on neighbourhood scale. This includes the impact of types of blockages, blockage extent, and temporal and spatial variability. Experimental studies can investigate how different types and extents of blockages affect the conveyance capacity of drainage segments, and statistical approaches can be used to detect how much, and where, the blockages must occur to have a considerable impact upstream.

Bibliography

[1] Gordon McGranahan, Deborah Balk, and Bridget Anderson. The rising tide: Assessing the risks of climate change and human settlements in low elevation coastal zones. *Environment and Urbanization*, 19(1):17–37, 2007. ISSN 09562478. doi: 10.1177/0956247807076960.

[2] Frederik Ramm, Jochen Topf, and Steve Chilton. *OpenStreetMap - Using and Enhancing the Free Map of the World*. UIT Cambridge Ltd., Cambridge, 2011. ISBN 978-1-906860-11-0.

[3] Robert Soden and Leysia Palen. From Crowdsourced Mapping to Community Mapping: The Post-earthquake Work of OpenStreetMap Haiti. In *COOP 2014 - Proceedings of the 11th International Conference on the Design of Cooperative Systems, 27-30 May 2014, Nice (France)*, pages 311–326. Springer International Publishing, Cham, 2014. doi: 10.1007/978-3-319-06498-7{_}19. URL `http://link.springer.com/10.1007/978-3-319-06498-7_19`.

[4] Mark Iliffe, James Goulding, and Hessel Winsemius. Towards a Conceptual Framework for Participatory Mapping in Developing Countries. *Gisruk 2017*, 2017. URL `http://huckg.is/gisruk2017/GISRUK_2017_paper_106.pdf`.

[5] Susan Hanson, Robert Nicholls, N. Ranger, S. Hallegatte, J. Corfee-Morlot, C. Herweijer, and J. Chateau. A global ranking of port cities with high exposure to climate extremes. *Climatic Change*, 104(1):89–111, 2011. ISSN 01650009. doi: 10.1007/s10584-010-9977-4.

[6] S. N. Jonkman. Global perspectives on loss of human life caused by floods. *Natural Hazards*, 34 (2):151–175, 2005. ISSN 0921030X. doi: 10.1007/s11069-004-8891-3.

[7] M. Haklay and P. Weber. OpenStreetMap: User-Generated Street Maps. *IEEE Pervasive Computing*, 7(4):12–18, 10 2008. ISSN 1536-1268. doi: 10.1109/MPRV.2008.80. URL `http://ieeexplore.ieee.org/document/4653466/`.

[8] Eskedar Gebremedhin. Participatory Modelling and Mapping for Flood Risk Managment - Urban Planning Study in Dar es Salaam Tanzania. Technical report, UNESCO-IHE Institute for Water Education, Delft, 2017.

[9] Judy L Baker. *Climate Change, Disaster Risk, and the Urban Poor: Cities Building Resilience for a Changing World*. The World Bank, Washington, DC, 2012. ISBN 9780821388457. URL `https://openknowledge.worldbank.org/handle/10986/6018`.

[10] Michael E. Schlesinger and Natalia G. Andronova. Causes of global temperature changes during the 19th and 20th centuries. *Geophysical Research Letters*, 27(14):2137–2140, 2000.

[11] Michael Mann, Jeffrey Park, and R.S. Bradley. Global interdecadal and century-scale climate oscillations during the past five centuries. *Nature*, 378:266–270, 1995.

[12] Natesan Mahasenan, Robert G. Watts, and Hadi Dowlatabadi. Low-frequency oscillations in temperature-proxy records and implications for recent climate change. *Geophysical Research Letters*, 24(5):563–566, 1997. ISSN 00948276. doi: 10.1029/97GL00319.

[13] Thomas G. Huntington. Evidence for intensification of the global water cycle: Review and synthesis. *Journal of Hydrology*, 319(1-4):83–95, 2006. ISSN 00221694. doi: 10.1016/j.jhydrol.2005.07.003.

[14] L O Mearns, M Hulme, T R Carter, R Leemans, M Lal, and P Whetton. Climate Scenario Development (Chapter 13). In Climate Change 2001: The Scientific Basis, Contribution of Working Group I to the Third Assessment Report of the IPCC. pages 583–638, 2001. ISSN 17498198. doi: 10.1111/j.1749-8198.2011.00426.x.

[15] Myles R. Allen and William J. Ingram. Constraints on future changes in climate and the hydrologic cycle. *Nature*, 419(6903), 2002. ISSN 00280836. doi: 10.1038/nature01092.

[16] S. Westra, H. Fowler, J. Evans, L. Alexander, P. Berg, F. Johnson, E. Kendon, G. Lenderink, and N. Roberts. Future changes to the intensity and frequency of short-duration extreme rainfall. *Reviews of Geophysics*, 52:522–555, 2014. doi: 10.1002/2015RG000500.

[17] Gavin D. Madakumbura, Hyungjun Kim, Nobuyuki Utsumi, Hideo Shiogama, Erich M. Fischer, Øyvind Seland, John F. Scinocca, Daniel M. Mitchell, Yukiko Hirabayashi, and Taikan Oki. Event-to-event intensification of the hydrologic cycle from 1.5 °C to a 2 °C warmer world. *Scientific Reports*, 9(1):1–7, 2019. ISSN 20452322. doi: 10.1038/s41598-019-39936-2.

[18] Aiguo Dai, Inez Y. Fung, Anthony D. Del Genio, Aiguo Dai, Inez Y. Fung, and Anthony D. Del Genio. Surface Observed Global Land Precipitation Variations during 1900–88. *Journal of Climate*, 10(11): 2943–2962, 11 1997. ISSN 0894-8755. doi: 10.1175/1520-0442(1997)010<2943:SOGLPV>2.0.CO;2. URL http://journals.ametsoc.org/doi/abs/10.1175/1520-0442%281997%29010%3C2943%3ASOGLPV%3E2.0.CO%3B2.

[19] Mike Hulme, Timothy J. Osborn, and Timothy C. Johns. Precipitation sensitivity to global warming: Comparison of observations with Had CM2 simulations. *Geophysical Research Letters*, 25(17): 3379–3382, 1998. ISSN 00948276. doi: 10.1029/98GL02562.

[20] J.L. Probst and Y. Tardy. Long range streamflow and world continental runoff fluctuations since the beginning of this century. *Journal of Hydrology*, 94(3-4):289–311, 10 1987. ISSN 0022-1694. doi: 10.1016/0022-1694(87)90057-6. URL https://www.sciencedirect.com/science/article/pii/0022169487900576.

[21] David Labat, Yves Goddéris, Jean Luc Probst, and Jean Loup Guyot. Evidence for global runoff increase related to climate warming. *Advances in Water Resources*, 27(6):631–642, 6 2004. ISSN 0309-1708. doi: 10.1016/J.ADVWATRES.2004.02.020. URL https://www.sciencedirect.com/science/article/pii/S0309170804000478.

[22] Joseph Alcamo, Petra Doell, Frank Kaspar, and Stefan Siebert. Global change and global scenarios of water use and availability: An Application of WaterGAP1.0. Technical report, Center for Environmental Systems Research (CESR), University of KasseL, 1997.

[23] Nigel W. Arnell. Climate change and global water resources. *Global Environmental Change*, 9: S31–S49, 10 1999. ISSN 0959-3780. doi: 10.1016/S0959-3780(99)00017-5. URL https://www.sciencedirect.com/science/article/pii/S0959378099000175.

[24] S. Manabe, R. T. Wetherald, P. C. D. Milly, T. L. Delworth, and R. J. Stouffer. Century-Scale Change in Water Availability:CO2 -Quadrupling Experiment. *Climatic Change*, 64(1/2):59–76, 5 2004. doi: 10.1023/B:CLIM.0000024674.37725.ca. URL http://link.springer.com/10.1023/B:CLIM.0000024674.37725.ca.

[25] United Nations. World Urbanization Prospects: The 2018 Revision. *United Nations Economic & Social Affairs*, pages 1–2, 2018.

[26] United Nations. World Urbanization Prospects: The 2014 Revision. *United Nations Economic & Social Affairs*, 2015.

[27] Shlomo Angel, Jason Parent, Daniel L. Civco, Alexander Blei, and David Potere. The dimensions of global urban expansion: Estimates and projections for all countries, 2000-2050. *Progress in Planning*, 75(2):53–107, 2011. ISSN 03059006. doi: 10.1016/j.progress.2011.04.001.

[28] European Parliament and Council of the European Union. Directive 2007/60/EC of the European Parliament and of the Council of 23 October 2007 on the assessment and management of flood risks. *Off. J. Eur. Union Legis*, 50:27–34, 2007.

[29] G. Berz, W. Kron, T. Loster, E. Rauch, J. Schimetschek, J. Schmieder, A. Siebert, A. Smolka, and A. Wirtz. World Map of Natural Hazards – A Global View of the Distribution and Intensity of Significant Exposures. *Natural Hazards*, 23(2/3):443–465, 2001. ISSN 0921030X. doi: 10.1023/A:1011193724026. URL http://link.springer.com/10.1023/A:1011193724026.

[30] J French and K Holt. Floods. In M.B Gregg, editor, *The Public Health Consequences of Disasters*. US Department of Health and Human Services, Atlanta, Georgia, 1989.

[31] David Butler, John Davies, and John Davies. *Urban Drainage, Third Edition.* CRC Press, 9 2010. ISBN 9781315272535. doi: 10.1201/9781315272535. URL https://www.taylorfrancis.com/books/9781315272535.

[32] Bernice R. Rosenzweig, Lauren McPhillips, Heejun Chang, Chingwen Cheng, Claire Welty, Marissa Matsler, David Iwaniec, and Cliff I. Davidson. Pluvial flood risk and opportunities for resilience. *Wiley Interdisciplinary Reviews: Water*, 5(6):e1302, 2018. ISSN 20491948. doi: 10.1002/wat2.1302. URL http://doi.wiley.com/10.1002/wat2.1302.

[33] R.H. Falconer, D. Cobby, P. Smyth, G. Astle, J. Dent, and B. Golding. Pluvial flooding: new approaches in flood warning, mapping and risk management. *Journal of Flood Risk Management*, 2(3):198–208, 9 2009. ISSN 1753318X. doi: 10.1111/j.1753-318X.2009.01034.x. URL http://doi.wiley.com/10.1111/j.1753-318X.2009.01034.x.

[34] Heejun Chang, Martin Lafrenz, Il-Won Jung, Miguel Figliozzi, Deena Platman, and Cindy Pederson. Potential Impacts of Climate Change on Flood-Induced Travel Disruptions: A Case Study of Portland, Oregon, USA. *Annals of the Association of American Geographers*, 100(4):938–952, 8 2010. ISSN 0004-5608. doi: 10.1080/00045608.2010.497110. URL http://www.tandfonline.com/doi/abs/10.1080/00045608.2010.497110.

[35] I. Douglas, S. Garvin, N. Lawson, J. Richards, J. Tippett, and I. White. Urban pluvial flooding: A qualitative case study of cause, effect and nonstructural mitigation. *Journal of Flood Risk Management*, 3(2):112–125, 2010. ISSN 1753318X. doi: 10.1111/j.1753-318X.2010.01061.x.

[36] R.L Wilby. A Review of Climate Change Impacts on the Built Environment. *Built Environment*, 33 (1):31–45, 3 2007. ISSN 02637960. doi: 10.2148/benv.33.1.31. URL http://openurl.ingenta.com/content/xref?genre=article&issn=0263-7960&volume=33&issue=1&spage=31.

[37] Lawrence B. Cahoon and Marc H. Hanke. Rainfall effects on inflow and infiltration in wastewater treatment systems in a coastal plain region. *Water Science and Technology*, 75(8):1909–1921, 4 2017. ISSN 0273-1223. doi: 10.2166/wst.2017.072. URL https://iwaponline.com/wst/article/75/8/1909-1921/19506.

[38] Elinor Ostrom. Polycentric systems for coping with collective action and global environmental change. *Global Environmental Change*, 20(4):550–557, 10 2010. ISSN 0959-3780. doi: 10.1016/J.GLOENVCHA.2010.07.004. URL https://www.sciencedirect.com/science/article/pii/S0959378010000634.

[39] Jonathan D. Paul, Wouter Buytaert, Simon Allen, Juan A. Ballesteros-Cánovas, Jagat Bhusal, Katarzyna Cieslik, Julian Clark, Sumit Dugar, David M. Hannah, Markus Stoffel, Art Dewulf, Megh R. Dhital, Wei Liu, Janak Lal Nayaval, Bhanu Neupane, Arnulf Schiller, Paul J. Smith, and Robert Supper. Citizen science for hydrological risk reduction and resilience building. *Wiley Interdisciplinary Reviews: Water*, 5(1):e1262, 2018. ISSN 20491948. doi: 10.1002/wat2.1262. URL http://doi.wiley.com/10.1002/wat2.1262.

[40] Global Water Partnership Technical Advisory Committee. *Integrated Water Resources Management. Background Paper No.4.* Number 4. 2000. ISBN 91-630-9229-8. URL www.gwpforum.org.

[41] United Nations. Sendai Framework for Disaster Risk Reduction 2015 - 2030. Technical report, 2015.

[42] Brenda Parker. Constructing community through maps? Power and praxis in community mapping. *Professional Geographer*, 58(4):470–484, 2006. ISSN 00330124. doi: 10.1111/j.1467-9272.2006.00583.x.

[43] Michael F. Goodchild. Citizens as sensors: the world of volunteered geography. *GeoJournal*, 69 (4):211–221, 11 2007. ISSN 0343-2521. doi: 10.1007/s10708-007-9111-y. URL http://link.springer.com/10.1007/s10708-007-9111-y.

[44] Alek Felstiner. Employment and Labor Law in the Crowdsourcing Industry. *Berkeley Journal of Employment and Labor Law*, 32(1):143–202, 2011. URL papers.ssrn.com/sol3/papers.cfm?abstract_id=1593853.

[45] Matthew Zook, Mark Graham, Taylor Shelton, and Sean Gorman. Volunteered Geographic Information and Crowdsourcing Disaster Relief: A Case Study of the Haitian Earthquake. *World Medical & Health Policy*, 2(2):6–32, 1 2010. ISSN 1948-4682. doi: 10.2202/1948-4682.1069. URL http://doi.wiley.com/10.2202/1948-4682.1069.

[46] Andrew J. Flanagin and Miriam J. Metzger. The credibility of volunteered geographic information. *GeoJournal*, 72(3-4):137–148, 2008. ISSN 03432521. doi: 10.1007/s10708-008-9188-y.

[47] Wouter Buytaert, Zed Zulkafli, Sam Grainger, Luis Acosta, Tilashwork C. Alemie, Johan Bastiaensen, Bert De Bièvre, Jagat Bhusal, Julian Clark, Art Dewulf, Marc Foggin, David M. Hannah, Christian Hergarten, Aiganysh Isaeva, Timothy Karpouzoglou, Bhopal Pandeya, Deepak Paudel, Keshav Sharma, Tammo Steenhuis, Seifu Tilahun, Gert Van Hecken, and Munavar Zhumanova. Citizen science in hydrology and water resources: opportunities for knowledge generation, ecosystem service management, and sustainable development. *Frontiers in Earth Science*, 2:26, 10 2014. ISSN 2296-6463. doi: 10.3389/feart.2014.00026. URL http://journal.frontiersin.org/article/10.3389/feart.2014.00026/abstract.

[48] Muki Haklay. Citizen Science and Volunteered Geographic Information: Overview and Typology of Participation. In *Crowdsourcing Geographic Knowledge*, pages 105–122. Springer Netherlands, Dordrecht, 2013. doi: 10.1007/978-94-007-4587-2{_}7. URL http://www.springerlink.com/index/10.1007/978-94-007-4587-2_7.

[49] Jeffrey C. Davids, Martine M. Rutten, Anusha Pandey, Nischal Devkota, Wessel David van Oyen, Rajaram Prajapati, and Nick van de Giesen. Citizen science flow - an assessment of citizen science streamflow measurement methods. *Hydrology and Earth System Sciences Discussions*, pages 1–28, 2018. doi: 10.5194/hess-2018-425.

[50] Mark Peter Iliffe. *The praxis of community mapping in developing countries*. PhD thesis, University of Nottingham, 2017.

[51] Roger Bilham. Lessons from the Haiti earthquake. *Nature*, 463(7283):878–879, 2 2010. ISSN 0028-0836. doi: 10.1038/463878a. URL http://www.nature.com/doifinder/10.1038/463878a.

[52] Martin Dittus, Giovanni Quattrone, and Licia Capra. Social Contribution Settings and Newcomer Retention in Humanitarian Crowd Mapping. pages 179–193. Springer, Cham, 11 2016. doi: 10.1007/978-3-319-47874-6{_}13. URL http://link.springer.com/10.1007/978-3-319-47874-6_13.

[53] Jen Ziemke. Crisis Mapping: The Construction of a New Interdisciplinary Field? *Journal of Map & Geography Libraries*, 8(2):101–117, 5 2012. ISSN 1542-0353. doi: 10.1080/15420353.2012.662471. URL http://www.tandfonline.com/doi/abs/10.1080/15420353.2012.662471.

[54] JB Harley. Deconstructing the map. *Cartographica: The International Journal for Geographic Information and Geovisualization*, 26(2):1–20, 10 1989. ISSN 0317-7173. doi: 10.3138/E635-7827-1757-9T53. URL https://utpjournals.press/doi/10.3138/E635-7827-1757-9T53.

[55] Rob Kitchin, Chris Perkins, and Martin Dodge. Thinking about maps. In Martin Dodge, Rob Kitchin, and Chris Perkins, editors, *Rethinking maps - New frontiers in cartographic theory*, chapter 1. Routledge, London, 2009.

[56] Glen Stellmacher. Mapping Kibera: New strategies for mapping and improving the slum. *ARCH 442 Middle East & Africa Seminar*, page 21, 2011.

[57] Erica Hagen. Putting Nairobi's Slums on the Map. *Development Outreach*, 12(1):41–43, 7 2010. ISSN 1020-797X. doi: 10.1596/1020-797X{_}12{_}1{_}41. URL http://elibrary.worldbank.org/doi/abs/10.1596/1020-797X_12_1_41.

[58] Nancy Lee Peluso. Whose woods are these? Counter-mapping forest territories in Kalimantan, Indonesia. *Antipode*, 27(4):383–406, 10 1995. ISSN 0066-4812. doi: 10.1111/j.1467-8330.1995.tb00286.x. URL http://doi.wiley.com/10.1111/j.1467-8330.1995.tb00286.x.

[59] Hansi Senaratne, Amin Mobasheri, Ahmed Loai Ali, Cristina Capineri, and Mordechai (Muki) Haklay. A review of volunteered geographic information quality assessment methods. *International Journal of Geographical Information Science*, 31(1):139–167, 2017. ISSN 13623087. doi: 10.1080/13658816.2016.1189556. URL http://dx.doi.org/10.1080/13658816.2016.1189556.

[60] Mordechai Haklay. How Good is Volunteered Geographical Information? A Comparative Study of OpenStreetMap and Ordnance Survey Datasets. *Environment and Planning B: Planning and Design*, 37(4):682–703, 8 2010. ISSN 0265-8135. doi: 10.1068/b35097. URL http://journals.sagepub.com/doi/10.1068/b35097.

[61] Jean-François Girres and Guillaume Touya. Quality Assessment of the French OpenStreetMap Dataset. *Transactions in GIS*, 14(4):435–459, 8 2010. ISSN 13611682. doi: 10.1111/j.1467-9671.2010.01203.x. URL http://doi.wiley.com/10.1111/j.1467-9671.2010.01203.x.

[62] Mohammad Forghani, Mahmoud Delavar, Mohammad Forghani, and Mahmoud Reza Delavar. A Quality Study of the OpenStreetMap Dataset for Tehran. *ISPRS International Journal of Geo-Information*, 3(2):750–763, 5 2014. ISSN 2220-9964. doi: 10.3390/ijgi3020750. URL http://www.mdpi.com/2220-9964/3/2/750.

[63] Hongchao Fan, Alexander Zipf, Qing Fu, and Pascal Neis. Quality assessment for building footprints data on OpenStreetMap. *International Journal of Geographical Information Science*, 28 (4):700–719, 4 2014. ISSN 1365-8816. doi: 10.1080/13658816.2013.867495. URL http://www.tandfonline.com/doi/abs/10.1080/13658816.2013.867495.

[64] Julian Will. Development of an automated matching algorithm to assess the quality of the OpenStreetMap road network : a case study in Göteborg, Sweden. *Student thesis series INES; (2014)*, 2014. URL https://lup.lub.lu.se/student-papers/search/publication/4464336.

[65] Pascal Neis, Dennis Zielstra, and Alexander Zipf. The Street Network Evolution of Crowdsourced Maps: OpenStreetMap in Germany 2007–2011. *Future Internet*, 4(1):1–21, 12 2011. ISSN 1999-5903. doi: 10.3390/fi4010001. URL http://www.mdpi.com/1999-5903/4/1/1.

[66] Michael F. Goodchild and Linna Li. Assuring the quality of volunteered geographic information. *Spatial Statistics*, 1:110–120, 5 2012. ISSN 2211-6753. doi: 10.1016/J.SPASTA.2012.03.002. URL https://www.sciencedirect.com/science/article/pii/S2211675312000097?via%3Dihub.

[67] Mordechai (Muki) Haklay, Sofia Basiouka, Vyron Antoniou, and Aamer Ather. How Many Volunteers Does it Take to Map an Area Well? The Validity of Linus' Law to Volunteered Geographic Information. *The Cartographic Journal*, 47(4):315–322, 11 2010. ISSN 0008-7041. doi: 10.1179/000870410X12911304958827. URL http://www.tandfonline.com/doi/full/10.1179/000870410X12911304958827.

[68] V. Antoniou and A. Skopeliti. Measures and indicators of vgi quality: An overview. *ISPRS Annals of the Photogrammetry, Remote Sensing and Spatial Information Sciences*, 2(3W5):345–351, 2015. ISSN 21949050. doi: 10.5194/isprsannals-II-3-W5-345-2015.

[69] Oxford English Dictionary. Authority, . URL www.oed.com.

[70] Oxford English Dictionary. Credibility, . URL www.oed.com.

[71] Ven te Chow, David R. Maidment, and Larry W. Mays. *Applied hydrology*. Mc Graw-Hill, Inc., 1988.

[72] Shervan Gharari. *On the role of model structure in hydrological modeling. Understanding models.* PhD thesis, Delft University of Technology, 2015.

[73] G. Schoups, N. C. van de Giesen, and H. H. G. Savenije. Model complexity control for hydrologic prediction. *Water Resources Research*, 44(12), 12 2008. ISSN 1944-7973. doi: 10.1029/2008WR006836@10.1002/(ISSN)1944-7973.ASSESS1. URL https://agupubs.onlinelibrary.wiley.com/doi/abs/10.1029/2008WR006836%4010.1002/%28ISSN%291944-7973.ASSESS1.

[74] Hubert H. G. Savenije. Analytical Expression for Tidal Damping in Alluvial Estuaries. *Journal of Hydraulic Engineering*, 124(6):615–618, 6 1998. ISSN 0733-9429. doi: 10.1061/(ASCE)0733-9429(1998)124:6(615). URL http://ascelibrary.org/doi/10.1061/%28ASCE%290733-9429%281998%29124%3A6%28615%29.

[75] M. S. Longuet-Higgins. Eulerian and Lagrangian aspects of surface waves. *Journal of Fluid Mechanics*, 173:683–707, 12 1986. ISSN 0022-1120. doi: 10.1017/S0022112086001325. URL https://www.cambridge.org/core/product/identifier/S0022112086001325/type/journal_article.

[76] UN-HABITAT. *Informal Settlements and Finance In Dar es Salaam, Tanzania.* 2010. ISBN 9789211321869. URL https://unhabitat.org/books/informal-settlements-and-finance-in-dar-es-salaam-tanzania/.

[77] African Development Bank. Tracking Africa's Growth in Figures. Technical report, 2014.

[78] Sally Brown, Abiy S Kebede, and Robert J Nicholls. Sea Level Rise and Impacts in Africa, 2000 to 2100. *Unpublished Report to Stockholm Environment Institute*, (April):Oxford, 2009.

[79] World Bank. Tanzania Urban Resilience Program. Annual Report 2018. Technical report, 2018. URL `http://documents.worldbank.org/curated/en/402541542394008047/Tanzania-Urban-Resilience-Programme-Annual-Report-2018`.

[80] Glory Pastory. Community initiatives in planning and management of storm water drainage in informal settlement. A case of Kingugi sub ward, Temeke Municipality, Dar es Salaam. Technical report, Ardhi University, 2018.

[81] Guy J-P. Schumann and Paul D. Bates. The Need for a High-Accuracy, Open-Access Global DEM. *Frontiers in Earth Science*, 6:225, 12 2018. ISSN 2296-6463. doi: 10.3389/feart.2018.00225. URL `https://www.frontiersin.org/article/10.3389/feart.2018.00225/full`.

[82] USBR (United States Bureau of Reclamation). Water Measurement Manual, 3rd Edition Revised Reprinted. Technical report, 2001. URL `www.usbr.gov/pmts/hydraulics_lab/pubs/wmm/`.

[83] Eliseo Clementini, Paolino Felice, and Peter Oosterom. A small set of formal topological relationships suitable for end-user interaction. In *Advances in Spatial Databases, Third International Symposium, SSD '93*, pages 277–295, Singapore, 1003. Springer. doi: 10.1007/3-540-56869-7{_}16.

Appendix A

Questionnaires

A.1 Flood extent survey

1. Record geopoint
2. How deep was the water on the street outside of your house this morning (3 March 2019)?
    - Only puddles
    - Finger depth [0-2 cm]
    - Ankle deep [2-10 cm]
    - Mid-shin deep [10-30 cm]
    - Knee deep [30-50 cm]
    - Waist deep [50-100 cm]
    - Chest deep [100-150 cm]
    - Person's height [150-200 cm]
    - Over person's height [+200 cm]

A.2 Solid waste blockage survey

1. Record geopoint
2. What kind of feature is this?
    - culvert
    - ditch
    - drain
3. What kind of blockage does it have?
    - Solid waste
    - Sand
4. What kind of other blockage does it have? (free text)
5. How blocked is the drain?
    - Half (50%)
    - Three quarters (75%)
    - Completely blocked (100%)

Appendix B

Field maps

This appendix presents the field maps that guided the mappers when they collected the flood extend and blockage survey on 3 March, 2019. The motivation of these maps is described in section 4.2.1. Note that the correct names of the first two *mitaa* are *Alimaua* A and B.

ALI AMUA A

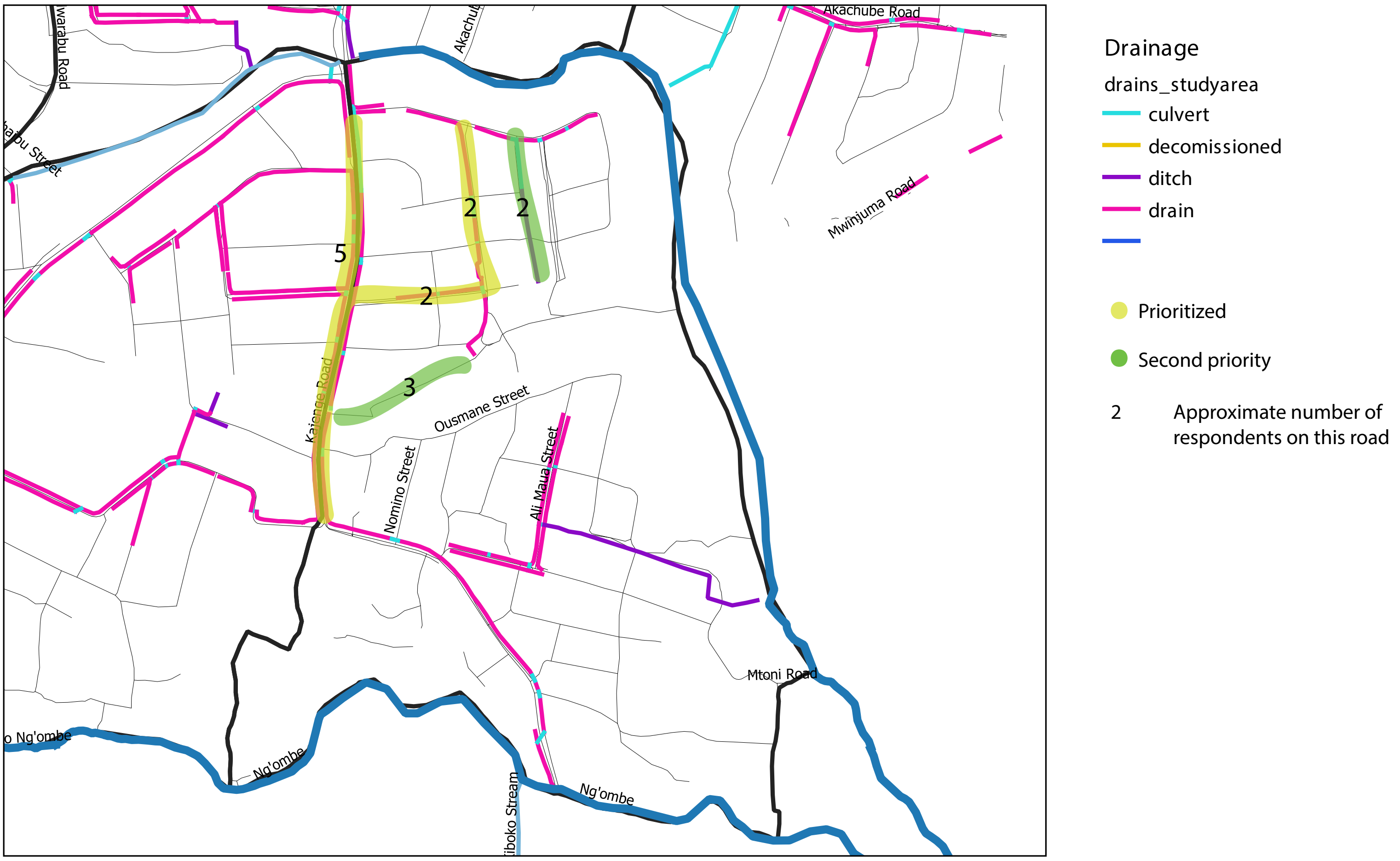

Akachube Road
Akachub
warabu Road
abu Street
Mwinjuma Road
Kajenge Road
Ousmane Street
Nomino Street
Ali Maua Street
Mtoni Road
o Ng'ombe
Ng'ombe
Ng'ombe
iboko Stream
5
2
2
2
3
Drainage
drains_studyarea
culvert
decomissioned
ditch
drain
Prioritized
Second priority
2
Approximate number of respondents on this road

ALI AMUA B

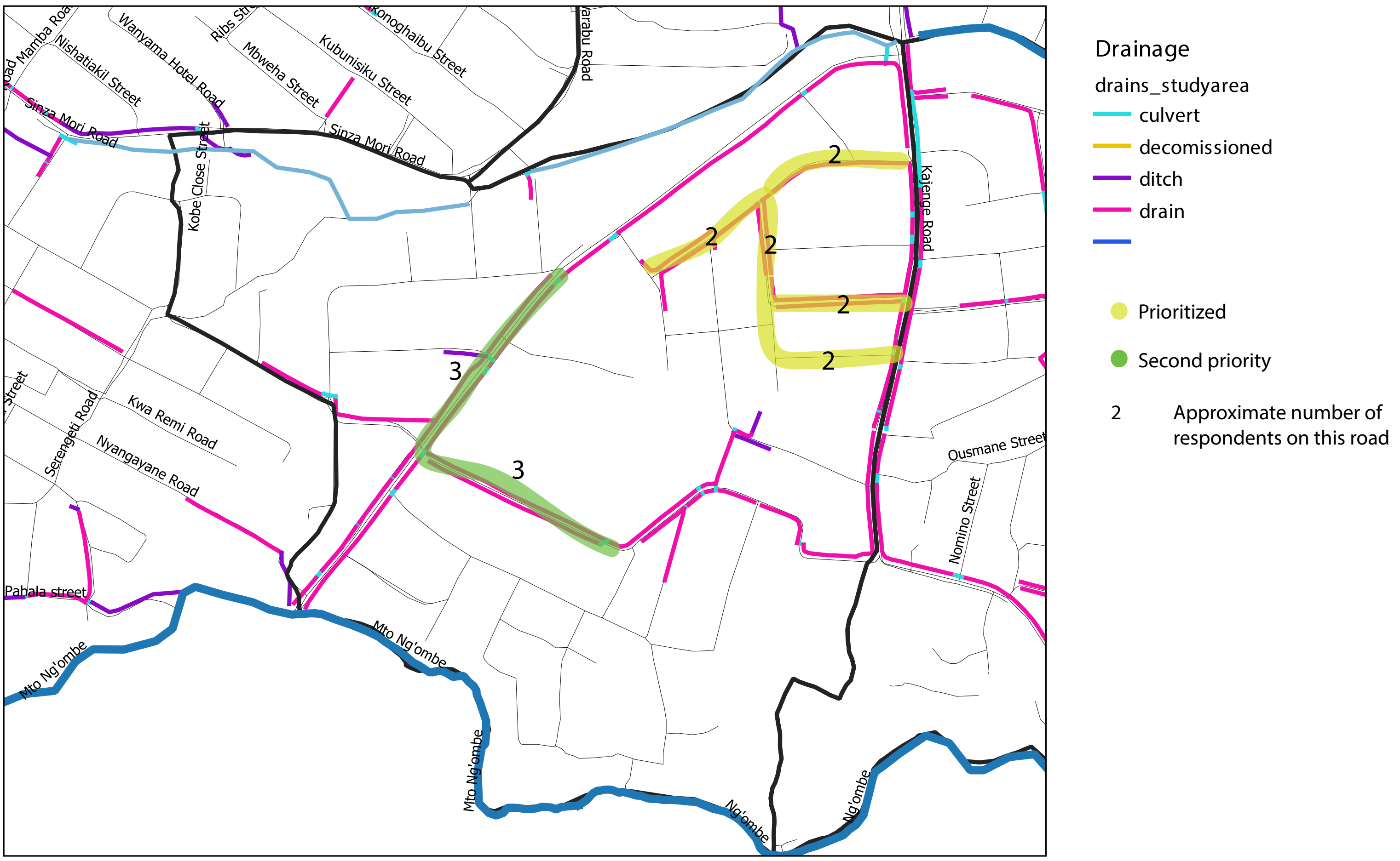

Sinza Mori Road
Kobe Close Street
Wanyama Hotel Road
Nishatiakil Street
Mbweha Street
Kubunisiku Street
Konoghaibu Street
Kwa Remi Road
Nyangayane Road
Serengeti Road
Pahala street
Mto Ng'ombe
Ng'ombe
Kajenge Road
Ousmane Street
Nomino Street
2
2
2
2
2
3
3
Drainage
drains_studyarea
culvert
decomissioned
ditch
drain
Prioritized
Second priority
2 Approximate number of respondents on this road

MPAKANI A

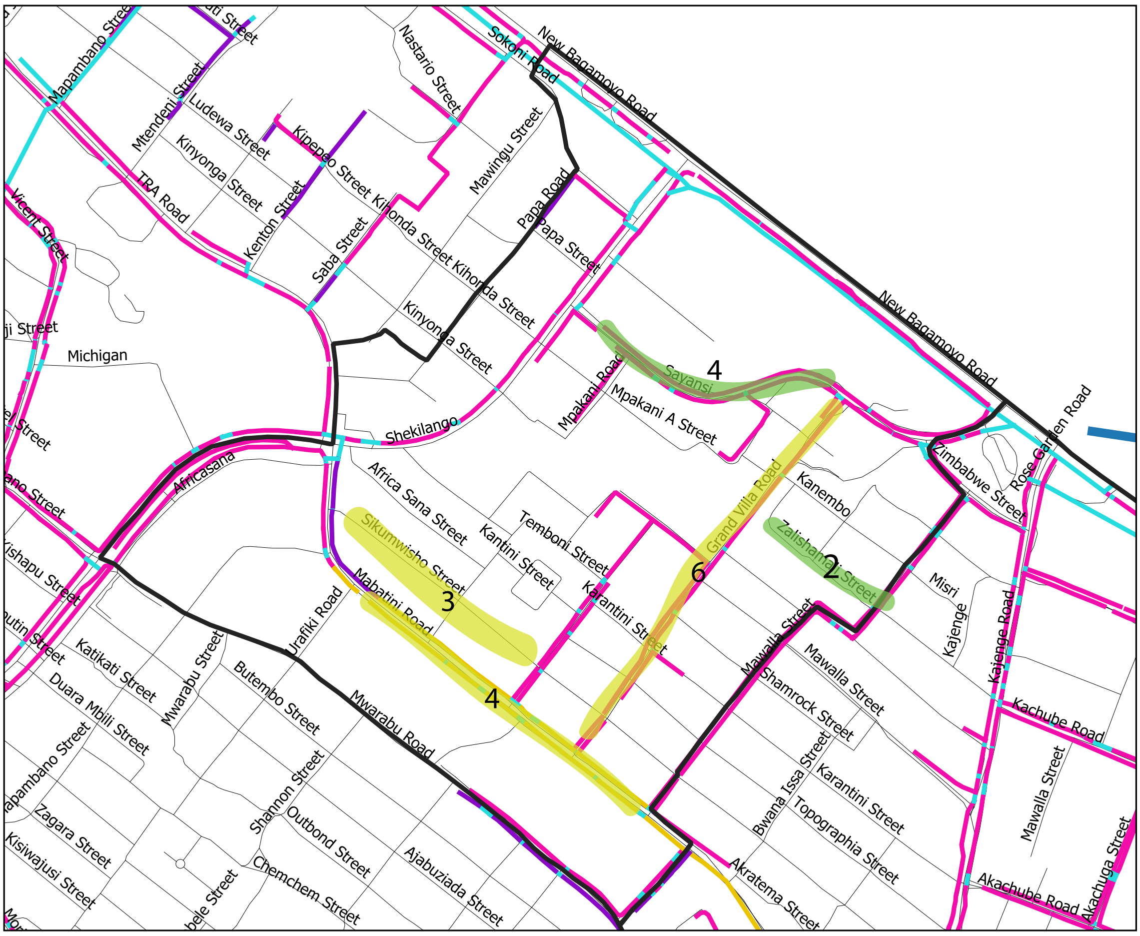

Drainage

drains_studyarea

- culvert
- decomissioned
- ditch
- drain

- Prioritized
- Second priority

2 Approximate number of respondents on this road

KIJITONYAMA (MTAA)

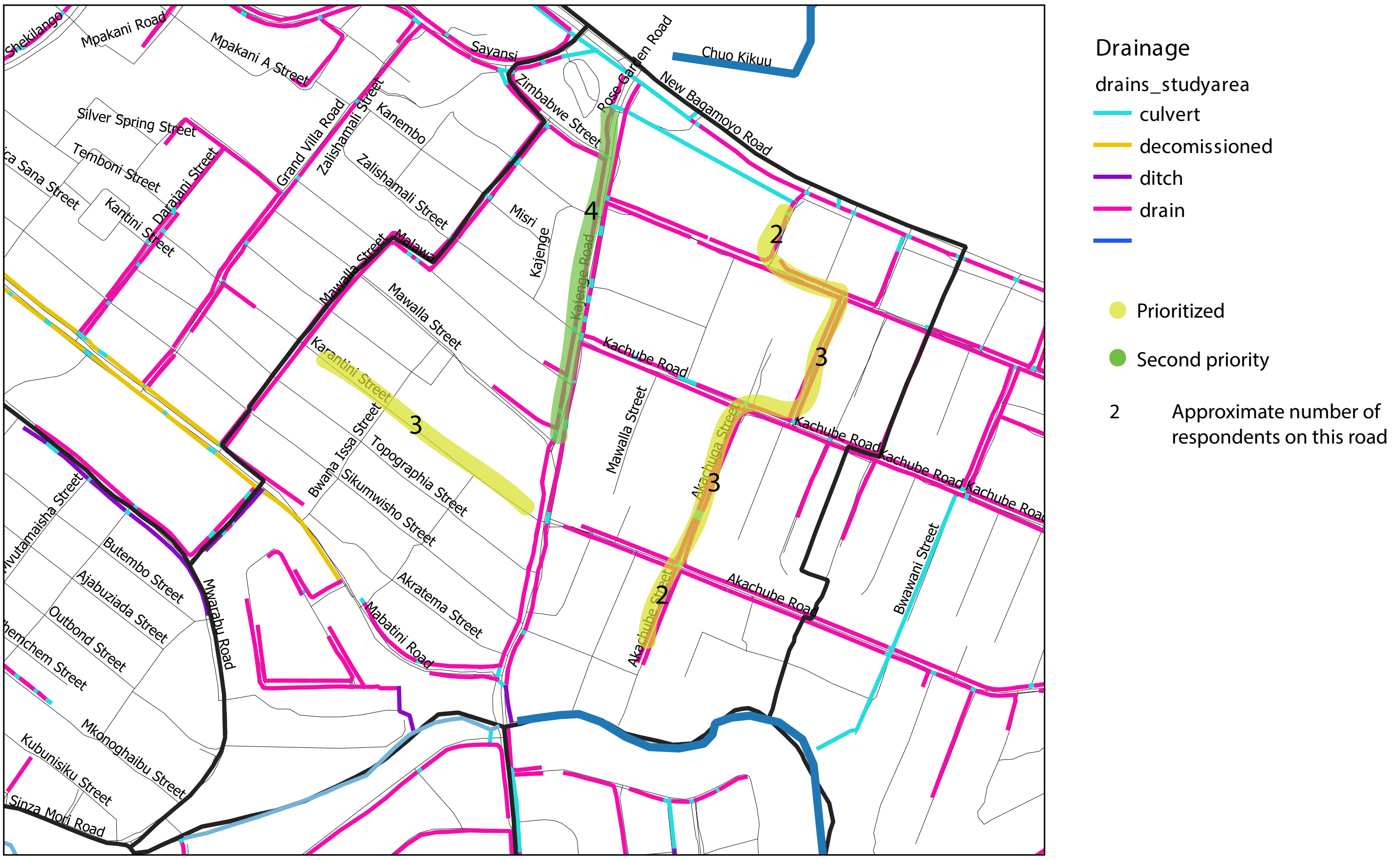

Appendix C

Crash course

How to build a flood model with community mapped drainage data

You need:

- Community mapped drainage data
- A digital terrain model (DTM) of your study area with high resolution
- Precipitation data
- A hydrodynamic modelling software for 1D schematisations[1]

Do like this:

C.1 Prepare model area

1. Download the drainage data in your study area as *.shp*- or *.gpkg*-files from https://export.hotosm.org/ by specifying a sufficient extent on the map. You also need a shapefile of the outline of your study area.
2. Open the drainage data, study area outline and the DTM in QGIS. You must work in a metric coordinate reference system.
3. Clip all drainage segments in your study area with *Vector → Geoprocessing Tools → Clip*. Use the drainage data as input layer, and the outline of the study area as overlay layer.
4. Some drainage might be located just outside of the study area, and is therefore excluded in the clipping, but is still part of the drainage system. An example is shown in Figure C.1. These features must be added manually by copying them in the downloaded drainage data set and paste them in the clipped data set (select *toggle editing* for the clipped data set, select the downloaded data set in the *Layers panel*, select the drainage outside of the study area, click *Copy features*, select the clipped data set in the *Layers panel* and click *Paste features*).
5. All segments must have an unique ID. If your drainage data has no IDs, you can assign it by creating a new field and type *$rownum* in the field calculator.
6. It might be an idea to divide the data set into more drain types than those predefined by *Ramani Huria*, that is *ditch*, *culvert*, *drain* and *decommissioned drain*. For example, your modelling software might treat open and closed drains differently, and then you must

[1]Note that this crash course explains how to prepare the data for SOBEK 2.16, and might not be applicable to other modelling programs.

easily know which segments that have these properties. In this thesis, ten different cross section types were identified, see section 4.1.1. Each cross section type was given a number, and was added as a field in the attribute table of the drainage data. For this thesis, the cross section type *culvert* was assigned with number 4, which is used in the adjustment of bed levels, see section C.5.

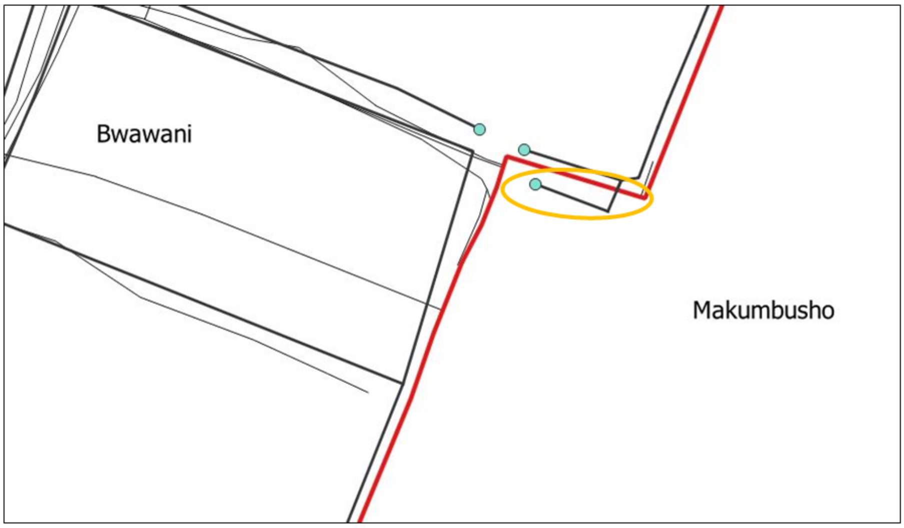

Figure C.1: Example of segment that must be added manually to the clipped data set.

C.2 Check connectivity

Load the shapefile of the drainage data in your modelling software to inspect the connectivity of the network. In SOBEK 2.16, this is done by selecting a flow connection node, pressing shift and then select another node. If the reaches between the nodes gets highlighted, they are connected. Disconnections can occur due to *T-junctions* as explained in section 5.1.1, and those segments must then be split with the *Edit* → *Split Features* tool. Other disconnections can be solved by snapping segments to each other.

C.3 Prepare locations of cross sections

All drainage segments must be assigned with cross sections in the modelling software. These cross sections contain information on the cross section dimensions, e.g. if it is a round or rectangular drain, bed levels and surface levels, and hydraulic roughness, see section 2.3.3. The cross sections should be as close as possible to the end of each segment. The bed- and surface levels will be interpolated between the two cross sections on each segment, and the remaining part between the cross section location and the end will be assumed to be straight by the modelling software. For this thesis, all cross sections are located 1 meter from the ends of each segment. The methodology to perform this is described here, but as will be illustrated, QGIS cannot perform the task satisfactory. For this thesis, the same steps were performed in ArcGIS, with adequate results.

1. Open the *Processing Toolbox*. Browse to *v.buffer* in the *GRASS* package. Choose the drainage data as input layer, and apply a 1.1 meter wide buffer. Check the box *Do not make caps at ends of polylines.*

2. Select the output layer, and apply a negative buffer of 1 meter. This step, unfortunately, creates problems in QGIS. You should get a polygon as output that has a 10 cm buffer

on both sides of the drainage segments, excluding 1 meter at each end, see the blue polygon in figure C.2. However, this operation fails in junctions with QGIS. Figure C.3 shows a junction with correct buffers to the left, and one where the application of buffers goes wrong in QGIS to the right.

3. Clip the drainage data with the buffer polygon as overlay layer. Now, you get a data set consisting of drainage segments that are one meter shorter at each end than the original data set. Add the coordinates of the downstream (DS) and upstream (US) point of each segment. Do this by open the attribute table of your clipped drainage data set, select *toggle editing* and open the *field calculator*. As *Ramani Huria* is starting the geotracing at the DS point of each segment in their mapping, the DS point is the beginning of the segment and the US point is the end of the segment. Select *Create new field*, and type the following in the *Expression* window:

Expression	**Result**	**Label**
x_at(0)	x-coordinate of DS point	ds_x
y_at(0)	y-coordinate of DS point	ds_y
x_ at(-1)	x-coordinate of US point	us_x
y_at(-1)	y-coordinate of US point	us_y

   Turn off *toggle editing*.

4. Save the layer as a *.csv*-file (*Export* → *Save features as...*). Make sure that it has the following attributes stored; ID, if it is covered or not, drain type, cross section type, material, smoothness, diameter, width, depth, top width, bottom width, elevation and downstream and upstream x- and y-coordinates. In the examples below, this file is called *clipped_segments.csv*.

5. Open the *.csv*-file in Excel, save it as *.xlsx*-file. Copy all IDs and paste them below in the same column, so that you have the IDs for each segment twice in that column. Add the suffix *"_ds"* to half of the IDs, and *"_us"* to the other half. Move the upstream coordinates to the upstream IDs. Remove all other attributes. Now you have an excel sheet with three columns; ID, x-coordinate and y-coordinate for all downstream and upstream cross sections.

6. Save the *.xlsx*-file as *.csv*-file again with a new file name, load it as delimited text layer in QGIS, and save it as a point shape file.

7. Load the shape file with the cross section locations in your modelling software. In SOBEK, this is called *reach elements*. Now you have all cross section locations implemented for all reaches in your schematisation. The next step is to assign dimensions, friction and bed- and surface levels to these cross sections. First, the bed- and surface levels must be calculated.

C.4 Calculate bed- and surface levels

This section describes the process to derive the bed level and surface level at the DS and US point of each drainage segment.

1. Import the *.csv*-file that you saved in step 4 in the previous section as delimited text file layer. Set the *X* and *Y*-field to the downstream coordinates (ds_x and ds_y). Repeat the procedure for the upstream coordinates. Save both layers as shape files.

2. The next step is to use these point layers to sample the values of the DTM at the DS and US point of each segment. Download the plugin *Point Sampling Tool*. Open it and

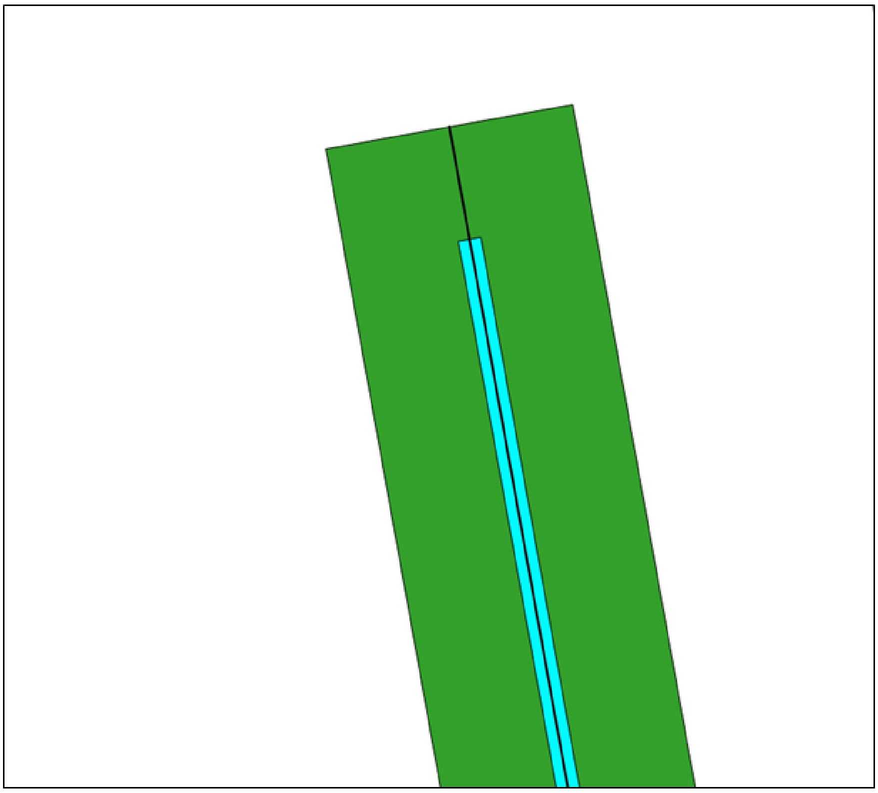

Figure C.2: Drainage segment (black line) with a 1.1 m wide buffer (green) and the overlay clipping layer (blue).

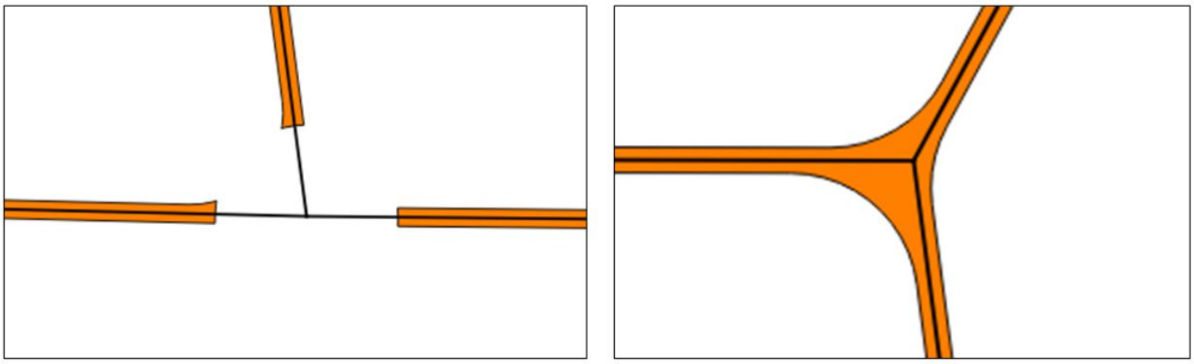

Figure C.3: A junction with correct buffers to the left, and one where the application of buffers goes wrong in QGIS to the right.

set the sampling point layer to your layer with DS points, and the DTM as layer to get values from. For the author, the sampling only succeeded if the output layer was saved as geopackage file, and not as shapefile. Repeat the procedure for the US points. Now you have two geopackage files with the DTM values at each DS and US point.

3. Now, the DTM values and the shapefile with shorter drainage segments from step 3 in section C.3 will be put together in a *joined layer*. Click *Vector* → *Data Management Tools* → *Join Attributes by Location*. Set the input layer to the layer with DTM DS points, and the join layer to the clipped drainage data layer. Set the *Geometric predicate* to *equal*[2]. Save the output file as geopackage. Repeat the procedure for the US points.

4. Open the attribute table of the DS joined layer, select *toggle editing* and open the *field*

[2]Spatial predicates are explained in detail by Clementin et al. [83], see also https://en.wikipedia.org/wiki/DE-9IM

calculator. Create a new field and calculate the bed level b as $b = DTM - e$, where DTM is the DTM value at each DS point and e is the measured elevation. Create a new field and calculate the surface level s as $s = DTM - e + d$ where d is the measured depth. Save the changes and repeat the procedure for the US points. Now you have two geopackage files with the attributes of each segment, including bed level and surface level, at all DS and US points. Save these files as *.csv*-files. In the examples below, they are called *ds_DTM.csv* and *us_DTM.csv*.

5. Inspect the points that now are missing bed level and surface level values. These points are likely missing data on dimension and elevation, but have an explanation of why this could not be measured. Decide on how to proceed with these points, for example by assuming dimension values.

C.5 Adjust bed levels

As explained in section 5.1.6, bed level gaps are introduced in the drainage network when assuming that the measured elevation is constant along the whole segment. As *Ramani Huria* is measuring the elevation at the upstream point of each segment, the upstream bed levels are most likely to represent the actual bed levels. All downstream bed levels will here be shifted to match the upstream bed levels. First, the actual end coordinates of each segment, that is, the end coordinates before the buffer was introduced in previous steps, must be added to the joined layer created in section C.4. An example of how this can be done in Python is shown below. Firstly, calculate the DS and US coordinates for your original, not-buffered drainage data, in the same way as described in section C.3. Save it as *.csv*-file. Here, this file is called *all_segments.csv*.

```
import numpy as np
import pandas as pd

clipped_file = 'clipped_segments.csv' #clipped drainage elements
notclipped_file = 'all_segments.csv' #original drainage data

clipped = pd.read_csv(clipped_file,sep = ',', na_values = ['NaN'])
not_clipped = pd.read_csv(notclipped_file,sep = ',', na_values = ['NaN'])


#add columns to store coordinates
clipped['ds_x'] = 'NaN'
clipped['ds_y'] = 'NaN'
clipped['us_x'] = 'NaN'
clipped['us_y'] = 'NaN'

#copy dataframe
add_coord = clipped.copy()

#check it
add_coord.head()

#add coordinates
for i in np.arange(np.size(add_coord.iloc[:,0])):
    for j in np.arange(np.size(not_clipped.iloc[:,0])):
        if add_coord.fid[i] == not_clipped.fid[j]:
            add_coord.ds_x[i] = not_clipped.ds_x[j]
            add_coord.ds_y[i] = not_clipped.ds_y[j]
            add_coord.us_x[i] = not_clipped.us_x[j]
            add_coord.us_y[i] = not_clipped.us_y[j]
```

```
#save it
add_coord.to_csv('add_coordinates.csv', sep=',')
```

Now, this saved *.csv*-file contains rows with the attributes of all segments, the coordinates of the cross section locations, and the start- and end coordinates of each segment. This file is loaded in another script, see below, to adjust the bed levels.

```
import numpy as np
import pandas as pd

fn = 'add_coordinates.csv'
df = pd.read_csv(fn,sep = ',', na_values = ['NaN'])

ds_file = 'ds_DTM.csv'
#File with attributes of all segments, and downstream bed- and surface levels.
ds_points = pd.read_csv(ds_file,sep = ',', na_values = ['NaN'])

us_file = 'us_DTM.csv'
#File with attributes of all #segments, and upstream bed- and surface levels.
us_points = pd.read_csv(us_file,sep = ',', na_values = ['NaN'])

#preallocate segment's own bed- and surface level
df['ds_bedlev'] = 'NaN'
df['ds_surflev'] = 'NaN'
df['us_bedlev'] = 'NaN'
df['us_surflev'] = 'NaN'

#preallocate downstream segments
df['ds_id1'] = 'NaN'
df['ds_id2'] = 'NaN'
df['ds_id3'] = 'NaN'

df['ds_bedlev1'] = 'NaN'
df['ds_bedlev2'] = 'NaN'
df['ds_bedlev3'] = 'NaN'

df['ds_surflev1'] = 'NaN'
df['ds_surflev2'] = 'NaN'
df['ds_surflev3'] = 'NaN'

#assign each segment's own upstream bed- and surface level
for i in np.arange(np.size(df.iloc[:,0])):
    for j in np.arange(np.size(us_points.iloc[:,0])):
        if df.fid[i] == us_points.fid[j]:
            df.us_bedlev[i] = us_points.us_bedlev[j]
            df.us_surflev[i] = us_points.us_surflev[j]

#assign each segment's own downstream bed- and surface level
for i in np.arange(np.size(df.iloc[:,0])):
    for j in np.arange(np.size(ds_points.iloc[:,0])):
        if df.fid[i] == ds_points.fid[j]:
            df.ds_bedlev[i] = ds_points.ds_bedlev[j]
            df.ds_surflev[i] = ds_points.ds_surflev[j]

#Each downstream point can have at most 3 other points connected to itself.
#These can be both us and ds points. We are only interested in the us-points
```

```
#that are connected downstream, as they are most likely to be represent
#the actual bed level. This is because Ramani Huria is measuring
#elevation from reference road at the upstream points of segments.

r = 0.5 #Arbritaty small radius, meter
k = 1 #counter

for i in np.arange(np.size(df.iloc[:,0])):
    for j in np.arange(np.size(df.iloc[:,0])):
        #distance between the downstream point of this segment,
        #and all other us points.
            if (df.ds_x[i] - df.us_x[ju]) ** 2 + (df.ds_y[i] - df.us_y[j])** 2
< r ** 2 and df.fid[i] != df.fid[j]:
            #then these segments are connected,
            #save the connected segment's attributes
               df['ds_id' + str(k)][i] = df.fid[j]
               df['ds_bedlev' + str(k)][i] = df.us_bedlev[j]
               df['ds_surflev' + str(k)][i] = df.us_surflev[j]
               k += 1
    if df.ds_bedlev1[i] != 'NaN':

    #if this column is NaN, then no upstream point is connected to this
    #downstream point. This downstream point is then an outflow, and the bed
    #level should remain the same. If this downstream point is not an outflow
    #(statement is True), then the bed level of it should be adjusted.
    #The bed level can be set to any of the connected us points bed levels,
    #because their bed levels should be equal or very similar.
    #If they are not, then that is an error in itself that we cannot influence.
    #The selection of bed level among the connected upstream points
    #does not matter.

        df.ds_bedlev[i] = df.ds_bedlev1[i]
        df.ds_surflev[i] = df.ds_bedlev1[i] + df.depth[i]
        #keep the depth of the segment
    k = 1

#making culverts almost straight, assuming a slope of 1:500

for i in np.arange(np.size(df.iloc[:,0])):
    if df.drain_type[i] == 4: #if it is a culvert
        #calculate the length of the culvert
        L = np.sqrt((df.ds_x[i] - df.us_x[i]) ** 2 +
        (df.ds_y[i] - df.us_y[i])**2)

        #assuming a small slope of 1:500 of all culverts,
        #adjusting the us bedlevel
        df.us_bedlev[i] = df.ds_bedlev[i] + 0.002 * L

        df.to_csv('adjusted_straightculverts.csv', sep=',')
```

Now all culverts are almost straight, and the final step is to adjust the downstream bed levels of the non-culverts to the upstream bed levels of the culverts. Open the file *adjusted_straightculverts.csv* in Excel. Split the output file in two parts, one *.csv*-file with only culverts, and one with all other drain types. In the example below, these files are called *culverts.csv* and *notculverts.csv*

```
import numpy as np
import pandas as pd

fn1 = 'notculverts.csv'
df_notculvert = pd.read_csv(fn1,sep = ';', na_values = ['NaN'])

fn2 = 'culverts.csv'
df_culvert = pd.read_csv(fn2,sep = ';', na_values = ['NaN'])

for i in np.arange(np.size(df_notculvert.iloc[:,0])):
    #for all segments that is not a culvert
    for column in df_notculvert[['ds_id1','ds_id2','ds_id3']]:
    #for the max 3 connected points
        #downstream of each non-culvert
        for j in np.arange(np.size(df_culvert.iloc[:,0])):

        #loop through the culverts
            #if the ds point of a non-culvert is connected to a culvert
            if df_notculvert[column][i] == df_culvert.fid[j]:
                #set bedlevel to the one of the culvert
                df_notculvert.ds_bedlev[i] = df_culvert.us_bedlev[j]

                df_notculvert.to_csv('final_notculverts.csv', sep=',')
```

Then, merge this output file with the *culverts.csv*-file to get your final 1D schematisation. How to assign the dimensions and bed levels to the cross section locations depends on the requirements of the modelling software that is used.

C.6 Add friction values

Finally, the hydraulic roughness should be allocated to each segment. *Ramani Huria* is recording the material of the drainage, and this material data should be converted to friction values, see section 4.1.1. In this thesis, eight different materials are present in the study area. Prepare a *.csv*-file with the IDs of all segments, and allocate a number for each material type. Here, the column with the material of the segments is called *smoothness*. The sources of the friction values chosen here can be found in section 5.1.5.

```
import numpy as np
import pandas as pd

fn = 'distributed_roughness.csv'
df = pd.read_csv(fn,sep = ';', na_values = ['NaN'])

#preallocate hydraulic roughness
df['roughness'] = 'NaN'

for i in np.arange(np.size(df.iloc[:,0])):
    if df.smoothness[i] == 1: #smooth concrete
        df.roughness[i] = 0.06
    if df.smoothness[i] == 2: #intermediate concrete
        df.roughness[i] = 0.5
    if df.smoothness[i] == 3: #rough concrete
        df.roughness[i] = 1
    if df.smoothness[i] == 4: #rock
        df.roughness[i] = 1
    if df.smoothness[i] == 5: #decommissioned with grass
        df.roughness[i] = 0.5
```

```
    if df.smoothness[i] == 6: #sand
        df.roughness[i] = 0.02
    if df.smoothness[i] == 7: #corrugated steel
        df.roughness[i] = 0.02
    if df.smoothness[i] == 8: #plastic
        df.roughness[i] = 0.01

df.to_csv('assigned_distributed_roughness.csv', sep=',')
```

If your modelling software has table environment where friction values can be assigned, you can now copy and paste the friction values from the output file.